

University of Alberta Library



0 1620 3370008 7

EX LIBRIS
UNIVERSITATIS
ALBERTAENSIS





Digitized by the Internet Archive
in 2018 with funding from
University of Alberta Libraries

<https://archive.org/details/investigationofr00winn>

An Investigation
of the
Rheological Properties
and
Pipeline Flow Characteristics
of
Clay Slurries.

UNIVERSITY OF ALBERTA
FACULTY of ENGINEERING

This is to certify that the undersigned
have read and recommend to the Committee on Graduate
Studies for acceptance, a thesis submitted
by M. D. Winning, B.Sc., entitled:

An Investigation
of the
Rheological Properties
and
Pipeline Flow Characteristics
of
Clay Slurries.

Professor

Professor

Professor

Thesis

An INVESTIGATION of the RHEOLOGICAL
PROPERTIES and PIPELINE FLOW CHARACTERISTICS
of CLAY SLURRIES.

Submitted in partial fulfillment of
the requirements for the degree of

Master of Science
in Chemical Engineering

by

M. D. Winning.

Under the direction of

Dr. G. W. Govier.

University of Alberta.

Edmonton

September 1948.

THE
OFFICE OF THE
SECRETARY OF THE
NAVY
WASHINGTON, D. C.

DEPARTMENT OF THE NAVY

NAVY DEPARTMENT

NAVY DEPARTMENT

NAVY DEPARTMENT

NAVY DEPARTMENT

NAVY DEPARTMENT

Acknowledgment.

The author wishes to express appreciation to Dr. G. W. Govier under whose supervision this project was carried out and whose criticism and assistance have contributed greatly to the investigation.

The author is indebted to

The National Research Council of Canada for their sponsorship.

The Research Council of Alberta for the use of their Stormer viscosimeter.

The Department of Chemical Engineering of the University of Alberta for the equipment and supplies used in the investigation.

Acknowledgment is also made to Mr. C. E. Newman, who helped with the construction of the flow circuit, and to Mr. G. E. Nickoloff for assistance with the calculation of the yield ratios.

The service rendered by Mr. T. W. Dalkin and Mr. R. M. Scott in the reproduction of the illustrations is greatly appreciated.

Table of Contents.

Table of Contents	(i)
List of Illustrations	(iv)
The Problem	(vi)
Summary	(vii)
I <u>Introduction</u>	1
II <u>Literature Review and Theory</u>	2
Rheology	2
Mechanism of Suspension Flow	9
The Flow Problem	10
Newtonian Fluids	10
Non-Newtonian Fluids	12
Summary and Comparison of Theory	27
Dimensional Analysis	30
Viscosimetry	33
The MacMichael Viscosimeter	35
The Stormer Viscosimeter	35
Mathematical Analysis of a Stormer Viscosimeter	36
III <u>Experimental Equipment</u>	43
Equipment for the Measurement of Suspension	
Rheological Properties	43
The Flow Circuit	43
Supply Tank	46
Pump and Motor	46
Test Sections	46
Scales and Weighing Tank	47
Pressure Taps and Sight Glasses	50
Manometers	50
Control	56

<u>IV Experimental Procedure</u>	58
Methods of Measuring the Suspension	
Rheological Properties	58
Pipeline Operation	59
Circulation of Slurry	59
Deaeration of Pressure Lines	60
Flow Rate-Pressure Drop Measurement	61
Water Tests	62
<u>V Experimental Data</u>	63
Calibration Data for Viscosimeter	64
Manometer Fluid Calibration	71
Suspension Rheological Properties	77
Supplementary Data	81
Water Flow Data	82
Suspension Flow Data	85
<u>VI Presentation of Results</u>	93
Computed Data obtained by Preliminary	
Calculations	93
Final Calculations and Correlation of	
Results	106
Water Flow Results	117
Suspension Flow Results	122
<u>VII Discussion of Results</u>	158
Calibration of Equipment	158
The Viscosimeter	158
The Manometer Fluids	160

Discussion of Results (con't)	
Pipeline Smoothness	160
Rheology	160
Pressure Drop-Rate of Flow Correlations	162
Recommended Method of Pressure Drop	
Estimation	165
<u>VIII Conclusions</u>	166
<u>IX Bibliography</u>	168
<u>X Appendix (Theoretical Derivations)</u>	169

List of Illustrations.

Fig.No.	Illustration	Page No.
1	Possible Rheological Relationships.	3
2	Rate of Shear-Shearing Stress-Time.	8
3	Caldwell and Babbitt's "Apparent Viscosity".	15
4	McMillen's Velocity-Reynolds Number Distribution.	26
5	Stormer Viscosimeter Load-Speed Relationship for a Newtonian Fluid.	38
6	Stormer Viscosimeter Load-Speed Relationship for a True Plastic.	40
7	The Stormer Viscosimeter.	42
8	Flow Sheet of the Pipeline.	44
9	Supply tank, Pump, and Motor.	45
10	End View of Test Sections.	48
11	Cross-section of a Pipe Joint.	49
12	The Scales and Weighing Tank.	51
13	A Pressure Tap and Sight Glass.	52
14	Cross-section of a Pressure Tap.	53
15	The Pressure Connections.	54
16	The Manometers.	55
17	Viscosimeter Calibration Data.	66
18	" " "	67
19	Viscosimeter Calibration Chart.	68
20	Expansion of the Curved Region of the Viscosimeter Calibration Chart.	69
21	Manometer Fluid #1 Calibration Chart.	73
22	" " #3 " "	74
23	" " #5 " "	75
24	" " #6 " "	76
25	Viscosimeter Data on the Suspensions.	79
26	" " " " " "	80
27	Yield Values vs. Percent Solids.	111
28	$\ln(m'+0.001)$ vs. Percent Solids.	112
29	Smoothed Yield Values vs. Percent Solids.	113
30	Coefficients of Rigidity vs. Percent Solids.	114
31	$\ln(\eta-\nu+0.042)$ vs. Percent Solids.	115
32	Smoothed Coefficients of Rigidity vs. Percent Solids.	116
33	Water Test Data.	121
34	Friction Factor vs. Reynolds Number $\frac{Dv}{\mu} f > 0.011$	132
35	As above $f < 0.011$	133
36	Friction Factor vs. Reynolds Number $\frac{Dv}{\mu} f < 0.011$	135
37	As above $f > 0.011$	136

Fig. No.	Illustration	Page No.
38	Friction Factor vs. Reynolds Number $\frac{DVP_3}{\eta_s} \left[1 - \frac{4}{3} \left(\frac{2Lm'}{RAP} \right) + \frac{1}{3} \left(\frac{2Lm'}{RAP} \right)^4 \right]$ Streamline Region	138
39	Figures (38) and (36) Combined. Friction Factor vs. Yield Ratio.	139
40	At Reynolds Number= 40	143
41	" 100	144
42	" 400	145
43	" 1000	146
44	" 4000	147
45	" 6000	148
46	" 8000	149
47	" 10^4	150
48	" 2×10^4	151
49	" 4×10^4	151
50	" 10^5	151
51	Friction Factor vs. Reynolds Number with Yield Ratio as Parameter.	157

The Problem.

The problem here undertaken is:

- (a) An interpretation of the theoretical equations, applying to flow of a plastic material, in terms of the friction concept.
- (b) An investigation of the rheological properties of clay slurries.
- (c) An experimental evaluation of the flow rate - pressure drop relationships for pipeline flow of clay slurries.
- (d) A correlation of the flow rate - pressure drop relationships in terms of slurry properties.

SUMMARY

Pressure drop - rate of flow data have been obtained for clay suspensions flowing through two twenty-foot lengths of smooth copper tube 0.786 and 1.277 inches in diameter respectively. Over the range of solids concentration encountered (0 to 40.4% solids by weight) the clay suspensions behaved in a manner very similar to true plastic materials.

The rheological properties of these suspensions were independently measured by means of a calibrated Stormer viscosimeter. For the particular suspensions used the yield values and the coefficients of rigidity were correlated as exponential functions of the percent solids. The equation relating the yield value (m^1) to the percent solids (x) was found to be

$$m^1 = 0.001 (e^{0.158x} - 1)$$

over the range of yield values from 0.0005 to 0.560 lbs/ft². The coefficients of rigidity (η_s) were related to the percent solids (x) by the equation

$$\eta_s = \nu + 0.042 (e^{0.159x} - 1)$$

where (ν) is the viscosity of water at the temperature of the suspension. Values of (η_s) covered the range from 0.000526 to 0.0155 lbs/ft.sec.

The rheological properties and pressure drop data were used to verify various methods of pressure drop estimation for suspensions flowing in pipelines.

Bingham's equation for streamline and/or plug flow of a plastic material was rearranged to show that the friction factor "f" may be obtained from

$$f = 16/N_{Re(III)}$$

$$\text{where } N_{Re(III)} = \frac{DV\beta_s}{\eta_s} \left[1 - \frac{4}{3} \frac{(2Lm)}{(R\Delta P)} + \frac{1}{3} \frac{(2Lm)^4}{(R\Delta P)^4} \right]$$

The scattering of data, which was as much as 1000 percent, indicated that this method is questionable.

Babbitt and Caldwell's method of obtaining the friction factor from the usual Reynolds number diagram using a modified Reynolds number $N_{Re(i)} = \frac{DV\beta}{\eta_s}$ was tested by correlating the data as "f" vs. " $\frac{DV\beta}{\eta_s}$ ". A scattering of data which varied with the solids concentration in the turbulent flow region and with both percent solids and diameter in the streamline flow region indicates that this method is only an approximation.

Dimensional analysis indicated the possibility of relating the friction factor to the three dimensionless groups

$$\left(\frac{DV\beta_s}{\eta_s} \right), \quad \left(\frac{\Delta}{D} \right), \quad \left(\frac{Dm\beta}{V\eta_s} \right)$$

The ratio $\left(\frac{DV\beta_s}{\eta_s} \right)$ has been defined as a modified Reynolds number $(N_{Re(II)})$ and the ratio $\left(\frac{Dm\beta}{V\eta_s} \right)$ as the yield ratio.

Since smooth copper tubes were used in the test sections the effect of the roughness factor $\left(\frac{\Delta}{D} \right)$ was assumed to be negligible. At high flow rates $\left(\frac{DV\beta_s}{\eta_s} \right) > 2 \times 10^4$

it was found that the friction factor was independent of the yield ratio. Further at high flow rates the data indicated that the friction factor may be predicted by means of the conventional Reynolds number diagram and the modified Reynolds number $\left(\frac{DV\beta}{\eta_s}\right)$. At low flow rates $\left(\frac{DV\beta}{\eta_s} < 2 \times 10^4\right)$ the friction factor was correlated with the modified Reynolds number using the yield ratio as a parameter. This correlation has been presented and has been found satisfactory in the estimation of the friction factors except at extremely low flow rates of the less dense suspensions. No attempt has been made to check the figure, which presents this correlation, by comparing it with pressure drop data from other investigations.

Thesis

An Investigation of the Rheological Properties and Pipeline Flow Characteristics of Clay Slurries.

I. Introduction.

The flow of slurries (solids suspended in a liquid) occurs with varying importance in many industries - to mention a few: the flow of sludges in sewage disposal, the flow of pulp in paper making, the flow of rock suspensions in the cement industry, the placement of concrete in construction work, the flow of mud in oil well drilling, and the handling of clay in the pottery industry. More and more, industry is attempting to use this economical method of moving solid materials rather than the older, costly, and very cumbersome systems. It becomes necessary then to be able to design equipment for the handling of solid suspensions. It would be very convenient if the design methods applicable to ordinary fluids could be used for slurries. However, suspensions of solids do not behave as Newtonian fluids and the usual methods for estimating pressure drop do not hold.

In this thesis the results of an investigation of the rheological properties and pressure drop-flow rate relationships for a series of clay-water suspensions are presented and discussed.

II Literature Review & Theory.

Rheology:

In the study of fluid flow much information may be obtained by considering the relationships between the applied shearing stress and the resultant rate of shear. In the case of flow of suspensions the properties of the Newtonian carrier fluid are modified by the presence of the solid being conveyed. Figure (1) below indicates some of the possibilities which may occur. Curve I represents a Newtonian fluid which can be characterized by its viscosity ν where

$$\nu = \beta \frac{s}{\left(\frac{dv}{dx}\right)} \quad (1)$$

with s = the tangential unit shearing force
 v = the relative velocity of two planes
 a distance x apart.

$$\beta = \text{a proportionality constant} \frac{(\text{mass.lbs. ft.})}{(\text{force.lbs.sec}^2)}$$

For a circular pipe dx becomes dr .

Curve II represents the rheological properties of a true plastic. Such a material is characterized by a yield point (m) and a coefficient of rigidity (η). The yield point can be defined as the maximum shearing stress at zero rate of shear. It is that portion of the applied stress which is used to overcome the internal elastic stresses.

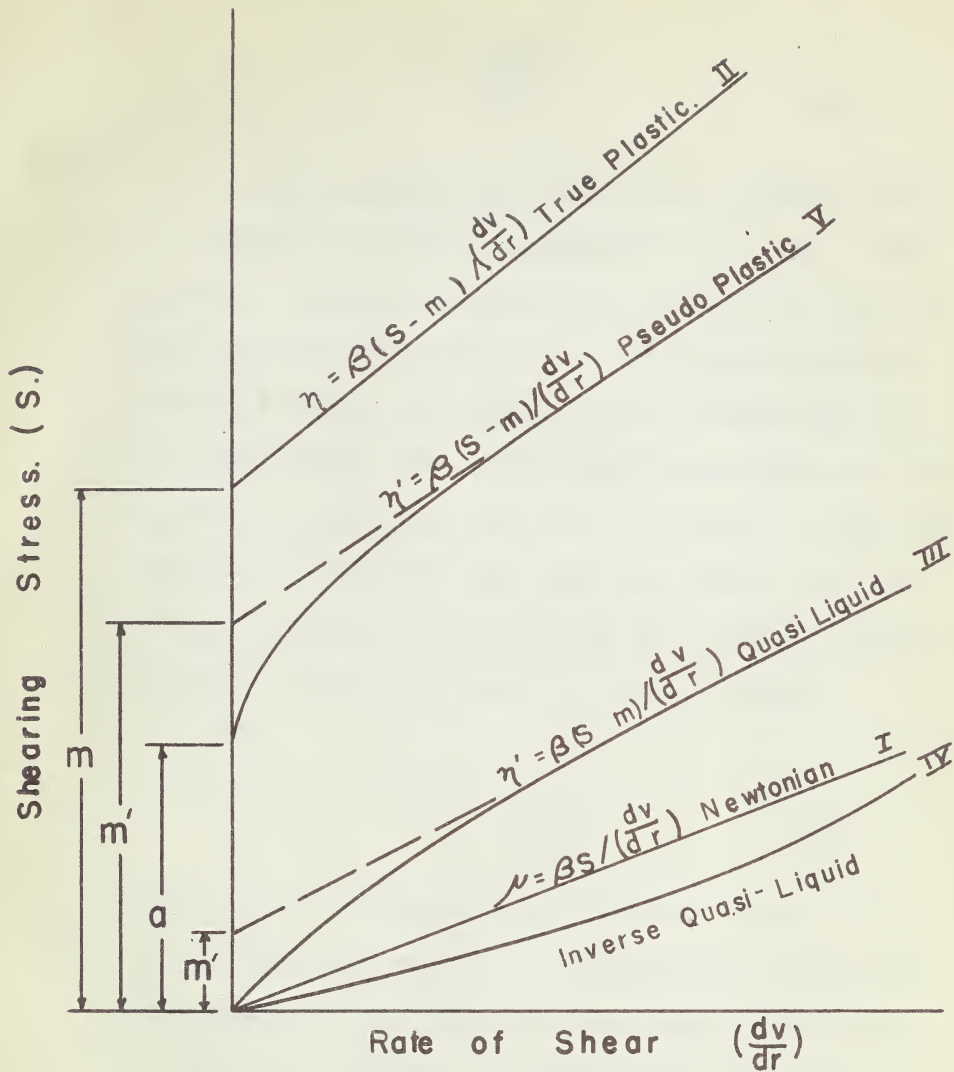


Fig. 1. Possible Rheological Relationships.

The coefficient of rigidity is given by the expression

$$\eta = \beta \frac{(S-m)}{\left(\frac{dv}{dx}\right)} \quad (2)$$

Most suspensions behave in a manner which is somewhere between a Newtonian fluid and a true plastic. Further possibilities which are known to occur are the pseudo-plastics and quasi-liquids. Curve III is that of a quasi-liquid which exhibits no yield point. The rheological properties of this type of material are complex in as much as the true relationship between the shearing stress and rate of shear cannot be represented by a simple linear equation. The relationship takes the form

$$\nu^* = \beta \frac{S^n}{\left(\frac{dv}{dx}\right)} \quad (3)$$

where n is an exponent greater than one. It is to be noted that when n is not equal to one the dimensions of ν^* are not the same as viscosity. Ostwald and de Waele (13) make use of the term "Strukturviskosität" for ν^* to distinguish it from viscosity ν . Fortunately at high rates of shear, such as are ordinarily encountered, it is possible to represent the shearing stress-rate of shear relationship by means of an apparent coefficient of rigidity (γ') and an apparent yield point (m')

as indicated in Figure I . The approximate relationship being

$$\eta' = \beta \frac{(S-m')}{\frac{dv}{dr}} \quad (4)$$

Curve IV indicates the behaviour of a quasi-liquid which follows equation (3)

$$\eta^* = \beta \frac{S^n}{\frac{dv}{dr}}$$

when the exponent n is less than one. Here again the rheological properties are very complex. This type of material has been called an inverse plastic by Babbett and Caldwell (1) and quasi-viscous by Houwink (7). It is not expected that any of the material being used in this investigation will behave as such.

Curve V is that of a pseudo-plastic. The rheological properties of which may be represented by

$$\eta^* = \beta \frac{(S-m)^n}{\frac{dv}{dr}} \quad (5)$$

where n is greater than one. Similarly to the case of the quasi-liquid the exponent alters the units so that η^* should not be expressed in the same dimensions as a coefficient of rigidity. As an approximation the behaviour of a pseudo-plastic may be characterized by an apparent coefficient of rigidity η' and an apparent yield point (m') such that

$$\eta' = \beta \frac{(S - m')}{\frac{dv}{dr}} \quad (6)$$

It is to be noted that in the case of a pseudo-plastic there is a second yield point "a" which does not coincide with m' . To avoid confusion the yield point "a" will be defined as the lower yield point and m' as the yield point.

The use of an apparent yield point m' which is permissible at high rates of shear should be restricted at low rates of shear to those suspensions which are very nearly true plastics. For those materials having a lower yield point which is only a small fraction of the apparent yield point, the use of the apparent value results in an estimated pressure drop which will be much greater than the actual value.

It is not expected that material behaving according to equation 5, with n less than one, will be encountered in this investigation.

Actually figure (1) presents only part of the picture. For materials whose rheological properties change with agitation a three dimensional representation is necessary to show the effect of time. Figure (2) gives a plot of shearing stress against rate of shear and time for the case where the rheological properties change with time. Surface II represents a true plastic and surface III a quasi-liquid. The case of pseudo plastic is given by surface IV. For comparison surface I represents a Newtonian fluid whose properties do not change with time.

Assuming that the rate of change of shearing stress with time $\left(\frac{ds}{dt}\right)$ is proportional to the amount by which the shearing stress at time θ exceeds the shearing stress after long agitation (S_{∞}) the following equation can be written

$$\frac{ds}{dt} = \frac{-(S_{\theta} - S_{\infty})}{\lambda} \quad (7)$$

where λ is a proportionality factor called the "time of relaxation" by Houwink (7).

Solving equation(7) results in the expression $\log \frac{S_{\theta} - S_{\infty}}{S_0 - S_{\infty}} = -\frac{\theta}{\lambda}$ (8)

where S_0 is the initial shearing stress.

This equation may be put in the form

$$S_{\theta} = S_{\infty} + (S_0 - S_{\infty}) e^{-\frac{\theta}{\lambda}} \quad (9)$$

Assuming equation (2) to hold it is possible to write

$$\eta_0 - \eta_{\infty} = \frac{\beta}{\frac{dv}{dr}} \{S_0 - m - S_{\infty+m}\} \quad (10)$$

or

$$\eta_0 - \eta_{\infty} = \frac{\beta}{\frac{dv}{dr}} (S_0 - S_{\infty}) \quad (11)$$

Similarly $\eta_0 - \eta_{\infty} = \frac{\beta}{\frac{dv}{dr}} (S_0 - S_{\infty}) \quad (12)$

Solving equations (11, 12) for the shearing stress and substituting in (9) results in

$$\eta_{\theta} = \eta_{\infty} + (\eta_0 - \eta_{\infty}) e^{-\frac{\theta}{\lambda}} \quad (13)$$

Equation (13) presents the variation of the coefficient of rigidity with time of agitation and suggests an exponential relationship between the two. This equation has never been verified experimentally.

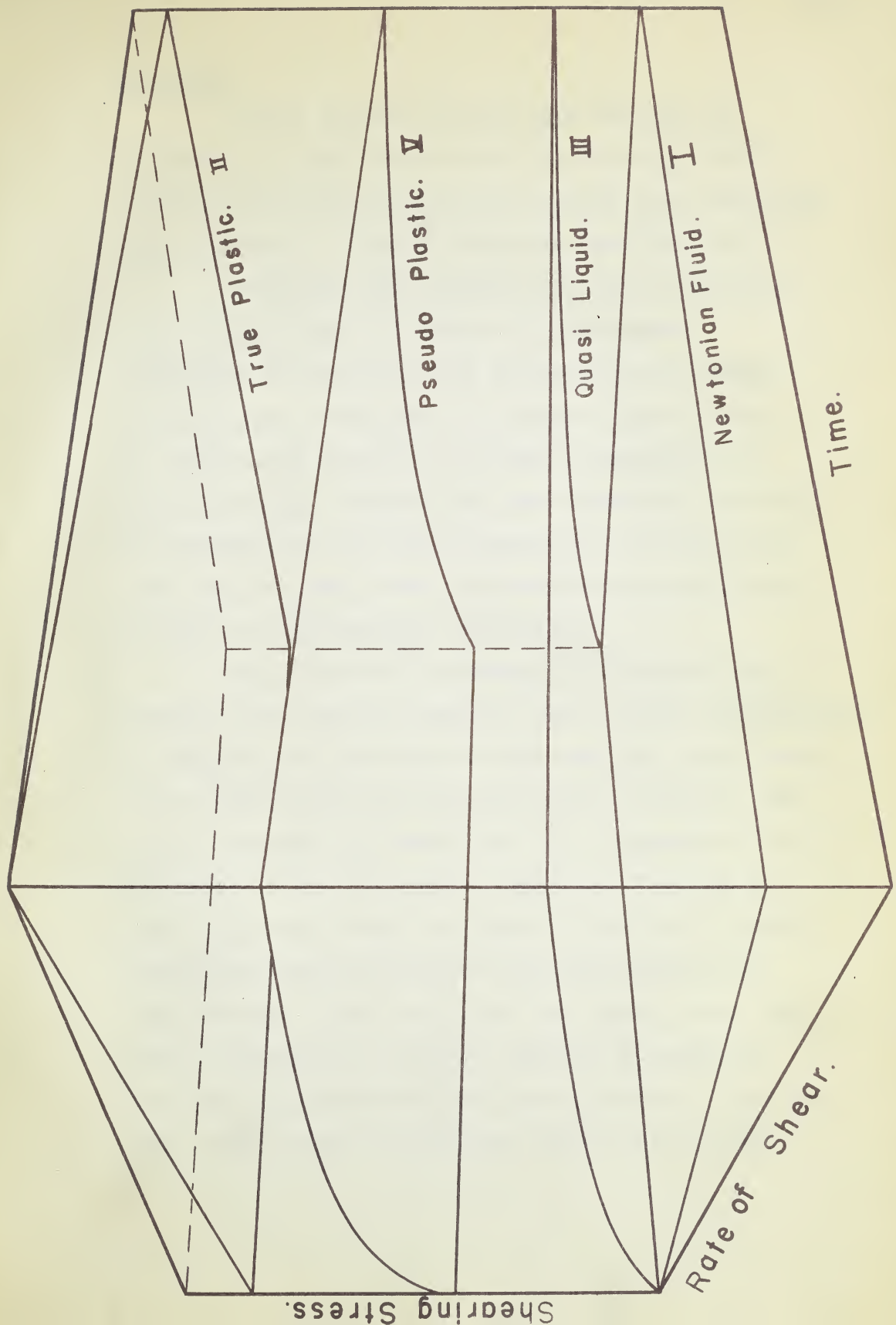


Fig. 2. Rate of Shear Shearing Stress Time.

Mechanism.

Several mechanisms have been advanced as explanation of the variation in the shearing stress - rate of shear relationship which occurs with increasing rates of shear. A few of these are mentioned below.

Williamson (15) suggests that the increasing rate of shear tends to deform or disintegrate aggregates of particles thus decreasing their resistance to flow. Hatschek (6) presents the same idea as applying to layers of solvation surrounding the solid particles. Neither of these mechanisms explains the increase in the rate of change of shearing stress with rate of shear, which occurs with increasing rates of shear in the turbulent flow region.

Reiner (10) and Staudinger (12) explain the change in the shearing stress - rate of shear relationship as being due to the effect of the shearing couple which exists between any two separate layers of fluid. The couple promotes the attenuation and alignment of solid particles in the fluid with a resultant decrease in flow resistance. This mechanism allows for a possible increase in rate of change of shearing stress with rate of shear in the turbulent flow region, since the radial components of velocity present in turbulent flow may disorientate the aligned particles. Just how much of the effect of turbulent flow is due to this

disorientation and how much is due to the inertia effects of the fluid is very difficult to determine.

The Flow Problems.

Many problems in the design of equipment for the unit operation of fluid flow may be handled by a mechanical energy balance. The equation most used takes the form:

$$(x_2 - x_1) \frac{g}{\beta} + \frac{v_2^2 - v_1^2}{2\beta} + \Sigma F + W + \int_1^2 v dp = 0 \quad (14)$$

where x = the height above a datum plane (ft. of fluid)

g = the gravitational constant (ft/sec²).

β = a proportionality constant

$$= 32.174 \frac{(\text{mass lbs.ft})}{(\text{force lbs.sec}^2)}$$

p = the pressure (force lbs/ft²).

v = the specific volume of the fluid (ft³/lb.mass)

V = the velocity (ft/sec).

W = the work done by the fluid (force lbs.ft/mass lb)

ΣF = the total friction due to flow (force lbs.ft/mass lb)

The subscripts indicate the section at which the quantity is measured. Actually ΣF is better defined as the term necessary to balance the equation. For the special case where ($w = x_2 - x_1 = v_2 - v_1 = 0$) and the change in specific volume is small it is possible to express the pressure drop as

$$-\Delta P = \rho \Sigma F \quad (15)$$

Newtonian Fluid.

For Newtonian fluids it may be shown by dimensional analysis that the pressure drop due to

friction in a pipeline is given by

$$\Delta P = \frac{V^2 \rho L}{8 R} \phi \left(\frac{2RV\rho}{\mu}, \frac{\Delta}{2R} \right) \quad (16)$$

where R = the radius of the pipe (ft)

L = the length of pipe (ft)

ρ = the density of the fluid (lbs mass/ft³)

μ = the absolute viscosity of the fluid (lbs mass/ft.sec)

ϕ = some unknown function.

$\frac{2RV\rho}{\mu}$ = a dimensionless ratio called Reynold's number

$\frac{\Delta}{2R}$ = the relative roughness.

The unknown function is given the symbol $2f$ so that

$$\Delta P = \frac{2 f V^2 \rho}{8 R} L \quad (17)$$

and it has been shown experimentally that the relationship $2f = \phi \left(\frac{2RV\rho}{\mu}, \frac{\Delta}{2R} \right)$ does exist. The relationship, in the region of turbulent flow, is rather complex and best represented graphically by the friction factor-Reynold's number graph which may be found in most Chemical Engineering textbooks. (14)

In the streamline flow region the relationship is much simpler. The effect of roughness disappears so the term $\frac{\Delta}{2R}$ drops out. The function then becomes

$$2f = \phi \left(\frac{2RV\rho}{\mu} \right) \quad (18)$$

and it can be shown experimentally that

$$f = \frac{16 \mu}{8 RV\rho} \quad (19)$$

Substitution of this equality for f in equation (17) results in

$$\Delta P = \frac{32 \mu VL}{(8R)^2 \rho} \quad (20)$$

Poiseuille by means of a theoretical analysis arrived at the same result as equation (20)
Non-Newtonian Fluids.

It is possible to use the friction factor Reynold s number graph for the evaluation of the pressure drop due to friction in a pipeline carrying a Newtonian fluid. In the case of a material whose rheological properties change with rate and time of application of shear the term viscosity is meaningless and the above method is inapplicable. In order however to permit a direct comparison between the pressure drops for Non-Newtonian and for Newtonian fluids it is convenient to assume that both may be represented by equation (17) in the form

$$-\Delta P = \frac{2f V^2 L \rho}{2R \beta} \quad (21)$$

This procedure is permissible provided it is understood that $2f$ no longer is defined by the equation

$$2f = \phi \left(\frac{2RV\rho}{\mu}, \frac{\Delta}{2R} \right) \quad (22)$$

but must be defined to satisfy equation (21)

Equation (21) may be rearranged to give

$$V^2 = \left(\frac{R}{L} \right) \left(\frac{\beta \Delta P}{\rho} \right) \frac{1}{f} \quad (23)$$

which is more suitable for comparative purposes.

For a true plastic (Figure 1) Bingham (3) has derived an equation for plug and streamline flow, characterizing the rheological properties of the plastic material by the yield value (τ_0) and the

coefficient of rigidity (γ). His derivation which is detailed in the appendix, leads to the following expression

$$V = \frac{\beta R^2 \Delta P}{8 L \gamma} \left[1 - \frac{4}{3 \Delta P} \left(\frac{2 L m}{R} \right) + \frac{1}{3 \Delta P^4} \left(\frac{2 L m}{R} \right)^4 \right] \quad (24)$$

This equation may be transformed as follows, ^usquaring both sides:

$$V^2 = \frac{\beta^2 R^4}{64 L^2 \gamma^2} \Delta P^2 \left[1 - \frac{4}{3 \Delta P} \left(\frac{2 L m}{R} \right) + \frac{1}{3 \Delta P^4} \left(\frac{2 L m}{R} \right)^4 \right]^2 \quad (25)$$

Multiplying and dividing the right side by ρ to obtain the form of equation (23):

$$V^2 = \frac{R}{L} \frac{\beta \Delta P}{\rho} \frac{\beta R^3 \Delta P \rho}{64 L \gamma^2} \left[1 - \frac{4}{3 \Delta P} \left(\frac{2 L m}{R} \right) + \frac{1}{3 \Delta P^4} \left(\frac{2 L m}{R} \right)^4 \right]^2 \quad (26)$$

Comparing equation (26) with equation (23) it follows that

$$\frac{1}{f} = \frac{\beta R^3 \Delta P \rho}{64 L \gamma^2} \left[1 - \frac{4}{3 \Delta P} \left(\frac{2 L m}{R} \right) + \frac{1}{3 \Delta P^4} \left(\frac{2 L m}{R} \right)^4 \right]^2 \quad (27)$$

Multiplying the right side of equation (27) by V and dividing by the equivalent of V from equation (24) results in

$$f = \frac{16 \gamma}{2 R V \rho} \frac{1}{\left[1 - \frac{4}{3 \Delta P} \left(\frac{2 L m}{R} \right) + \frac{1}{3 \Delta P^4} \left(\frac{2 L m}{R} \right)^4 \right]} \quad (28)$$

Comparing equations (29) with the expression for the friction factor for streamline flow of a Newtonian fluid

$$f = \frac{16 \nu}{2 R V \rho} \quad (19)$$

the effect of the yield value is immediately apparent. Equations (28) and (19) indicate the possibility of defining an "apparent" viscosity ν where

$$\nu = \frac{\gamma}{\left[1 - \frac{4}{3 \Delta P} \left(\frac{2 L m}{R} \right) + \frac{1}{3 \Delta P^4} \left(\frac{2 L m}{R} \right)^4 \right]} \quad (29)$$

It can be seen that considering a Newtonian fluid as the special case of a plastic having a yield value (m) of zero, the coefficient of rigidity (γ) becomes equal to the viscosity and $f = \frac{16 \mu}{2 R V} \quad (19)$ Equation (24) and its equivalent equation (29) were verified experimentally by Bingham working with true plastic materials.

Babbitt and Caldwell (1) carried out an investigation of the flow of sewage sludges at the Engineering Experimental Station at the University of Illinois and at the sewage treatment plant at Decatur, Illinois. The sludges ranged in solids content from 2% to 18% and had ^{an} average specific gravity about 1.05. Determinations were made using 3/8, 1, 2 and 3 inch pipes. The range of yield values (m) was 0.0 to 1.58 lbs/ft² and coefficients of rigidity (γ) 0.001 to 0.040 lbs/ft sec.

Relationships were developed between the shearing stress (m) and the yield load used on a Stormer type viscosimeter and between the coefficient of rigidity (γ) and the slope of the load versus speed curve for the viscosimeter. This permits the evaluation of the two significant quantities required to characterize the rheological behaviour of true plastics.

The viscosimeter calibration data indicates that the sewage sludge behaved as a true plastic. In correlating their data obtained from pipeline measurements Babbitt and Caldwell accepted Bingham's theoretical

approach but assumed that the last term of equations (24) and (28) $\frac{1}{3\Delta P^4} \left(\frac{2Lm}{R}\right)^4$ was negligible at high rates of shear. They further assumed β numerically equal to 32 instead of 32.174. These assumptions allow a slight simplification of the expressions for velocity and friction factor to give

$$V = \frac{4 R^2 \Delta P}{\eta L} \left[1 - \frac{4}{3\Delta P} \left(\frac{2Lm}{R} \right) \right] \quad (30)$$

$$\text{and } f = \frac{16 \eta}{2 R V \beta} \frac{1}{\left[1 - \frac{4}{3\Delta P} \left(\frac{2Lm}{R} \right) \right]} \quad (31)$$

Babbitt and Caldwell assumed that the normal Reynolds number friction factor relationship held if an "apparent viscosity" μ' replaces the Newtonian viscosity. They defined μ' arbitrarily as the shearing stress divided by the rate of shear. The significance of this is shown graphically in Figure (3) where μ' , the "apparent viscosity" at A, is the slope of the line OB.

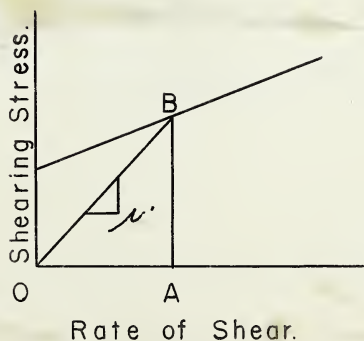


Fig. 3.

Equations (32) to (35) have been deleted from the original thesis on the suggestion of the examiners.

It is to be noted that the "apparent viscosity" ν' has no actual significance. A more appropriate apparent viscosity is found by comparing equations (31) and (19) to give

$$\nu'' = \frac{\eta}{\left[1 - \frac{4}{3\Delta P} \left(\frac{2Lm}{R}\right)\right]} = \eta + \eta \frac{4}{3} \frac{(2Lm)}{P(R)} + \eta \left[\frac{4}{3\Delta P} \left(\frac{2Lm}{R}\right) \right]^2 \quad (36)$$

$$\text{or } \nu'' = \eta \left\{ \left[1 + \frac{4}{3\Delta P} \left(\frac{2Lm}{R}\right) \right] + \left[\frac{4}{3\Delta P} \left(\frac{2Lm}{R}\right) \right]^2 \right\} \quad (37)$$

Parent (9) used Bingham's equation (24) as the starting point in obtaining an expression for head loss due to the flow of a suspension. His method is detailed in the appendix. The resulting equation is

$$h = \frac{32 V \eta}{4g\rho R^2 \left[1 - \frac{16}{3} \left(\frac{\beta_m}{g\rho h 2R}\right) + \frac{256}{3} \left(\frac{\beta_m}{g\rho h 2R}\right)^4 \right]} \quad (38)$$

Since the head loss due to friction (h) is an implicit function here Parent changed the general form to

$$y + \frac{1}{3y^3} = x + \frac{16}{3} \quad (39)$$

$$\text{where } y = \frac{h \rho g R^3}{\Delta P} \quad (40)$$

$$\text{and } x = \frac{32 V \eta}{4 g \rho R^2} \quad (41)$$

and presented graphs of x vs y to aid in solution for h . Parent in his definition of h gives

$$h = - \frac{\Delta P}{\rho g} \quad (42)$$

Substituting this in equation (38) gives

$$-\Delta P = \frac{32 V L \eta}{4 R^2 \beta \left[1 - \frac{4}{3 \Delta P} \left(\frac{2 L m}{R} \right) + \frac{1}{3 \Delta P} \left(\frac{2 L m}{R} \right)^4 \right]} \quad (43)$$

And comparison with equation (21) yields directly

$$f = \frac{16 \eta}{2 R V \rho \left[1 - \frac{4}{3 \Delta P} \left(\frac{2 L m}{R} \right) + \frac{1}{3 \Delta P} \left(\frac{2 L m}{R} \right)^4 \right]} \quad (28)$$

as found from Bingham's theory. Parent used the data of Caldwell and Babbitt to verify equation (38).

Buckingham (4) previously in 1920 derived equations, for the case where streamline and plug flow exist together, on the assumption that there was a thin "lubricating layer" of carrier fluid at the pipe wall which behaved as a Newtonian fluid. Also he assumed that the suspension moves as a plug within this lubricating layer until the yield value m is attained at the pipe wall. Buckingham assumes further that the

applied shearing stress at the pipe wall exceeds the critical stress required for slip between the wall and the material. At stresses higher than m the plug begins to break down and the streamline shell grows radially inward.

His derivation which is detailed in the appendix leads to the expression

$$V = \frac{R^2 \beta}{8 L \eta} \left[\Delta P - \frac{4(2Lm)}{3(R)} + \frac{1}{5 \Delta P^3} \left(\frac{2Lm}{R} \right)^2 \right] + \frac{R \epsilon \phi \beta \Delta P}{2 L} \quad (44)$$

where ϵ is the thickness of the initial "lubricating layer" and ϕ is its viscosity. Buckingham did not present experimental data to verify his theoretical derivation.

Note:

In their present forms equations (44) and (28) cannot be separated to show the difference between the plug and the streamline shell. If the expressions for the velocity are given in an unsimplified form the difference is apparent. For example in equation (45) below which is part of Buckingham's derivation the first bracket shows the effect of the plug and the second the effect of the shell

$$V = \left\{ \frac{4 \beta}{\eta} \frac{L^2 m^2}{\Delta P^2 R^2} \left[\frac{\Delta P R^2}{4 L} + \frac{m^2 L}{\Delta P} - m \eta \right] + \frac{(4 L^2 m^2)}{(\Delta P^2 R^2)} \eta R \right\} + \left\{ \frac{2 \beta}{R} \frac{\Delta P}{\eta} \frac{1}{16} \frac{1}{L} - \frac{m R^3}{6} + \frac{R^2 \eta}{2 \beta} - \frac{R^2 L m^2}{2 \Delta P} + \frac{2 R L^2 m^3}{\Delta P^2} - \frac{8}{3} \frac{L^3 m^4}{\Delta P^3} - \frac{2 \eta R^2 L^2 m^2}{\Delta P \beta} \right\} \quad (45)$$

This equation can be transformed to

$$V = \frac{\beta R^2 \Delta P}{8 L \eta} \left\{ \left[\frac{2}{\Delta P^4} \left(\frac{2 L m}{R} \right)^4 \right] + \left[1 - \frac{4}{3 \Delta P} \left(\frac{2 L m}{R} \right) - \frac{5}{3 \Delta P^4} \left(\frac{2 L m}{R} \right)^4 + \frac{8 \eta L}{\beta R^2 \Delta P} \nu_R \right] \right\} \quad (40)$$

Equation (46) may be put in the form

$$V = \frac{\beta R^2 \Delta P}{8 L \eta} (X + Y) \quad (47)$$

where $X = \frac{2}{\Delta P^4} \left(\frac{2 L m}{R} \right)^4$ (due to the plug) (48)

and $Y = \left[1 - \frac{4}{3 \Delta P} \left(\frac{2 L m}{R} \right) - \frac{5}{3 \Delta P^4} \left(\frac{2 L m}{R} \right)^4 + \frac{8 \eta L}{\beta R^2 \Delta P} \nu_R \right]$
(due to the streamline shell) (49)

with $\nu_R = \frac{c \phi R \Delta P \beta}{8 L}$ according to Buckingham's assumption.

For Bingham's equation the term including ν_R is dropped from the expression for Y.

Three distinct possibilities exist as to the relationship between the applied stress and the yield point

- (i) Applied stress < yield point
- (ii) Applied stress = yield point
- (iii) Applied stress > yield point.

When the applied stress is less than the yield point X is relatively large Y is small. When the applied stress equals the yield point $X = 2$ and $Y = -2 + \frac{8 \eta L}{\beta R^2 \Delta P} \nu_R$ the

net result being $V = \nu_R$. When the applied stress is greater than the yield point X becomes small and Y increases so that the streamline shell contributes more to the flow

than the plug.

Equation (47) may be transformed as follows:

Square both sides,

$$V^2 = \frac{\beta^2 R^4 \Delta P^2}{8^2 \eta^2 L^2} (X + Y)^2 \quad (50)$$

Multiply numerator and denominator by ρ and separate terms to obtain the form of equation (23)

$$V = \frac{R}{L} \frac{\beta \Delta P}{\rho} \frac{\beta R^3 \rho \Delta P}{64 L \eta^2} (X + Y)^2 \quad (51)$$

Comparing equations (23) and (51) shows that

$$\frac{1}{f} = \frac{\beta R^3 \rho \Delta P}{64 L \eta^2} (X + Y)^2 \quad (52)$$

Multiplying the right side of equation (52) by V and dividing by the equivalent of V from equation (47) results in

$$f = \frac{16 \eta}{2 R V \rho} \frac{1}{(X + Y)} \quad (53)$$

This expression for (f) the friction factor is valid for both plug and streamline flow of a true plastic. It also holds approximately for pseudo plastics and quasi liquids.

Scott-Blair and Crowther (11) carried out an investigation on clay pastes by means of a capillary type viscosimeter. They found definite evidence of several stages of motion which are listed below:

(1) There is no motion until a well defined critical shearing stress is reached at the pipe wall.

(2) In the first stage of motion the suspension moves as a solid plug. The volumetric flow is linearly related to the pressure drop but there are no criteria

for determining the upper velocity limits of plug flow.

(3) As the velocity is increased the clay flows as a central plug with a streamline shell of increasing thickness. This region shows up as a curve on a flow rate - pressure drop graph. There is no way of establishing the upper or lower limits although this is a very definite transition region.

(4) The streamline shell finally fills the whole pipe. The upper limits at which streamline flow will occur are known but not the lower limits. The methods of correlation have not been tested very extensively but only over the range 0 to 20% solids.

The following two stages of motion were noticed by other investigators but will be included here to complete the list:

(5) The fourth stage of motion is that which shows a transition from streamline to turbulent flow. The limits may be predicted but the correlation requires further testing.

(6) The final stage is that of fully developed turbulence. This has a lower limit but no known upper limit. The present correlation of data covers the range from 0 to 30% solids and this should be extended.

In correlating their data, which covered both streamline and plug flow, Scott-Blair and Crowther attempted to use Buckingham's equation as given above (equation (44)). They found it necessary, however, to modify the last term of the equation. The first modifi-

cation was to replace the pressure drop by $(\Delta P - \Delta p)$ where " Δp " is the pressure equivalent of the critical shearing stress required for slip between the wall and the fluid. Secondly, rather than attempt an evaluation of ϵ the thickness of the "lubricating layer" and $\frac{1}{\phi}$ its viscosity they employed graphical methods to find $\frac{\epsilon \phi}{R}$ which they represented by $\epsilon \theta$

Their final equation takes the form

$$V = \frac{R^2 \beta}{8 L \gamma} \left\{ \Delta P - \frac{4}{3} \left(\frac{2 L m}{R} \right) + \frac{1}{3 \Delta P^3} \left(\frac{2 L m}{R} \right)^4 \right\} - \frac{R^2 \beta \epsilon \theta}{2 L} (\Delta P - \Delta p) \quad (54)$$

Equation (54) has the same form as Buckingham's equation and does not permit a separation of the plug flow effect from the streamline flow effect. If equation (46) is extended by substituting for V_R and ΔP in the last term equation (55) results

$$V = \frac{\beta R^2 \Delta P}{8 L \gamma} \left\{ \left[\frac{2}{\Delta P^4} \left(\frac{2 L m}{R} \right)^4 \right] + \left[1 - \frac{4}{3 \Delta P} \left(\frac{2 L m}{R} \right) - \frac{5}{3 \Delta P^4} \left(\frac{2 L m}{R} \right)^4 + \frac{4 \epsilon \theta \gamma}{\Delta P} (\Delta P - \Delta p) \right] \right\} \quad (55)$$

The expression for the friction factor which arises from equation (55) is

$$f = \frac{16 \gamma}{2 R V \rho} \frac{1}{(X + Y)} \quad (56)$$

where Y is redefined as

$$Y = \left[1 - \frac{4}{3 \Delta P} \left(\frac{2 L m}{R} \right) - \frac{5}{3 \Delta P^4} \left(\frac{2 L m}{R} \right)^4 + \frac{4 \epsilon \theta \gamma (\Delta P - \Delta p)}{\Delta P} \right] \quad (57)$$

Scott-Blair and Crowther evaluated several of the quantities graphically as follows:

Stage of flow.

I and II ΔP = pressure equivalent to the critical shearing stress required to initiate motion.

III $\epsilon \theta = \frac{\epsilon \phi}{R} = \frac{L}{R^3} \cdot \text{slope } \frac{dQ}{dP}$

IV $\frac{4}{3}(\frac{2Lm}{R})$ = the intercept of the extrapolated asymptote to Q vs ΔP curve with the pressure axis.

$$\gamma = \frac{R^4}{L} \cdot \frac{1}{\text{slope } \frac{dQ}{dP}}$$

Equations (54) to (57) assume merely that a critical shearing stress must be exceeded at the wall before any motion takes place. This is more general than Buckingham's assumption that a thin envelope layer, behaving as a Newtonian fluid, surrounds the moving plug at wall shearing stresses less than m .

Scott-Blair and Crowther presented data which verified equation (54).

Buckingham has attempted to represent the slip at the wall (V_R) by properties of the carrier fluid. However, V_R is not dependent upon fluid properties alone. The actual resistance to motion may be considered as a frictional force between the pipe wall and the plug. Scott-Blair and Crowther have perhaps obtained a better representation by using their data in graphical plots

to obtain the constants ϵ & θ

McMillen (8) makes use of Bingham's original expression in the form

$$\eta = \frac{(S_w - m)}{\frac{dv}{dr}} \beta \quad (2)$$

In solving of this differential equation McMillen does not make the substitution $r_0 = \frac{2 L m}{P}$. He uses C , the ratio of the plug radius to the pipe radius (i.e. $C = \frac{r_0}{R}$) and X , the ratio of the radius of any layer to the pipe radius (i.e. $X = \frac{r}{R}$) to simplify the solution. This simplification gives rise to the following expressions:

Velocity at any point in the streamline shell

$$V_{R-r_0} = \frac{\beta R m}{\eta} \alpha \quad (58)$$

Velocity of the plug

$$V_p = \frac{\beta R m}{\eta} b \quad (59)$$

Volumetric rate of flow

$$Q = \frac{\beta \pi R^3 m}{\eta} \alpha \quad (60)$$

Average velocity

$$V_{ave} = \frac{\beta R m}{\eta} \alpha \quad (61)$$

Where

$$\alpha = \frac{C^4 - 4C + 3}{12C} \quad (62)$$

$$b = \frac{(1 - c)^2}{2c} \quad (63)$$

$$\delta = \frac{\alpha}{b} \quad (64)$$

$$\eta = \left(\frac{1 - 2c + 2cX - X^2}{2c} \right) \quad (65)$$

Other dimensionless ratios which McMillen found useful are

$$W = \frac{1}{4 c \alpha} \quad (66)$$

$$X_m = c + \frac{4 c (1 - c)^2}{3} \quad (67)$$

$$Z = n_m \left(1 - \frac{c}{X_m} \right) (1 - X_m) \quad (68)$$

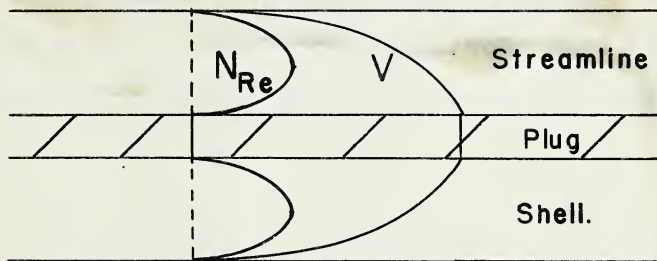
$$Y = \left(1 - \frac{c}{X} \right) \quad (69)$$

$$\text{Reynold's } No = \frac{\beta^2 R^2 m}{\eta^2} \rho n \gamma (1 - X) \quad (70)$$

With these equations McMillen suggests a trial and error method of obtaining m and γ from pressure drop measurements at any two different flow rates. This method is outlined in the appendix.

McMillen does not accept Buckingham's theory that the suspension slips through the pipe as a solid plug. His data which is for a quasi-liquid indicates that the slip at the wall V_R is negligible. He further suggests that a yield value is an entirely fictitious concept and if any stress is applied to a suspension it will deform permanently provided enough time is allowed for the flow to take place. This is equivalent to classifying all suspensions as quasi-liquids.

McMillen points out that it is possible to have plug, streamline, and turbulent flow existing together. McMillen considers that turbulent flow occurs first at the axis of the pipe (i.e. at maximum Reynolds number) and spreads towards the pipe wall. However, for plug flow the apparent viscosity is infinite at the plug boundary, giving a zero value of Reynolds number N_{Re} so that the Reynolds number distribution is as shown below in figure (4)



Velocity- Reynolds Number Distribution.

Fig. 4.

It will be noted that the maximum Reynolds number exists between the plug and the pipe wall. McMillen therefore suggests that there will be a tendency to form a turbulent annulus while there is still a plug core.

SUMMARY AND COMPARISON OF THEORY

The results of the several theoretical approaches may be summarized as follows:

1. Poiseuille's expression for Newtonian fluids in streamline motion results in an expression for the friction factor of

$$f = \frac{16}{2 R V} \frac{\eta}{\rho} \quad (\text{Figure 1, Curve I})$$

2. Bingham's analysis applies to true plastics and approximately, at high rates of shear, to quasi liquids and pseudo plastics. His analysis is for the case where the applied stress exceeds that required for flow. The resultant form of the friction factor is

$$f = \frac{16}{2 R V} \frac{\eta}{\rho} \frac{1}{\left[1 - \frac{4}{3 \Delta P} \left(\frac{2 L m}{R} \right) + \frac{1}{3 \Delta P^2} \left(\frac{2 L m}{R} \right)^2 \right]}$$

(Figure 1, Curves II, III, V)

3. The simplifications made by Babbitt and Caldwell reduce the application of Bingham's equation to an approximation for true plastics or a second approximation for pseudo plastics and quasi-liquids. The friction factor is given by

$$f = \frac{16}{2 R V} \frac{\eta}{\rho} \frac{1}{\left[1 - \frac{4}{3 \Delta P} \left(\frac{2 L m}{R} \right) \right]}$$

(Figure 1, Curves II, III, V)

4. Parent by a different approach has arrived at the same results as Bingham for a true plastic flowing in streamline motion with a plug core.

5. Buckingham has obtained a more general representation of the case of a true plastic by including the wall effect when the applied stress is less than the yield point but greater than the critical stress required to initiate flow. The expression for the friction factor which arises out of his work is given below and applies also as an approximation to quasi-liquids and pseudo-plastics.

$$f = \frac{16\eta}{2RV} \frac{1}{\rho \left[\frac{2}{\Delta P^4} \left(\frac{2Lm}{R} \right)^4 \right] + \left[1 - \frac{4}{3\Delta P} \left(\frac{2Lm}{R} \right) - \frac{5}{3\Delta P^4} \left(\frac{2Lm}{R} \right)^4 + \frac{4\eta}{R} \epsilon \phi \right]}$$

(Figure 1, Curves II, III, V)

6. Scott-Blair and Crowther have altered Buckingham's equation to include the effect of the critical stress required to overcome the friction at the wall. By redefining terms they have avoided the use of a "lubricating layer" to explain the wall effect when only plug flow exists. The expression for the friction factor using their theory is

$$f = \frac{16\eta}{2RV} \frac{1}{\rho \left[\frac{2}{\Delta P^4} \left(\frac{2Lm}{R} \right)^4 \right] + \left[1 - \frac{4}{3\Delta P} \frac{2Lm}{R} - \frac{5}{3\Delta P^4} \left(\frac{2Lm}{R} \right)^4 - \frac{4\eta \epsilon \theta (\Delta P - \Delta p)}{\Delta P} \right]}$$

(Figure 1, Curves II, III, V)

7. McMillen has used Bingham's analysis, together with certain dimensionless ratios which he claims make calculations easier, to investigate plastic flow. His data

indicate that the slip at the wall (V_R) is non-existent which is very convenient since it is so difficult to evaluate. Further the data indicate that the material with which he was working is a quasi-liquid rather than a true plastic. The fact that he was able to correlate his data by means of equations based on the flow of plastic materials indicates that at practical flow rates the assumption of a yield value is justifiable.

The dimensionless ratios, and equations derived by McMillen allow a visualization of the flow process under investigation. They also give a method of calculating Reynolds number at any point in a plastic flowing within a circular pipe.

The material which has been discussed above has been applied largely to those flow rates below the transition from streamline to turbulent. Very little investigation has been reported for turbulent flow of suspensions. The data of Babbitt and Caldwell (2) in an extension of their previous work indicated that for turbulent flow the friction factor (f) may be correlated with $\frac{DV\rho_s}{\mu}$, where ρ_s is the density of the suspension and μ is the viscosity of the carrier liquid, to give lines coinciding with that of the Reynolds friction factor diagram already referred to in (14). They explain the different curves which they get on the basis of the effect of the relative roughness of the pipe used.

It was noted previously that for a Newtonian fluid it is possible to obtain the same expressions for

pressure drop due to friction by dimensional analysis or analytically (Poiseuille's method). The theoretical methods which may be applied to the flow of suspensions have also been discussed. It is of interest to see whether similar expressions may be obtained by dimensional analysis.

Dimensional Analysis

The factors which are expected to influence the flow of a true plastic (and which approximately represent quasi-liquids and pseudo-plastics) (Fig. 1, Curves II, III, V) are listed below:

- R - the radius of the pipe
- Δ - the roughness depth
- L - the length of pipe
- V - the velocity of flow
- ρ - the density of the flowing fluid.
- η - the coefficient of rigidity
- m - the yield value
- β - a proportionality constant
- $-\Delta p$ - the pressure drop.

Assume a power function and let

$$-\Delta p = 2R^a L^b V^c \rho^d \eta^e m^f \beta^g (2R)^h \quad (71)$$

The dimensions of this equation are:

$$\frac{F}{L^2} = L^a L^b \left(\frac{L}{\theta}\right)^c \left(\frac{M}{L^3}\right)^d \left(\frac{M}{L\theta}\right)^e \left(\frac{F}{L^2}\right)^f \left(\frac{M L}{F \theta^2}\right)^g \left(\frac{L}{L}\right)^h \quad (72)$$

For this equation to hold true the following conditions must be satisfied:

$$F = 0 = -1 + f - g \quad (73)$$

$$M = 0 = d + e + g \quad (74)$$

$$L = 0 = 2 + a + b + c - 3d - e - 2f + g \quad (75)$$

$$\theta = 0 = -c - e - 2g \quad (76)$$

Letting b, d, and g be independent variables

then $a = d + g - b$

$$b = b$$

$$c = d - g$$

$$d = d$$

$$e = -d - g$$

$$f = 1 + g$$

$$g = g$$

Substituting in equation (71) gives

$$-\Delta P = 2R^{d+g-b} L b v^{d-g} \rho^d \eta^{-d-g} m^{1+g} \rho^g \left(\frac{\Delta}{2R}\right)^h \quad (77)$$

$$-\Delta P = \left(\frac{2RV}{\eta}\right)^d \left(\frac{2Rm\rho}{V\eta}\right)^{g+1} \left(\frac{L}{2R}\right)^b \left(\frac{\Delta}{2R}\right)^h \frac{V\eta}{2R\rho} \quad (78)$$

It is known that pressure drop is proportional to length

so $b = 1$ then letting ϕ be some unknown function

$$-\Delta P = \frac{V\eta}{2R\rho} \frac{L}{2R} \phi \left\{ \frac{2RV}{\eta}, \frac{\Delta}{2R}, \frac{2Rm\rho}{V\eta} \right\} \quad (79)$$

however by convention $-\Delta P = \frac{V^2 \rho L}{2 R \rho} 2f \quad (17)$

$$\text{so } \frac{V^2 \rho L}{2 R \rho} 2f = \frac{LV\eta}{(2R)^2 \rho} \phi \left\{ \frac{2RV}{\eta}, \frac{\Delta}{2R}, \frac{2Rm\rho}{V\eta} \right\} \quad (80)$$

$$\text{or } f = \frac{\eta}{2RV\rho} \phi \left\{ \frac{2RV}{\eta}, \frac{\Delta}{2R}, \frac{2Rm\rho}{V\eta} \right\} \quad (80a)$$

$$\text{finally } f = \phi \left\{ \frac{2RV}{\eta}, \frac{\Delta}{2R}, \frac{2Rm\rho}{V\eta} \right\} \quad (81)$$

Equation (81) suggests possible means of correlating the friction factor. However since it is based on a power function and the theoretical derivations indicate series functions its usefulness is questionable. A second point to be noted is that equation (81) does not contain the pressure drop implicitly and if it could be used would eliminate much "trial and error" calculation. This does not simplify the problem, however, since there is still the matter of the unknown function term in equation (81).

The results of the theoretical work indicate that a certain amount of "trial and error" calculation is to be expected in estimating the friction factor since the pressure drop, which depends on the friction factor, must be chosen first, then the friction factor calculated and finally the pressure drop checked. For this reason it is believed that the simplest method of obtaining a first approximation of the friction factor should be used. The methods of Buckingham and Scott-Blair and Crowther, while giving accurate results, appear rather complex for industrial use. Babbitt and Caldwell present the simplest method but as Parent pointed out it is inaccurate.

For the streamline region Parent's method of pressure drop estimation gives reliable results and the method of Babbitt and Caldwell may be used where extreme accuracy is not required. McMillen's dimensionless ratios give a picture of local conditions at a point within the pipe. They simplify the calculation of the properties

of the suspension from flow data. The method of Babbitt and Caldwell for the turbulent region is at present the only one available.

It would appear then that it is possible to use the current methods of pressure drop estimation for liquids combined with the proper rheological properties to design pipe lines for handling solid suspensions. However, the published data are rather scarce, covering only a limited range of solids concentration and the following question remains to be answered: Are the present methods of pressure drop calculation applicable over wide ranges of solids concentration and for all rates of flow? It is with this question in mind that the present investigation is being carried out.

Viscosimetry

The theoretical discussion has indicated that the rheological properties of plastic which must be determined in order to evaluate the flow characteristics are the yield value and the coefficient of rigidity. These in turn may be obtained by measuring the rate of shear at different shearing stresses. Of the many devices which are used to measure rheological properties three general types appear to be readily applicable to the measurement of rate of shear and shearing stress. These are:

1. The type of instrument making use of flow through a capillary tube.
2. The instrument which causes the tangential

displacement of two cylinders or plates immersed in the material being tested.

3. The torque type of instrument which measures the torque exerted on one cylinder by the rotation of a second cylinder about their common axis when the space between the two is filled with the material being tested.

A capillary tube viscosimeter proves unsatisfactory for the measurement of the rheological properties of a suspension due to the tendency of the solid particles to plug the bore if a high percentage of solids is present. If the percentage of solids is low enough to prevent plugging there will be a tendency to settle out. A further point, which is not a defect but which complicates the use of a capillary, is the necessity of applying kinetic energy corrections for the end effects, and correcting for any change in temperature which may arise from these kinetic effects.

Any viscosimeter employing the tangential displacement of cylinders or plates is not suited for materials containing water since the surface tension, being so great in relation to the viscosity, completely masks the effect of the latter. A second and very serious disadvantage of this type of instrument is that the relationship between plate *displacement* and shearing stress is not linear even for a Newtonian fluid.

The torque type of instrument has none of the above mentioned defects to any appreciable extent so it

is to be recommended for the measurement of the rheological properties of a suspension. The final choice is between two subtypes of this class, the MacMichael and the Stormer.

The MacMichael Viscosimeter

The MacMichael viscosimeter consists of two concentric cylinders. The outer cylinder is rotated at a fixed rate of speed and holds the sample being tested. The inner cylinder is solid and is suspended by means of a torque wire so as to be almost completely immersed in the sample. A pointer and scale are used in conjunction with the torque wire to indicate the deflection of the inner cylinder. This viscosimeter requires calibration to establish the relationships between shearing stress and the viscosity or coefficient of rigidity and the observed^{rv} deflection and relative rotation between the cylinders. This instrument requires great care in use to prevent overrange of the torque wire. For this reason it is not commonly used in industry.

The Stormer Viscosimeter.

In the Stormer viscosimeter the outer cylinder is fixed. The inner cylinder is hollow and rotates about a baffle attached to the bottom of the outer cylinder. A thermometer well is also attached to the outer cylinder or cup. The inner cylinder or rotor is supported from above by means of a shaft which is geared to a small drum. Weights are attached to a cord which is wound round the

drum. The weights, when allowed to fall, impart a rotation to both drum and rotor. The revolutions of the rotor are indicated by means of a counter attached to the top of the rotor shaft.

The shearing stress is readily obtainable from the applied weights but the viscosity and coefficient of rigidity are only obtainable by calibration. The mechanism of this instrument is much more rugged than the MacMichael and for this reason it is preferred by industrial users even though the latter instrument will measure lower shearing stresses.

A Stormer viscosimeter (Fig.7) was used in this study since:

- (a) A Stormer viscosimeter was readily available;
- (b) It is the type which most industrial establishments could be expected to have;
- (c) A preliminary calibration indicated that it could be used over the range of results expected.

A Mathematical Analysis of the Stormer Viscosimeter

The torque applied to the rotor of the viscosimeter is given by

$$T = \frac{A}{R} r w \quad (82)$$

where T = torque

A = radius of small gear of load transmission system

R = radius of large gear of load transmission system

r = radius of line drum

w = load applied to line.

If the applied torque gives rise to a stress S at the wall of the rotor then this torque and stress are related by $T = 2 \pi A S l A$ (83)

where A = the radius of the rotor

l = the length of the rotor.

Since both the inside and outside of the rotor are acting to produce a stress, then the torque at the rotor wall is given by

$$T_1 = 2 \pi l S (A_1^2 + A_2^2) \quad (84)$$

where A_1 = outside radius

A_2 = inside radius.

On the underside of the rotor the shearing stress on an element a distance "a" from the centre is given by

$$S \frac{a}{A_1} \quad (85)$$

The area of this element is $2 \pi a d a$ (86)

so the shearing force is $2 \pi a^2 \frac{S}{A_1} d a$ (87)

The total torque on the bottom of the rotor is then

$$T_2 = \int_0^{A_1} \frac{2 \pi S a^3 d a}{A_1} \quad (88)$$

$$\text{or } T_2 = \frac{2 \pi S}{A_1} \int_0^{A_1} a^3 d a \quad (88)$$

$$= \frac{\pi S A_1^3}{2} \quad (89)$$

The total torque on the rotor is then

$$T = \frac{A}{R} r w = S \left[2 \pi l (A_1^2 + A_2^2) + \frac{1}{2} \pi A_1^3 \right] \quad (90)$$

$$\text{or } S = \frac{A r w}{R \left[2 \pi l (A_1^2 + A_2^2) + \frac{1}{2} \pi A_1^3 \right]} \quad (91)$$

For the particular viscosimeter used

$$S = 0.0021 \frac{w^2}{\lambda}$$

where S = shearing stress in lb s/ft²

w = load in grams.

To obtain the yield value of the material being tested substitute the load at zero rate of shear for w . This analysis assumes that the mechanical friction of the instrument is negligible.

The relationship between viscosity, rate of shear and shearing stress of a Newtonian fluid in stream-line motion is shown in Fig. 1 (page 3). The equation giving this relationship is

$$S = \frac{\mu}{\beta} \frac{dv}{dx} \quad (1)$$

which for a circular pipe becomes

$$S = \frac{\mu}{\beta} \frac{dv}{dr} \quad (92)$$

A similar relationship is noticed for Storrer viscosimeter as shown in the figure below:

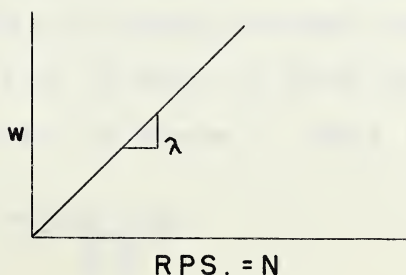


Fig. 5

w = the load

N = the revolutions per second

λ = the slope of the line.

The equation giving the relationship is

$$w = \lambda N \quad (93)$$

$$\text{Now } N \propto \frac{d v}{d r}$$

$$\text{so let } N = k_1 \frac{d v}{d r} \quad (94)$$

Also $w \propto S$

$$\text{so let } w = k_2 S \quad (95)$$

$$S = \frac{\lambda}{k_2} k_1 \frac{d v}{d r} \quad (96)$$

Equating this to equation (92) results in

$$\frac{\mu}{\beta} \frac{d v}{d r} = \lambda \frac{k_1}{k_2} \frac{d v}{d r} \quad (97)$$

$$\text{or } \mu = \lambda K \quad (98)$$

Since K for the instrument appears to be a function of $\frac{d v}{d r}$ a graph of viscosity (μ) vs slope ($\lambda = \frac{\text{load}}{\text{RPS}}$) may be obtained by a preliminary calibration of the viscosimeter.

The relationship between coefficient of rigidity, shear and rate of shear is given by equation (2) and is illustrated in Figure 1 (page 3)

$$\eta = \frac{\beta (S - m)}{\frac{d v}{d r}} \quad (2)$$

For a circular pipe this becomes

$$S - m = \frac{\eta}{\beta} \frac{d v}{d r} \quad (99)$$

The corresponding relationship for a Stormer viscosimeter is shown in Figure 6 below

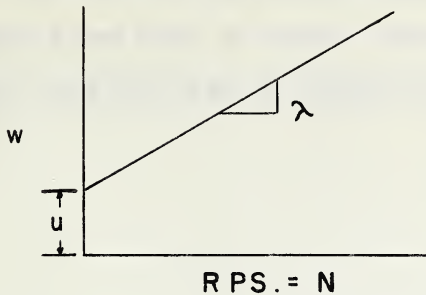


Fig. 6

The resulting equation is

$$(w - u) = \lambda(N) \quad (100)$$

which since

$$N \propto \frac{d v}{d r} = k, \quad \frac{d v}{d r} \quad (101)$$

becomes

$$(w - u) = k, \lambda \frac{d v}{d r} \quad (102)$$

$$\text{but } w = k_2 S \quad (103)$$

$$\text{and } u = k_2 m \quad (104)$$

$$\text{so } w - u = (k_2 S - k_2 m) \quad (105)$$

$$= k_2 (S - m) \quad (106)$$

Substituting equation (106) in equation (102) results in

$$(S - m) = \frac{k_1}{k_2} \lambda \frac{d v}{d r} \quad (107)$$

Equating this to equation (99) gives

$$\frac{k_1}{k_2} \lambda \frac{d v}{d r} = \frac{\eta}{\beta} \frac{d v}{d r} \quad (108)$$

or $\eta = \lambda K$

Therefore the calibration chart for the instrument obtained from data on known viscosities may be interpreted to give coefficients of rigidity.



Fig. 7. Stormer Viscosimeter.

3 Experimental Equipment.

The experimental equipment may be considered under two general headings;

1. Apparatus used to determine the suspension properties.

2. The flow circuit.

Suspension properties;

The equipment used to obtain the density, percent solids and viscosimeter data is largely standard laboratory equipment and a list is given below;

1. 1000ml graduate cylinder.
2. 9"x 7"x 2" enamel pan.
3. Cenco Type B. drying oven.
4. Standard 0-100°C Thermometer.
5. Cenco triple beam balance.
6. Elgin Stopwatch reading in 1/10 of seconds.
7. Stormer viscosimeter.

The Stormer viscosimeter has been described previously (page 38) and a photograph of it is given on page 42 (Fig. 7).

The Flow Circuit:

The flow circuit (Fig. 8 page 44) consists of several distinct units. These are:

1. The supply tank.
2. The pump and motor.
3. The test sections.
4. The weighing tank and scales.
5. The pressure taps and sight glasses.
6. The manometers.
7. The controls.

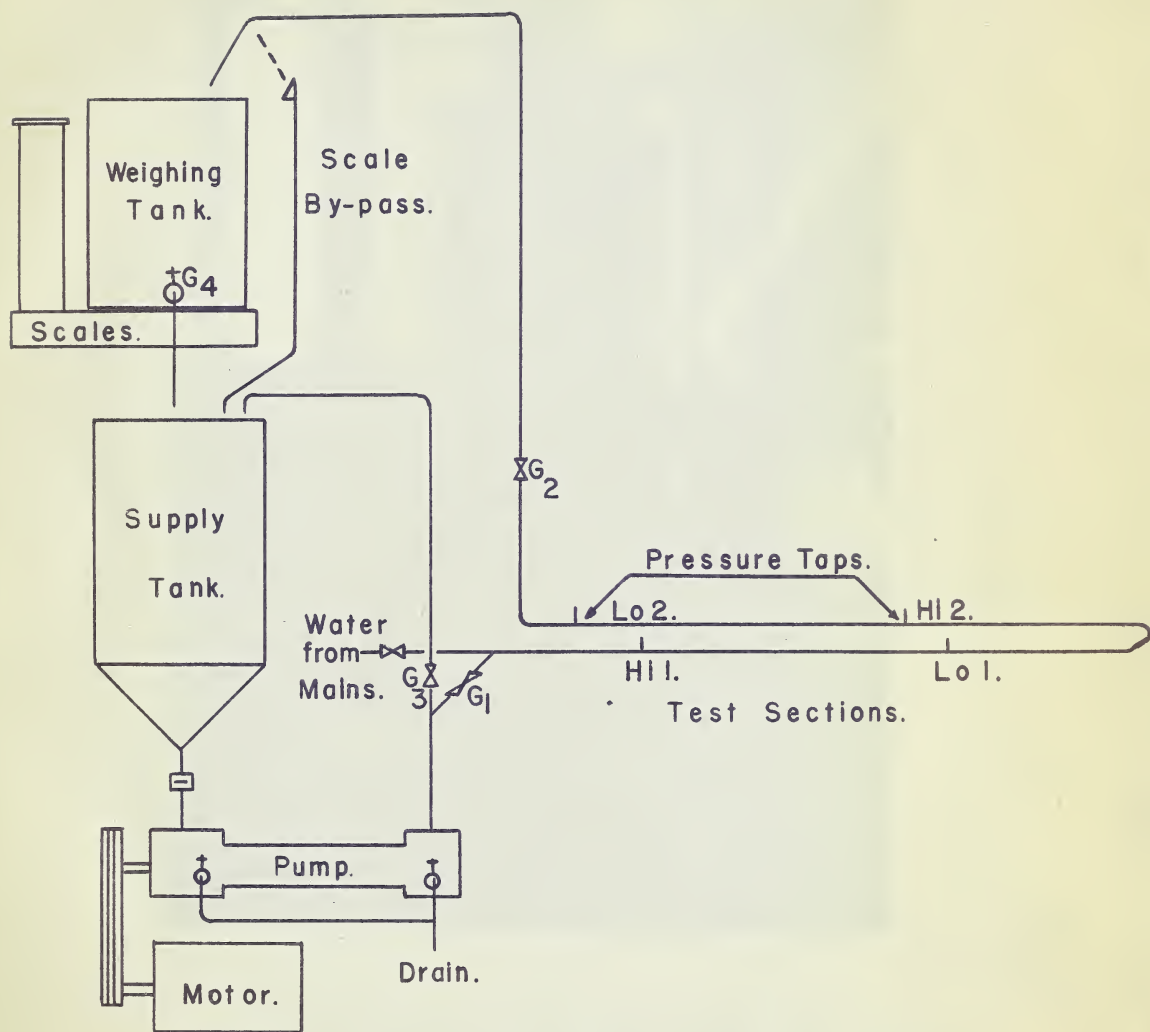


Fig. 8. Flow Circuit.



Fig. 9. Supply tank, Pump and Motor.

A detailed description of these units is given below.

The Supply Tank.

The supply tank (Figs. 8,9) is constructed of 18 gauge galvanized iron, welded to form a cylinder 3' long by 2' in diameter with a conical bottom. The inside of the tank is coated with asphalt to protect it against corrosion. A light frame of 1" angle iron serves to support the tank directly above the inlet of the pump. In order that the tank may be removed for repairs when necessary, a union is attached to the bottom. A Tee is inserted between the union and the pump in order that a by-pass may be placed across the pump at some future date.

The Pump and Motor.

A Moyno positive displacement pump (Fig.9) is used to circulate the slurry. To effect the positive displacement this pump employs a steel screw rotating at 770 RPM. within a rubber lined shell. At this speed the rated performance is 35 gpm. against a pressure of 75psi. The pump is driven by means of a 5 HP, 3 phase, 220 volt, electric motor, the two being connected by Vee belts.

The Test Sections.

The test sections consist of two 40' lengths of hard drawn copper tube, 0.786" and 1.277" actual inside diameter, and $\frac{3}{4}$ " and $1\frac{1}{4}$ " nominal outside diameter. They are supported on angle iron brackets

in such a manner as to parallel the building wall and be sufficiently far from it to allow insulation to be applied to the tubes if necessary. One end of each tube is connected by appropriate fittings so as to form a return bend. A Tee in this bend serves as a thermometer well when needed. The other end of the $\frac{1}{2}$ " tube is connected to a Tee which allows either water from the mains, or suspension from the pump outlet, to be run through the test sections. The $1\frac{1}{4}$ " tube is connected to a vertical pipe which leads to the weighing tank directly above the supply tank. An end view of the test sections is shown in Fig.10 page 48.

Note: Special care was exercised in joining the supplied 12' lengths of copper tube to insure that the whole 40' would be as smooth as possible. The lengths were cut so that only one joint would fall within the section over which the pressure drop was to be measured. Test joints were made and cut open to determine what procedure resulted in the smoothest joint. A photograph of one of these is shown in Figure 11.

Scales and Weighing Tank.

A set of Fairbanks Scales, capacity 500 lbs. and graduated in half pounds, weighs the discharge of each run. The weighing tank is an oil drum with one end removed and a gate valve (G4) set into the other end to allow the tank to be emptied. The scales and

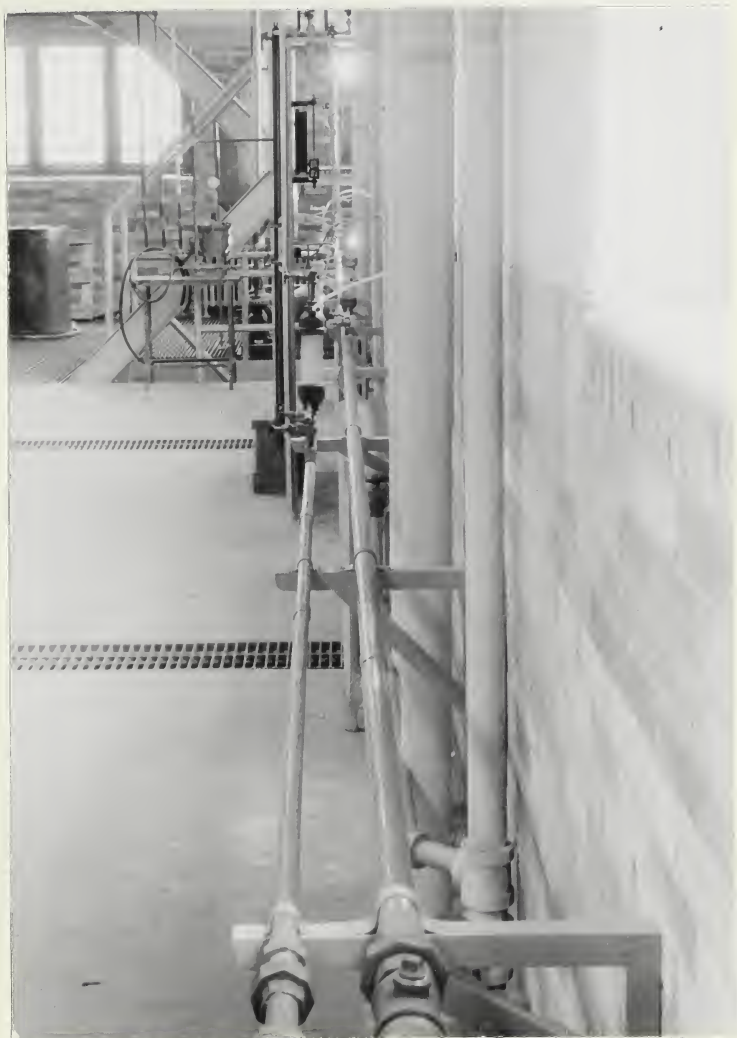


Fig. 10. End View of Test Sections.



Fig. 11. Cross Section of Pipe Joint.

tank are so positioned as to allow the slurry to run from the weighing to the supply tanks by gravity flow. A 3" pipe at the side of the scales acts as a by-pass when the tank is being emptied. A photograph of this setup is given in Figure 12, ^{page} 51.

The Pressure Taps and Sight Glasses.

Pressure taps and sight glasses are located 11.5' and 31.5' from the inlet of the $\frac{3}{4}$ " tube and 17' and 37' from the inlet of the $1\frac{1}{4}$ " tube. (The calculated required calming lengths are 9.16' and 14.8' respectively.) The actual construction of these is best described by means of a diagram. A sketch of a pressure tap cross section is shown in Figure 14 and a photograph of both a pressure tap and a sight glass is given in Figure 13. The plastic line from the upper side of the sight glass leads to the manometer board. The two taps are for the purpose of flushing and deaerating the equipment and adjusting the slurry level in the sight glass.

The Manometers.

Two 5' double cleanout Meriam manometers are used to measure pressures. They are connected to the sight glasses with $\frac{1}{4}$ " plastic tubing, the arrangement of these pressure leads is shown in Figure 15 page 54. One of the manometers is used in the upright position with fluids heavier than water. The other is inverted for use with fluids lighter than water. (Figure 16) Two

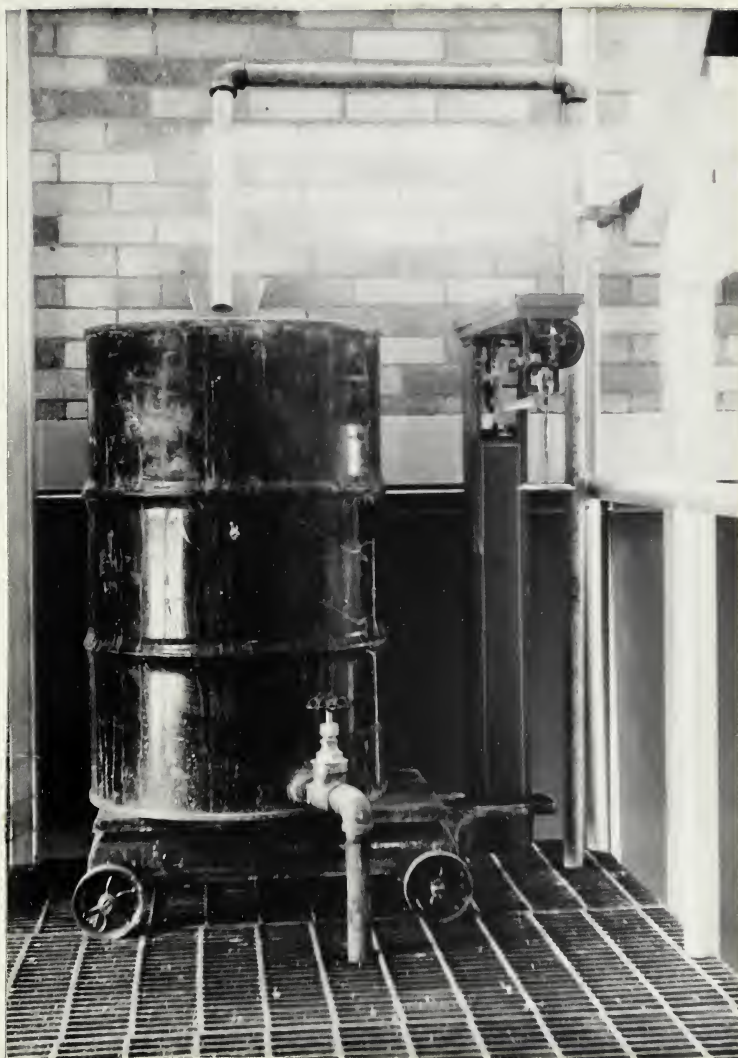
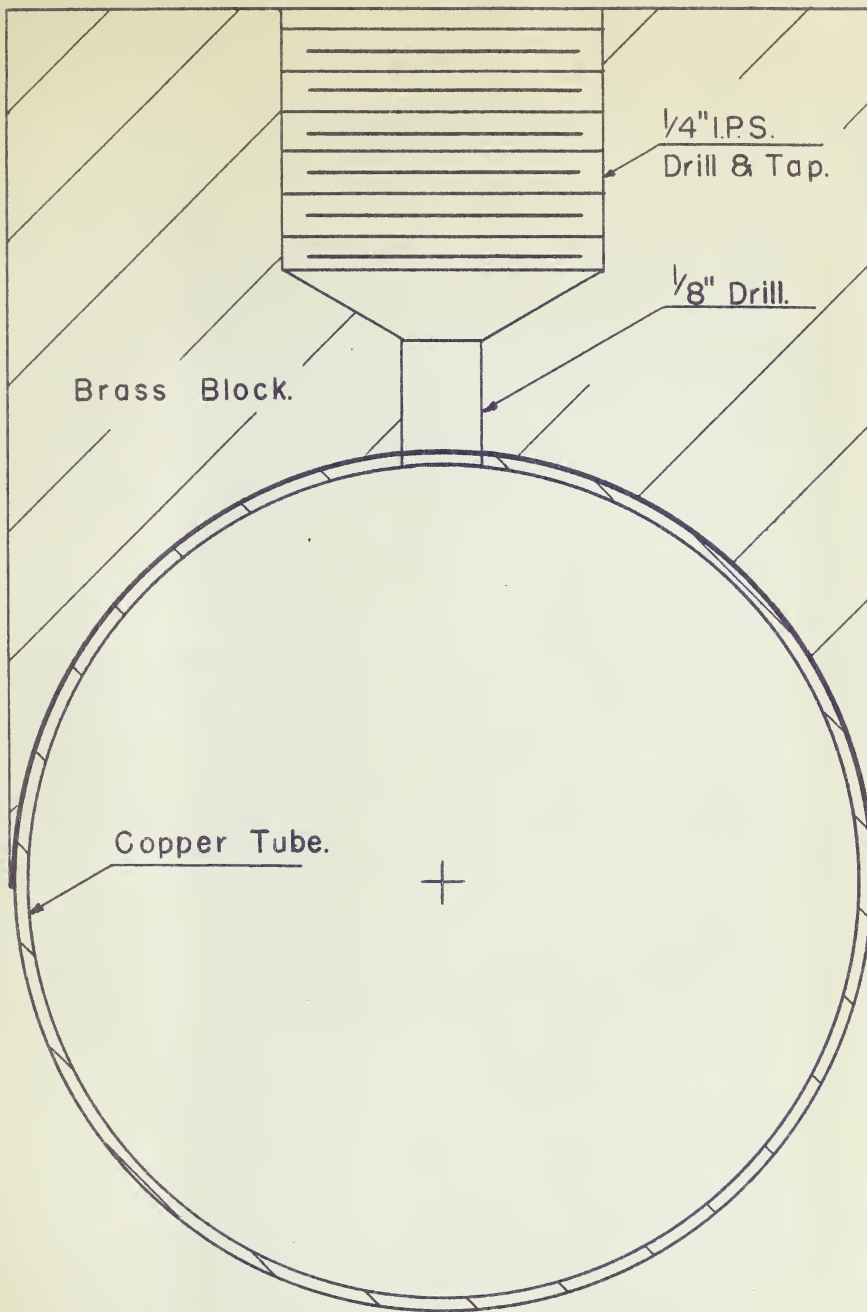


Fig. 12. Scales and Weighing Tank



Fig. 13. Pressure Tap and Sight Glass.



Brass to copper joint soft soldered.

Fig. 14. Cross Section of a
Pressure Tap.



Fig. 15 Pressure Connections.



Fig. 16. Manometers.

traps are inserted in the pressure leads just before they connect to the upright manometer to prevent any mercury from being blown out of the manometer into the copper tubes. These traps also serve as manifolds to catch any air which may collect in the manometer lines, and to admit flushing water to the system.

The six manometer fluids used are listed below with their approximate effective specific gravities. These fluids in the 5' manometers allow a pressure measurement range of 10^{-4} to 750 inches of water.

Manometer Fluid	Effective Sp.G.	
1. Carbon <u>tetrachloride-Turpentine</u>	0.010	Lighter
Water		than
2. <u>Air</u>	1.00	water.
Water		
3. <u>Water</u>	0.10	Heavier
Carbon tetrachloride-Turpentine		than
4. <u>Water</u>	12.53	water.
Mercury		
5. <u>Carbon tetrachloride-Turpentine</u>	0.10	Lighter
H ₂ O		than
6. <u>Carbon tetrachloride-Turpentine</u>	0.050	water.
H ₂ O		

Calibration charts for numbers 1,3, 5 and 6 are given on pages 73, 74, 75, and 76

Control.

Two control valves are in the flow circuit. A coarse control of the flow rate is obtained by means of a gate valve in the by-pass from the pump to the supply tank (G₃ Fig.8). The fine adjustments of flow control are made possible by a diaphragm valve inserted

in the vertical line leading from the $1\frac{1}{4}$ " tube to the weighing tank. This valve (G_2 Fig.8) is operated by remote control from the manometer panel.

To obtain this remote control a Selsyn motor is mounted on the diaphragm valve. A second Selsyn motor is mounted on the panel board with a small handle attached to its rotor. The two rotors are loaded with 20 volt 60 cycle single phase electricity. The motor stators are connected by three strand signal cable. Operation of the Selsyn mounted on the manometer board causes the rotor of the other Selsyn to open or close the diaphragm valve.

IV. Experimental Procedure.

Suspension Properties:

The experimental procedures followed in obtaining the properties of the suspensions (i.e. density, percent solids, and viscosimeter data,) are detailed below:

Density:

To determine the density of the suspension a tared graduated flask or cylinder was filled exactly to the one litre mark with slurry and the weight noted. The net weight in kilograms was then taken as the density of the suspension (in Metric units).

Percent Solids:

To find the percent of solids in the slurry a tared pan was partly filled with a sample of the suspension and the weight noted. The pan was then placed in a drier at 100°C. and weighed periodically, until constant weight was attained. The final net weight, after drying, divided by the original net weight times 100% was used as the percent solids.

Shearing stress-rate of shear:

A standard Stormer Viscosimeter (Fig. 7, page 42) was employed to obtain shearing stress-rate of shear data. The time required for one hundred revolutions of the rotor was noted for each of at least five different loads. The loads used were selected so as to give data in the streamline flow region.

Pipeline Measurements:

The procedures used in securing data on suspensions and on water differ slightly. The methods for handling suspensions will be described first and the simplification possible when water is the fluid will be mentioned later.

It was necessary to soak the clay being used for some time previous to the start of the set of experiments. This was done by filling an empty oil drum half full of water and adding clay until the drum was nearly full. This stock was added to the supply tank as required, to bring up the solids concentration of the suspension.

Circulation:

The by-pass from the pump (G_3 Fig. 8, Page 44) to the supply tank was always examined at the start of each run to insure that it was open. After this was checked the pump was started and the suspension allowed to circulate between the supply tank and the pump for a period of at least ten minutes. During this time, any solids required to adjust the composition of the suspension were added to the supply tank. When the composition had been adjusted the gate valve (G_1 Fig. 8) which isolates the pipeline from the pump was opened. Following this the discharge valve (G_2 Fig. 8) was opened allowing the suspension to flow through the pipeline. Circulation under "wide open" conditions was continued for ten minutes. It was necessary to rinse out the weighing tank to insure that

any material from previous runs was removed.

Suspension properties:

When circulation had continued long enough to thoroughly agitate and mix the suspension, samples were removed for the determination of the properties of the suspensions as described previously.

Deaeration of lines:

When the above preliminary data had been secured the pressure taps and manometer lines were de-aerated in preparation for the pressure drop-flow rate measurements. The gate valves below the sight glasses (Fig.13, page 52) were opened to allow any air trapped under them to rise into the lines. A small volume of suspension was allowed to flow out at the same time in order to clear the pressure taps of any material from the previous run. The gate valves were then closed and water admitted to the high pressure side of the manometers by means of a line connected to the mercury trap (Fig.15, page 54). All of the high pressure lines were then flushed clear of air and suspension by opening needle valves on the appropriate sight glass. With the high pressure side flushed and closed off the water was turned on to the low pressure lines and the process repeated.

Note, The low pressure side should never be open at the same time as the high pressure side. Finally with the water shut off the gate valves below the sight glasses were re-opened and slurry admitted to the glasses until it filled

them to the level line marked on each.

Flow rate -pressure drop-measurements:

When the lines had been completely flushed out the flow through the pipeline was cut back to zero and if any pressure difference was noted on the manometers it was recorded. Then the discharge valve was gradually opened until a very small flow was definitely established. When this flow had continued long enough to allow the manometers to attain equilibrium, the flow rate and pressure drop over both test sections were recorded.

The lower flow rates were measured by noting the time required to collect a definite volume in a graduated cylinder. The higher flow rates were gauged by recording the time required to collect a definite weight of the suspension. The pressure drops across the test sections were obtained by connecting the test sections to a manometer filled with a liquid of appropriate density. The differences in level of the two arms of the manometer were recorded in hundredths of an inch.

After each set of readings had been taken the discharge valve was opened slightly to increase the flow. The level of the slurry in the glasses was brought back to the mark and time allowed for the manometers to come to equilibrium before the next readings were taken. The temperatures of the suspension and of the manometer liquids were recorded at each flow rate. Periodically samples were withdrawn to check the density.

Shut down of equipment:

At the conclusion of the run the isolation gate valve (G₁ Fig. 8 page 44) was closed and water from the mains was admitted to the pipes to flush all of the suspension into the supply tank. Finally the pump was shut off and the whole apparatus washed to remove any caked slurry.

Water runs:

When water alone was being used in the apparatus it was not necessary to determine the density every few runs since it could be readily obtained from tables once the temperature was known. Further the water was used directly from the mains, excepting at the very high flow rates, and this eliminated the use of the pump to a considerable extent.

V EXPERIMENTAL DATA.

The following section presents the experimental data. Table 1 lists calibration data for the viscosimeter. A Westphal balance was used to obtain the specific gravities of the calibration fluids (glycerol-water mixtures). The viscosities could then be obtained from handbooks (5). Table 2 lists data from a preliminary study of the clay being used in this investigation. In table 3 are listed the effective specific gravities of the manometer fluids. The specific gravity of the fluids was measured by means of a Westphal balance. The effective specific gravity was then taken as the difference in gravities between the fluid and water at the same temperature. The density of water may be obtained from a handbook (5). Table 4 gives the properties of the slurries which were pumped through the pipe circuit. Supplementary data pertaining to the pipeline and the viscosimeter are given in table 5.

The flow data are presented in tables 6 to 17.

The viscosimeter calibration data are presented graphically in Figures (17) and (18). Figures (19) and (20) are the final calibration charts constructed from figures (17) and (18). The manometer fluid calibrations are presented in Figures (21) to (24) to allow interpolation of the calibration data. Figures (25) and (26) present the viscosimeter data on the suspensions encountered in this investigation.

V EXPERIMENTAL DATATABLE IStormer Viscosimeter Calibration

Water at 20.6°C		Slope 4.47				gm sec/R
Load (gms)	10	15	20	25	30	
Time for 100 revs.*	23.5	23.0	21.6	17.7	14.4	
RPM	137	212	278	339	390	
Glycerol-H ₂ O 20°C		Slope 5.82				gm sec/R
Load (gms)	10	15	20	25	30	
Time for 100 revs.*	40.3	36.7	29.7	24.0	20.5	
RPM	99.5	135.5	206	250	293	
Glycerol H ₂ O 20°C		Slope 5.13				gm sec/R
Load (gms)	10	15	20	25	30	
Time for 100 revs.*	37.7	34.5	32.2	32.7	27.6	24.1
RPM	69	110	146	184	211	249
Glycerol H ₂ O 20°C		Slope 4.28				gm sec/R
Load (gms)	10	15	20	25	30	
Time for 100 revs.*	72.6	48.6	36.5	29.3	24.7	
RPM	72.4	124	165	205	232	
Glycerol H ₂ O 20°C		Slope 9.175				gm sec/R
Load (gms) ²	10	15	20	25	30	35
Time for 100 revs.*	100.6	82.0	75.3	68.3	62.1	57.2
RPM	59.5	97	131	163	193	221
Glycerol H ₂ O 20°C		Slope 24.4				gm sec/R
Load (gms) ²	20	30	40	50	60	70
Time for 100 revs.*	125.3	82.8	61.2	49.5	41.1	34.0
RPM	47.8	72.5	98	122	146	172
Load (gms)		80	90	100	110	120
Time for 100 revs.*	30.6	27.3	24.8	22.6	20.7	17.9
RPM	196	220	242	266	290	353
Glycerol H ₂ O 20°C		Slope 11.9				gm sec/Rev
Load (gms)	10	20	30	40	50	
Time for 100 revs.*	131.9	58.9	29.8	30.2	24.5	
RPM	45.5	102	151	198	245	

* Average time for 3 trials in seconds.

TABLE I CONTINUED

Sterner Viscometer Calibration

Glycerol H ₂ O 20°C	73.6	Centipoise.	Slope 30.7	gm.sec/R			
Load (gms) ^c	50	75	100	125	150	175	200
Time for 100revs.*	59.5	40.1	30.5	21.1	20.5	18.1	15.9
RPM	101	150	197	239	293	332	378

Glycerol H ₂ O 20°C	271.6	Centipoise.	Slope 65.8	gm sec/R					
Load (gms) ^c	150	200	250	300	350	400	450	500	600
Time for 100revs.*	63.2	48.0	37.5	31.0	26.5	23.4	20.8	18.9	15.6
RPM	95	125	160	194	226	256	288	317	385

Glycerol H ₂ O 20°C	138.5	Centipoise.	Slope 48.5	gm sec/R			
Load (gms) ^c	100	150	200	250	300	350	400
Time for 100revs.*	48.1	32.1	24.4	19.6	18.0	16.5	15.0
RPM	175	187	246	306	314	373	432

Water 0°C	1.792	Centipoise.	Slope 4.92	gm sec/R			
Load (gms)	10	12	15	17	20	25	30
Time for 100revs.*	52.6	42.5	32.5	28.5	24.5	20.5	16.5
RPS	1.91	2.35	3.08	3.5	4.08	4.88	5.76

Water 20.2°C	1.00	Centipoise.	Slope 4.2	gm sec/R			
Load (gms)	10	12	15	17	20	25	30
Time for 100revs.*	43.0	35.2	27.5	24.4	20.9	17.4	14.0
RPS	2.32	2.84	3.62	4.1	4.78	5.72	6.86

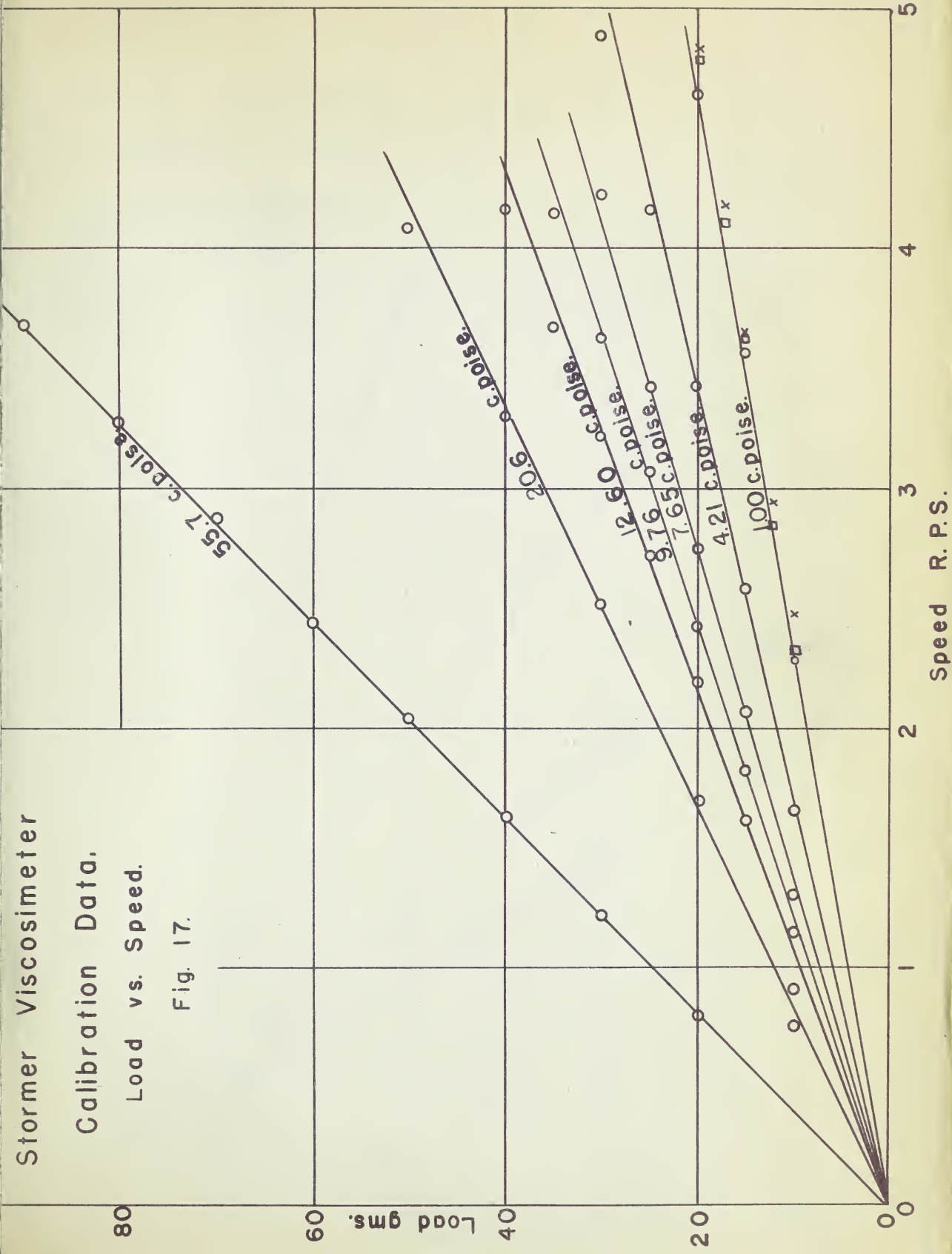
Glycerol H ₂ O 20°C	1.469	Centipoise.	Slope 4.43	gm sec/R			
Load (gms)	10	12	15	17	20	25	30
Time for 100revs.*	47.9	36.8	29.0	25.8	22.3	18.8	15.3
RPS	2.07	2.72	3.45	3.87	4.48	5.31	6.21

Glycerol H ₂ O 20°C	3.273	Centipoise.	Slope 5.29	gm sec/R			
Load (gms)	10	12	15	17	20	25	30
Time for 100revs.*	56.6	47.7	34.8	31.0	26.8	22.6	18.4
RPS	1.77	2.24	2.88	3.22	3.73	4.42	5.16

Glycerol H ₂ O 20°C	3.996	Centipoise.	Slope 5.46	gm sec/R			
Load (gms)	10	15	20	25	30	35	40
Time for 100 revs.*	61.5	36.6	27.8	22.9	19.8	16.7	13.6
RPS	1.62	2.74	3.60	4.56	5.56	6.59	7.64

Water at 20.2 C	1	Centipoise.	Slope 4.14	gm sec/R			
Load (gms)	10	12	15	17	20	25	30
Time for 100revs.*	40.5	34.0	27.5	23.9	20.7	17.4	14.1
RPS	2.47	2.94	3.64	4.18	4.83	5.72	6.74

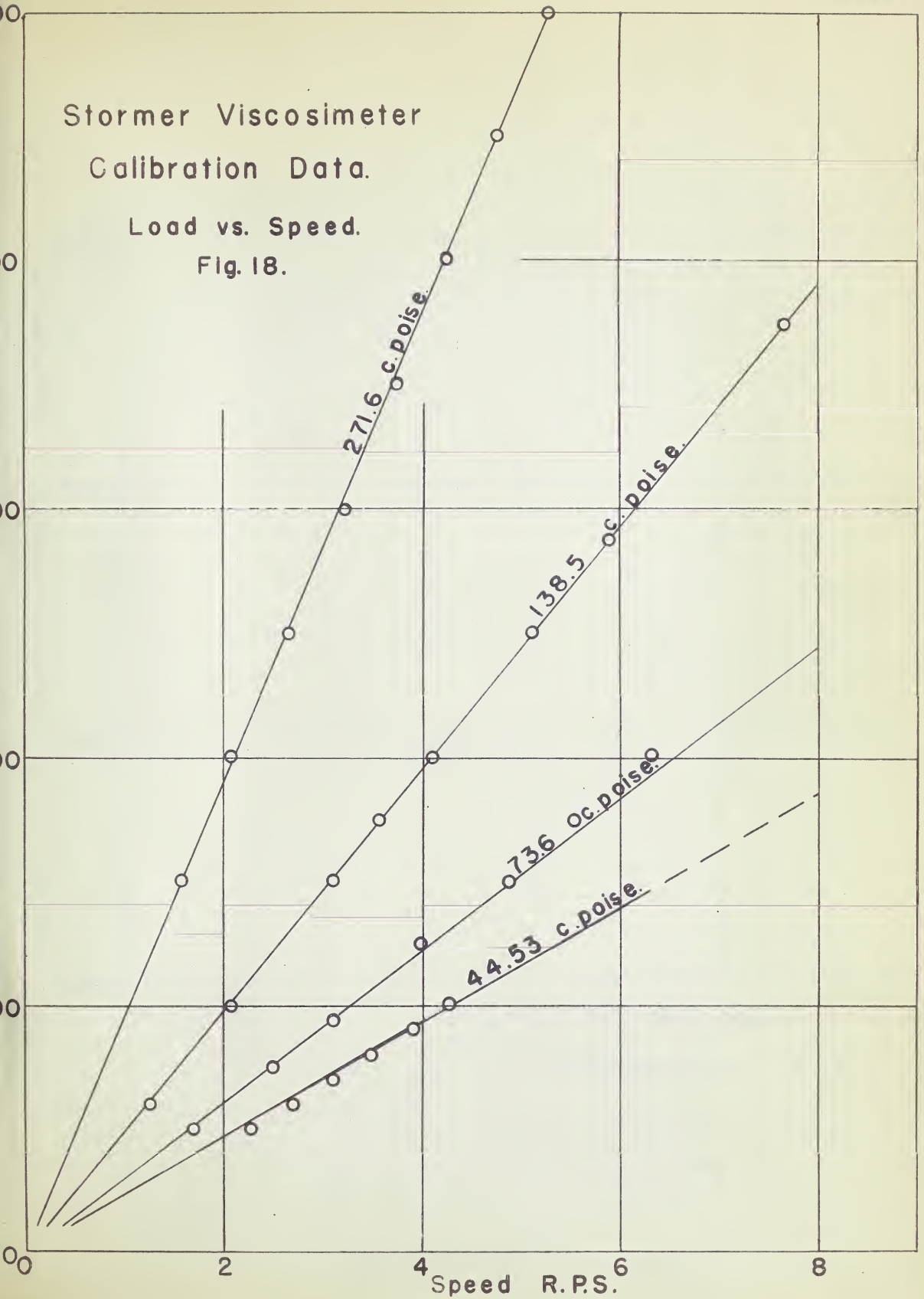
*Average time for 3 trials in Seconds

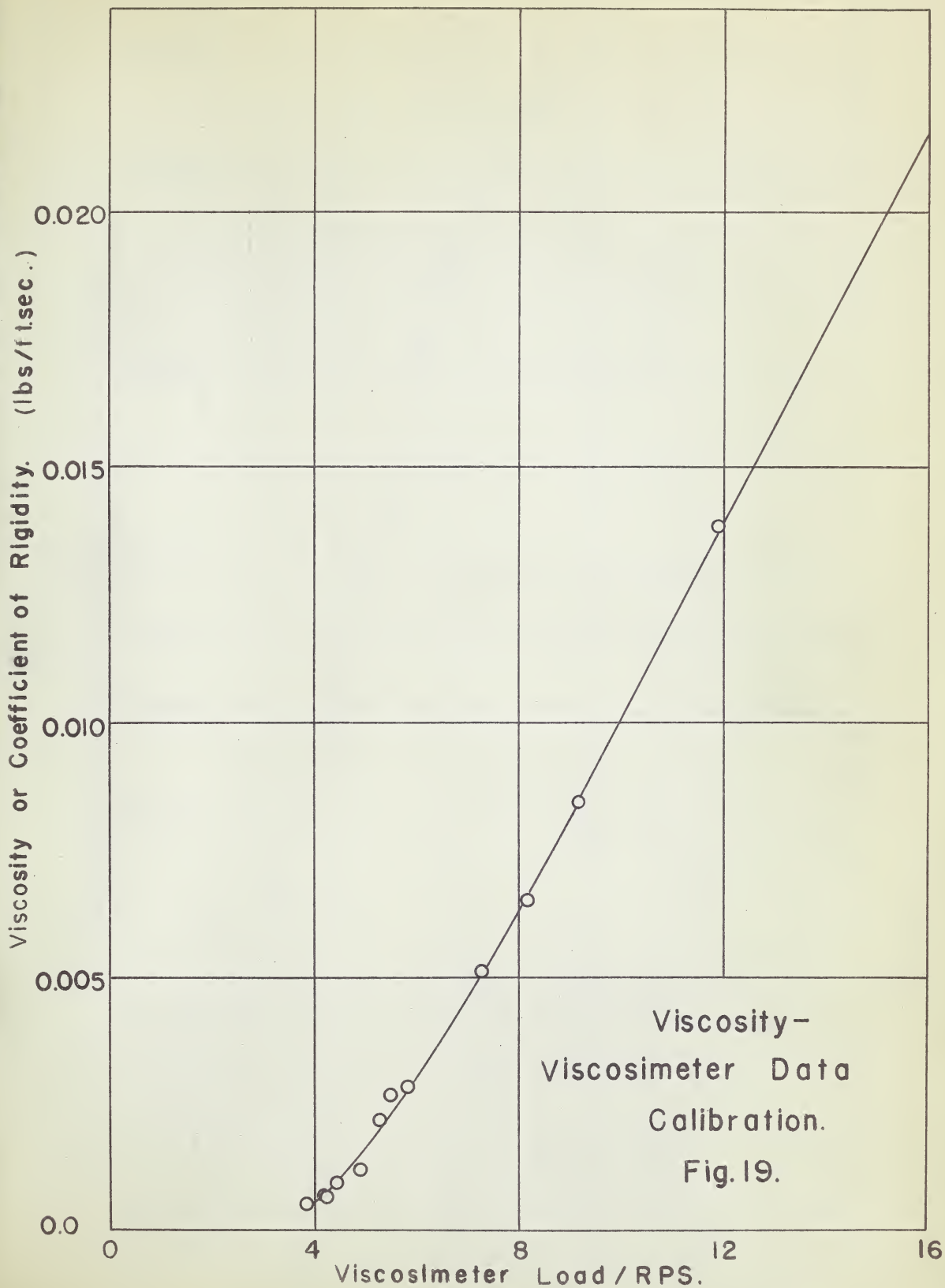


Stormer Viscosimeter Calibration Data.

Load vs. Speed.

Fig. 18.





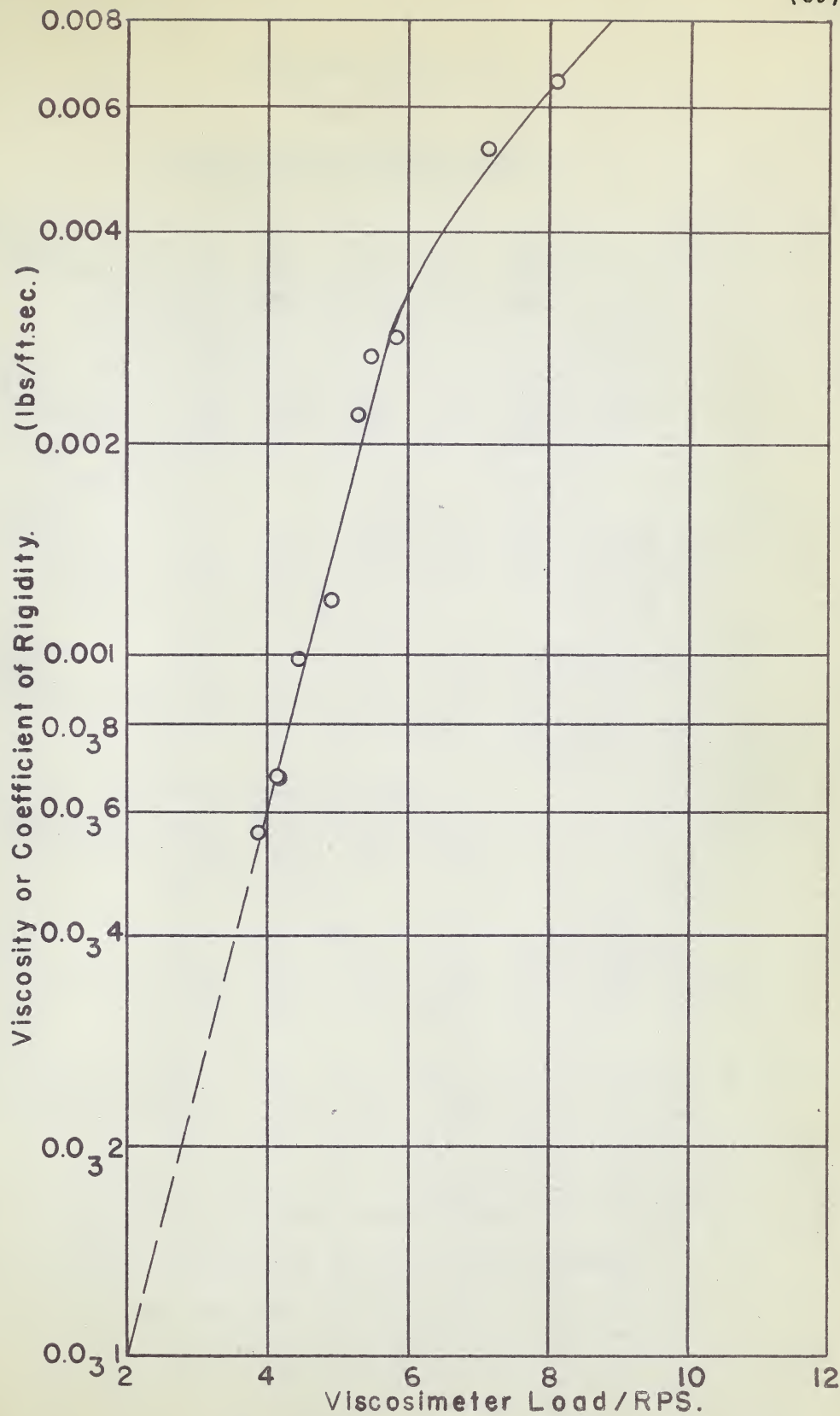


Fig. 2 O. Viscosimeter Calibration.

EXPERIMENTAL DATATABLE IIStormer Viscosimeter Data on Clay
(Preliminary Data Only).

10% Solids

Load (gms)	10	15	20	25	30
Time for 100revs.*	27.7	33.3	22.7	19.6	16.2
RPM	125	198	264	322	370

20% Solids.

Load (gms)	15	17	20	22	24	25
Time for 100revs.*	41.0	39.8	22.3	28.3	25.8	24.8
RPM	118	151	186	212	232	243

30% Solids

Load (gms)	40	45	50	55	60	65	70
Time for 100revs.*	141.8	31.3	20.2	26.8	23.3	17.8	16.4
RPM	51.5	110	129	224	259	337	346

40% Solids.

Load (gms)	65	70	75	80	85	90	100
Time for 100revs.*	37.3	39.8	22.3	21.2	20.0	14.2	13.5
RPM	142	101	247	283	333	370	444

50% Solids. (Fresh unagitated samples)

Load (gms)	500	525	550	575
Time for 100revs.*	26.9	21.0	15.1	12.3
RPM	163	242	397	487

50% Solids. (Agitated for 1 hour)

Load (gms)	350	375	400	425	455	465	475
Time for 100revs.#	77.0	51.4	33.9	24.5	16.9	15.2	13.5
RPM	78	117	117	225	355	395	145

Load (gms)	500	525	545	560
Time for 100revs.#	110	9.5	8.7	8.0
RPM	545	630	690	750

% Solids are on a weight basis.

* Average time for three trials in seconds.

Average time for one trial.

Experimental DataTable IIIManometer Fluid Calibration

Fluid No. 1 (Fig. 21)

<u>Temperature °C</u>	<u>Effective Specific Gravity</u>
28.9	0.012,5
24.0	0.009,6
20.5	0.007,6
22.4	0.008,4
26.5	0.011,9

Fluid No. 3 (Fig. 22)

<u>Temperature °C</u>	<u>Effective Specific Gravity</u>
27.2	0.104
19.6	0.109
21.8	0.107
23.6	0.104
25.7	0.103
29.6	0.099

Fluid No. 5 (Fig. 23)

<u>Temperature °C</u>	<u>Effective Specific Gravity</u>
28.9	0.090,6
21.1	0.091,9
24.1	0.092,7
26.4	0.094,1
19.3	0.089,6
20.0	0.089,4
24.5	0.093,2
27.8	0.095,2
29.5	0.095,3

Fluid No. 6 (Fig. 24)

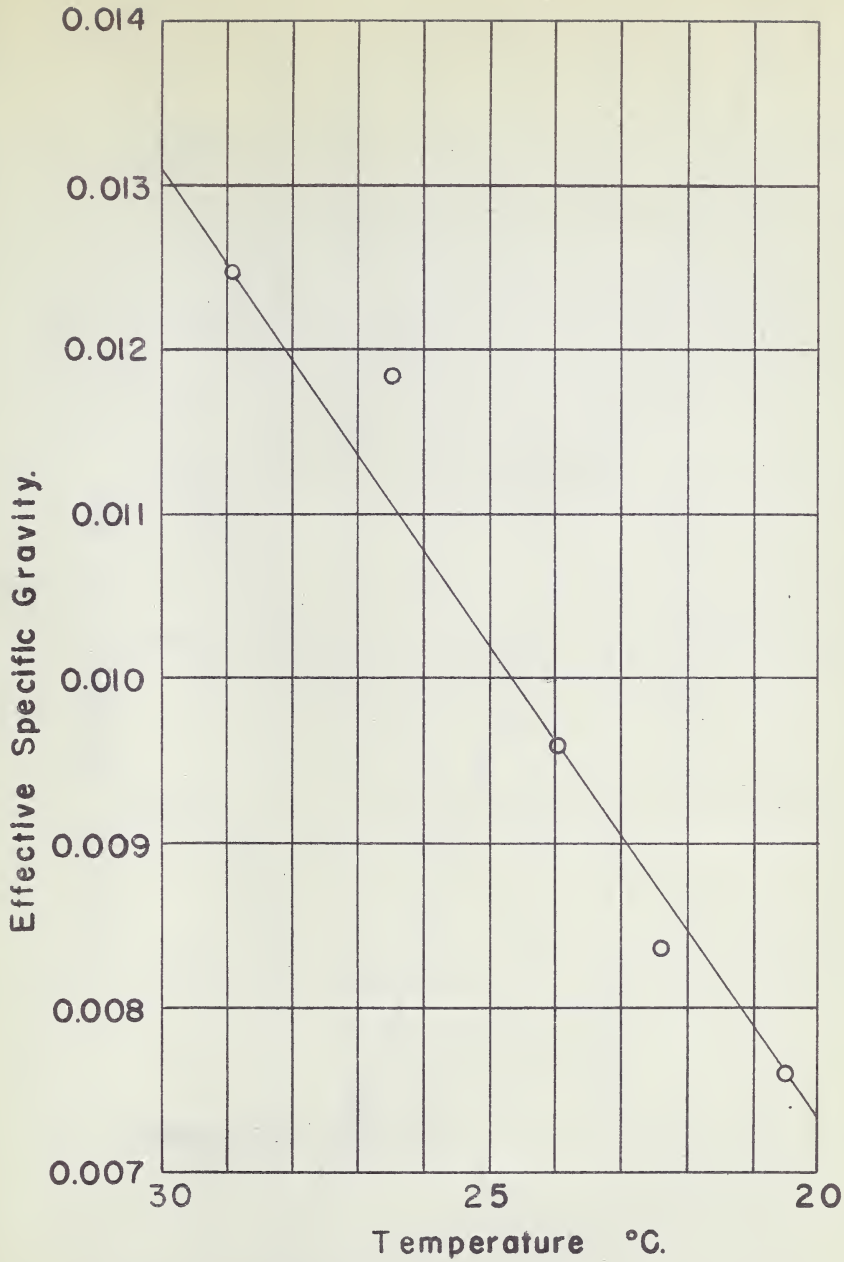
<u>Temperature °C</u>	<u>Effective Specific Gravity</u>
30.8	0.033,9
19.2	0.025,9
19.8	0.026,4
21.8	0.027,9
22.9	0.029,7
23.8	0.030,6
25.1	0.030,7
26.2	0.032,4
26.9	0.033,0
28.6	0.034,7
21.4	0.027,1
22.8	0.028,1

Table III - Continued

Fluid No. 6 (Fig. 24)

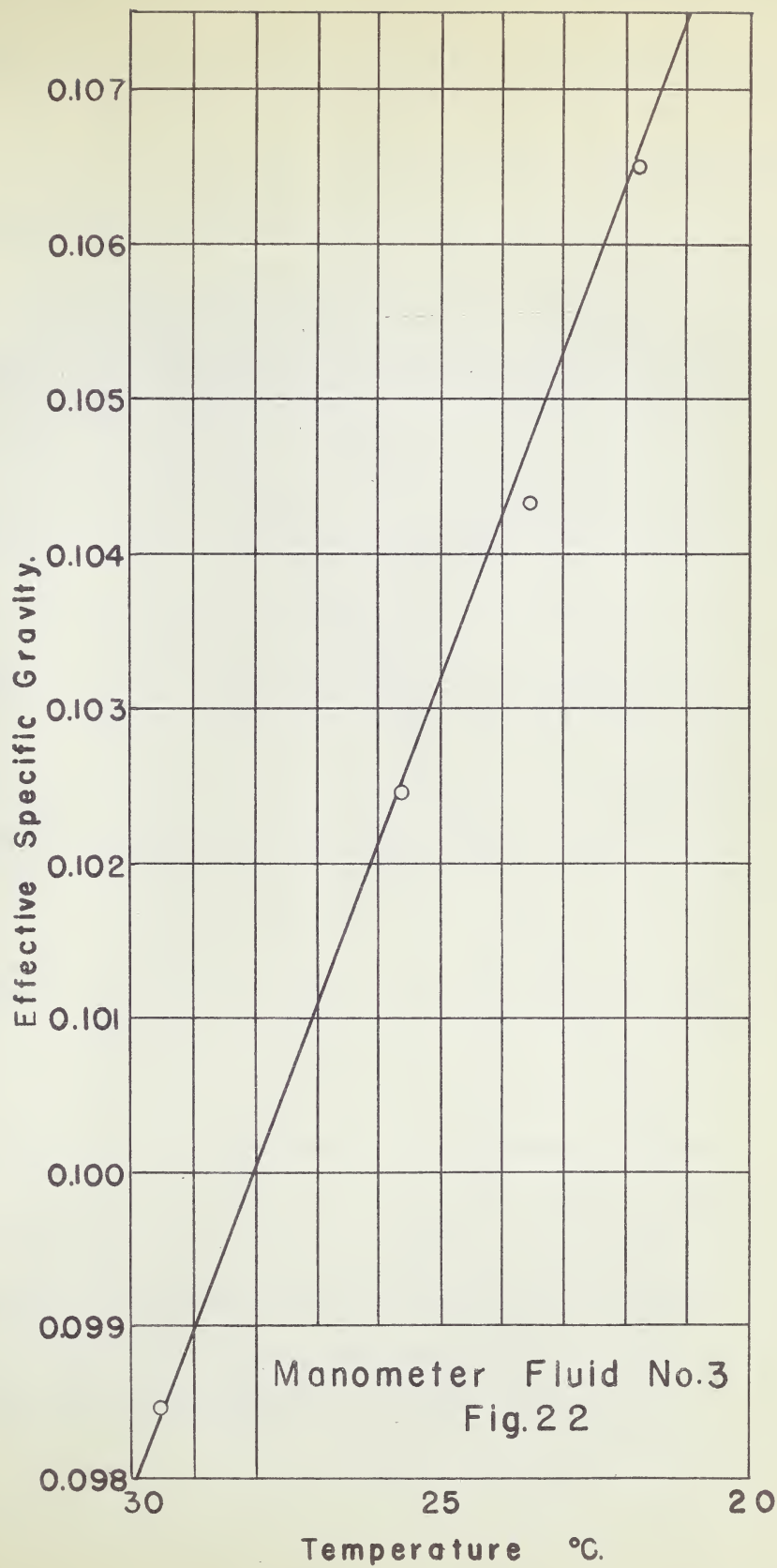
Temperature °CEffective Specific Gravity

25.0	0.030,8
26.5	0.031,8
21.1	0.026,8
22.7	0.029,4
25.3	0.031,5
27.6	0.033,5
29.8	0.034,4



Manometer Fluid No. 1

Fig. 21.



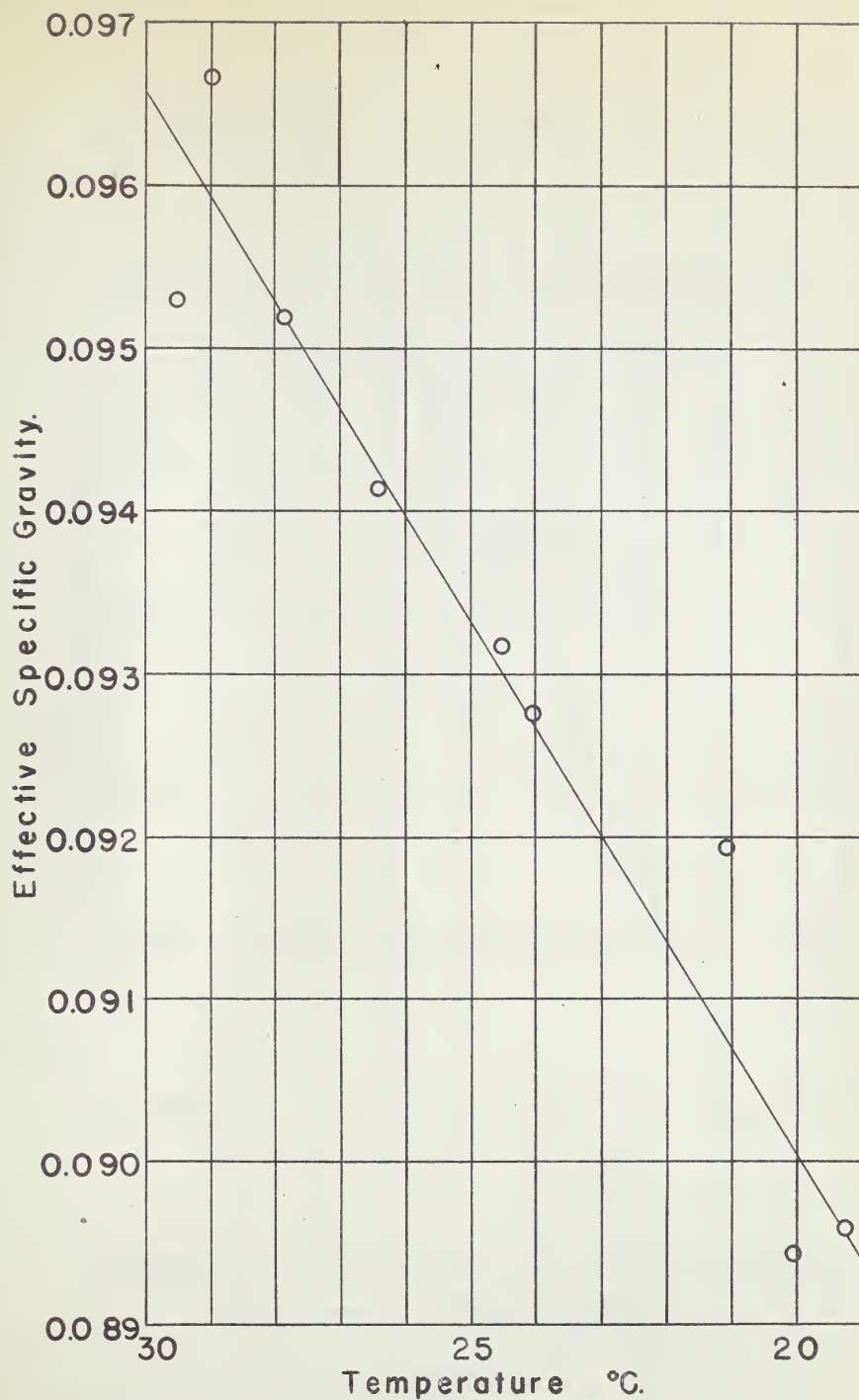
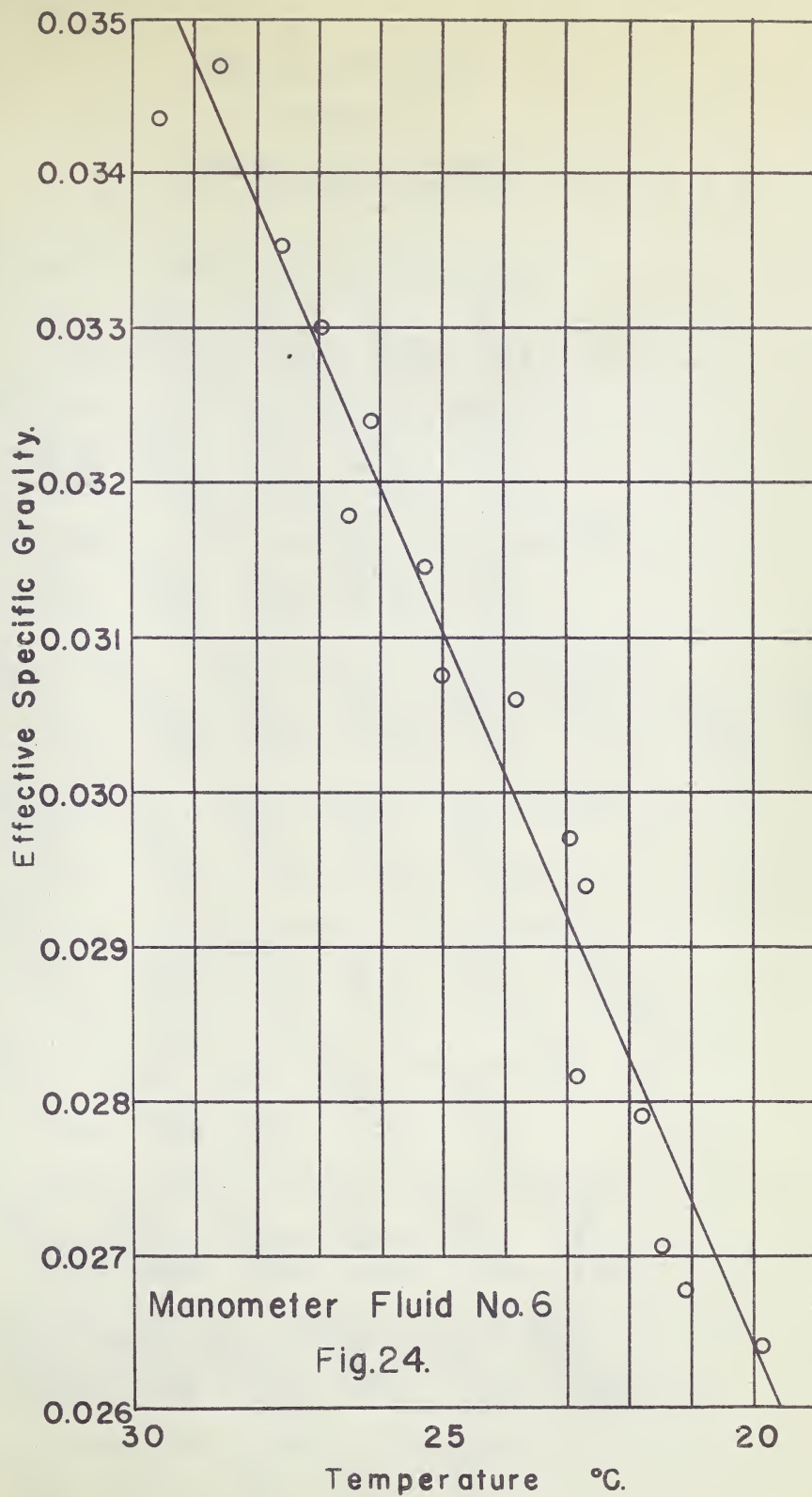


Fig. 23. Manometer Fluid No. 5



Experimental DataTable IVSuspension Properties

A.	2.5% Solids	30°C	Density 63.01lbs/ft ³			
Load	10	12	15	17	20	
Time	39.0	31.7	25.7	22.2	20.0	
R.P.S.	2.56	3.16	3.89	4.51	5.0	
B.	8.8% Solids	31°C	Density 65.01lbs/ft ³			
Load	10	12	15	17	20	
Time	44.0	34.9	27.7	24.3	21.4	
R.P.S.	2.27	2.86	3.61	4.12	4.67	
C.	14.3% Solids	28°C	Density 67.1 lbs/ft ³			
Load	12	15	17	20	22	
Time	56.6	39.4	33.1	27.7	24.5	
R.P.S.	1.77	2.54	3.02	3.61	4.08	
D.	21.2% Solids	28°C	Density 71.2 lbs/ft ³			
Load	20	21	22	23	24	25
Time	72.3	63.1	55.3	46.1	43.6	41.8
R.P.S.	1.26	1.57	1.81	2.17	2.29	2.39
						3.54
						4.50
E.	25.0% Solids	28°C	Density 73.2 lbs/ft ³			
Load	30	35	40	45	50	
Time	99.1	50.4	30.9	23.9	19.7	
R.P.S.	1.01	1.98	3.24	4.18	5.07	
F.	31.9% Solids	29°C	Density 77.51lbs/ft ³			
Load	75	80	85	90	95	100
Time	106.5	59.9	44.6	32.4	26.2	21.8
R.P.S.	0.94	1.67	2.24	3.62	3.82	4.58
G.	36.8% Solids	29°C	Density 79.8 lbs/ft ³			
Load	150	160	170	175	180	
Time	64.4	45.5	29.7	24.1	21.5	
R.P.S.	1.55	2.20	3.37	4.15	4.65	
H.	39.2% Solids	31°C	Density 81.2 lbs/ft ³			
Load	200	210	220	230	240	250
Time	125.5	69.6	42.8	29.6	22.9	19.7
R.P.S.	0.795	1.44	2.34	3.38	4.36	5.08
I.	40.4% Solids	27°C	Density 82.4 lbs/ft ³			
Load	260	270	280	290	300	321
Time	104.2	63.3	46.0	35.2	25.7	22.1
R.P.S.	0.962	1.58	2.22	3.84	3.89	4.52
Water run.	0% Solids	28°C	Density			
Load	10	12	15	17	20	
Time	39.2	31.9	26.0	22.6	19.2	
R.P.S.	2.55	3.14	3.85	4.42	5.20	

Experimental DataTable IVSuspension PropertiesNOTES:

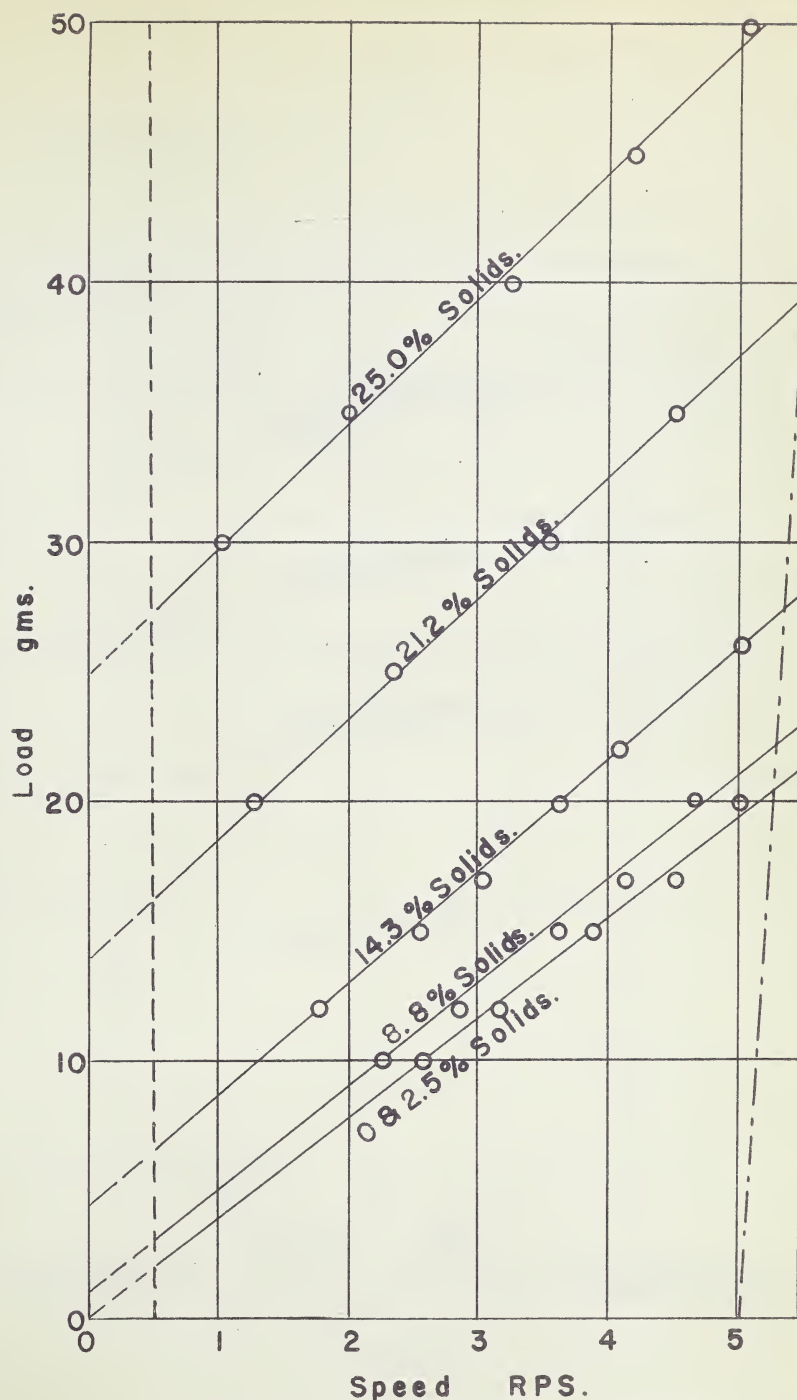
The loads are expressed in grams.

The time is given as the number of seconds required for 100 revs. of the viscosimeter rotor.

The percent solids is on a weight basis.

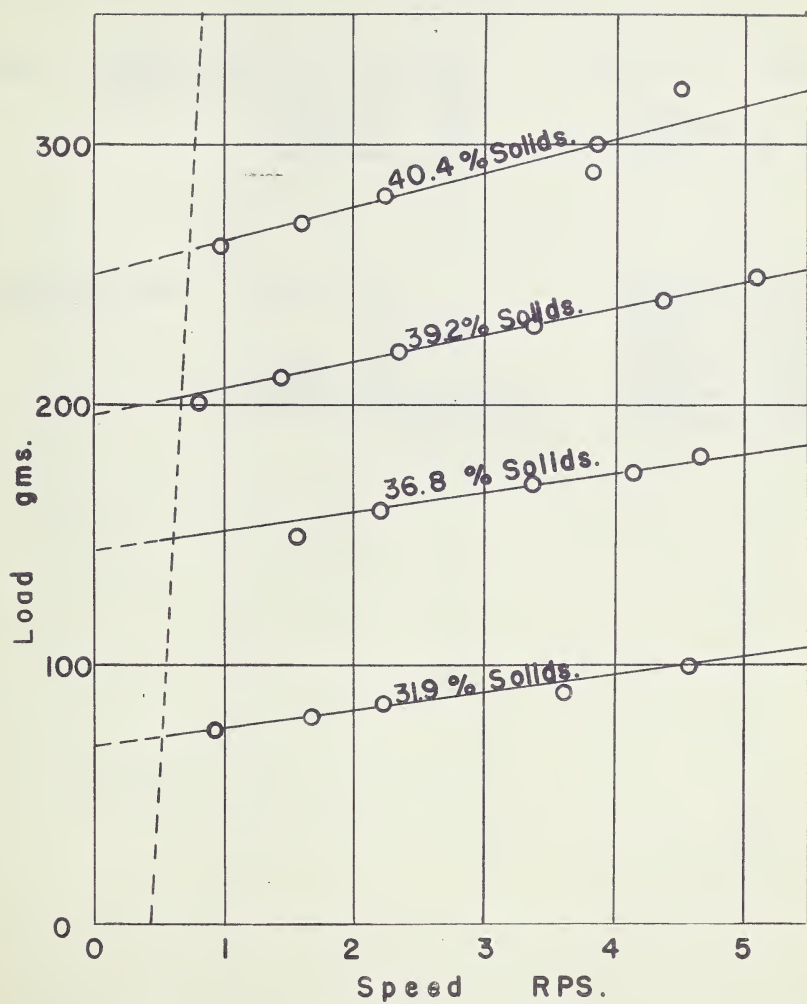
The temperature is that at which the viscosimeter data were obtained.

The density is the average of a number of readings taken during the pipeline measurements.



Viscosimeter Data on Clay Suspensions.

Fig. 25.



Viscosimeter Data on Clay Suspensions.

Fig. 26.

Table No. VSupplementary Data

Pipe	length of test sections	20.0ft. \pm	0.01 ft.
	Inside diameter of pipe		
	Nominal $\frac{3}{4}$ "	= 0.786"	\pm 0.001"
	Nominal $1\frac{1}{4}$ "	= 1.277"	\pm 0.001"
Viscosimeter	Rotor ID	1.190"	\pm 0.002"
	OD	1.250"	\pm 0.002"
	Length	1.367"	\pm 0.002"
	Cup ID	1.873"	\pm 0.002"
	Gears Small pitch	0.500"	\pm 0.002"
	Large pitch	5.687"	\pm 0.002"

EXPERIMENTAL DATA

Table VI

WATER FLOW DATA

Run #1

Test No.	Flow Rate			Pressure Drop							Suspension Temp. °C.
	Volume ml.	Weight lbs.	Time min.	3/4" Tube			1 1/4" Tube				
				Manometer Difference inches	Fluid No.	Fluid Temp. °C.	Manometer Difference inches	Fluid No.	Fluid Temp. °C.		
1		60	9.82	5.1	5	28.6	-	5	28.6	25.2	
2		100	11.01	11.0	"	28.4	1.00	"	28.4	"	
3		100	9.27	15.1	"	28.3	2.00	"	28.3	"	
4		100	7.65	21.6	"	28.3	2.55	"	28.3	"	
5		100	7.00	25.4	"	28.2	3.10	"	28.2	"	
6		100	6.34	30.3	"	28.0	3.40	"	28.0	"	
7		110	6.50	34.7	"	28.0	4.00	"	28.0	"	
8		100	5.47	39.8	"	27.8	4.50	"	27.8	"	
9		200	12.02	3.3	2	27.7	0.40	2	27.7	"	
10		200	8.34	6.3	"	27.5	0.60	"	27.5	"	
11		200	6.36	10.1	"	27.5	1.00	"	27.5	"	
12		200	5.06	15.0	"	27.2	1.50	"	27.2	"	
13		250	5.37	20.1	"	27.1	2.00	"	27.1	"	
14		300	5.72	25.3	"	27.6	2.50	"	27.6	"	
15		300	5.17	30.4	"	27.6	3.00	"	27.6	"	
16		325	5.06	36.0	"	27.5	3.70	"	27.5	"	
17		325	3.71	4.8	4		2.60	"	27.8	"	
18		350	2.72	9.9	"		12.10	"	27.8	"	
19		375	2.28	14.7	"		18.00	"	27.8	"	
20		400	2.00	20.2	"		2.10	4		"	
21		450	2.00	25.4	"		2.60	"		"	

EXPERIMENTAL DATA

Table VII

WATER FLOW DATA

Run #2

Test No.	Flow Rate			Pressure Drop						Suspension Temp. °C.
	Volume ml.	Weight lbs.	Time min.& seconds	3/4" Tube		1 1/4" Tube				
				Manometer Difference inches	Fluid No. Temp. °C.	Manometer Difference inches	Fluid No. Temp. °C.			
1		100	21:23.9	5.83	6	25.4	-	6	25.4	28
2		100	18:00.7	11.65	"	25.4	-	"	25.4	"
3		101.5	15:36.7	15.97	"	25.5	2.27	"	25.5	"
4		100	13:51.4	20.45	"	25.4	2.37	"	25.4	"
5		100	12:13.2	27.17	"	25.6	3.12	"	25.6	"
6		100	11:05.2	31.96	"	25.8	3.70	"	25.8	29
7		100	10:12.1	12.98	3	25.9	-	"	25.9	"
8		100	8:28.2	17.66	"	26.0	4.50	"	26.0	"
9		150	11:40.8	21.92	"	25.5	4.62	"	25.5	"
10		150	10:00.5	27.05	"	25.8	6.15	"	25.8	"
11		150	8:58.0	33.00	"	25.3	7.19	"	25.3	30
12		150	8:14.5	38.46	"	25.2	8.66	"	25.2	"
13		150	7:41.0	43.58	"	25.8	10.21	"	25.8	"
14		150	7:16.5	47.97	"	25.7	11.02	"	25.7	"
15		150	6:57.8	52.18	"	25.5	12.10	"	25.5	"
16		150	6:30.9	58.43	"	25.5	14.44	"	25.5	31
17		200	6:22.2	10.27	2	25.5	10.75	3	25.6	"
18		200	5:02.4	15.23	"	25.5	14.40	"	25.5	"
19		225	5:15.4	18.13	"	25.8	17.35	"	25.8	"
20		250	4:52.9	25.27	"	25.9	23.97	"	25.9	"
21		275	4	30.30	"	24.8	29.15	"	24.8	32
22		300	4:45.3	35.18	"	25.9	33.67	"	25.9	"
23		300	4:11.1	42.75	"	25.8	43.08	"	25.8	"
24		300	3:43.4	4.25	4		5.1	2	25.5	"
25		300	2:13.4	10.50	"		13.1	"	25.7	33
26		400	1:55.6	21.97	"		25.87	"	25.7	"
27		400	1:42.8	26.94	"		32.02	"	25.7	"
28		400	1:31.4	33.20	"		41.66	"	25.5	34

EXPERIMENTAL DATA

Table VIII

WATER FLOW DATA

Run #3

Test No.	Flow Rate			Pressure Drop						Suspension Temp.
	Volume ml.	Weight lbs.	Time seconds	3/4" Tube			1 1/4" Tube			
				Manometer Difference inches	Fluid No.	Fluid Temp. °C.	Manometer Difference inches	Fluid No.	Fluid Temp. °C.	
1	1000		174.5				0.31	1	25.2	25.0
2	1000		149.2				0.44	1	25.2	"
3	1000		108.1				0.61	1	25.2	"
4	1000		72.4				1.13	1	25.3	"
5	1000		49.3	8.90	1	27.9				"
6	1000		28.7	17.93	1	27.9				"
7	1000		27.4	25.94	1	27.9				"
8	1000		21.7	35.61	1	27.9				"
9	1000		19.6	43.16	1	25.9				"

Run #4.

Test No.	Flow Rate			Pressure Drop						Suspension Temp. °C.
	Volume ml.	Weight lbs.	Time mins. & seconds	3/4" Tube			1 1/4" Tube			
				Manometer Difference inches	Fluid No.	Fluid Temp. °C.	Manometer Difference inches	Fluid No.	Fluid Temp. °C.	
1	1000		1:52.7	0.50	3	21.4	-	1	21.6	22.7
2	1000		1:23.1	0.65	"	21.4	-	"	21.8	22.6
3	1000		1:02.3	0.89	"	21.4	-	"	21.8	22.4
4	1000		33.7	1.68	"	22.2	-	"	22.2	22.5
5		50	9:20.1	3.79	"	22.7	-	"	22.6	22.6
6		50	8:27.7	4.98	"	23.0	-	"	22.5	22.8
7		50	6:15.2	8.77	"	23.0	0.52	"	22.8	22.6
8		50	4:47.3	14.27	"	23.0	4.43	"	22.9	22.3
9		75	5:20.0	23.70	"	23.0	12.46	"	22.9	22.3
10		100	6:03.3	33.33	"	23.0	21.38	"	22.9	22.7
11		100	5:06.8	43.65	"	23.0	30.06	"	22.9	22.0
12		125	5:47.0	52.31	"	22.4	38.28	"	22.4	22.0
13		125	5:40.0	5.27	2	21.6	5.16	3	21.5	22.0
14		200	5:00.5	15.60	"	21.3	14.37	"	21.2	21.9
15		200	3:53.8	24.88	"	21.2	23.30	"	21.1	21.1
16		200	3:13.9	33.10	"	21.1	31.66	"	21.0	20.8
17		200	2:44.0	44.99	"	21.0	42.38	"	21.0	22.0
18		200	2:30.3	52.53	"	20.9	49.16	"	20.9	22.4
19		200	2:14.4	5.06	4	20.2	6.48	2	20.8	22.7
20		300	1:48.1	15.25	"	20.3	18.74	"	20.9	23.1
21		350	1:31.6	26.38	"	20.3	32.88	"	21.0	23.6
22		350	1:25.5	30.12	"	20.3	36.12	"	20.5	22.2

EXPERIMENTAL DATA

Table IX

SUSPENSION A 2.5% SOLIDS

Test No.	Flow Rate			Pressure Drop						Suspension Temp.
	Volume ml.	Weight lbs.	Time mins. & seconds	3/4" Tube			1 1/4" Tube			
				Manometer Difference inches	Fluid No.	Fluid Temp. °C.	Manometer Difference inches	Fluid No.	Fluid Temp. °C.	
1	1000		5:01.9	0.09	3	24.0	2.60	1	24.3	30.0
2	1000		1:36.1	0.57	"	24.2	3.39	"	24.3	"
3	1000		25.0	4.00	"	24.1	3.93	"	24.2	"
4		50	6:59.8	7.29	"	23.0	4.71	"	24.2	"
5		50	6:15.4	10.81	"	23.9	7.08	"	24.1	"
6		100	9:07.7	15.44	"	23.7	9.65	"	24.1	"
7		100	7:50.0	20.59	"	23.9	13.57	"	24.0	"
8		100	7:26.1	21.95	"	23.8	18.33	"	23.0	"
9		100	6:33.3	26.31	"	24.6	32.68	"	24.9	31.0
10		100	5:52.7	32.65	"	24.1	49.56	"	24.1	"
11		125	6:10.0	4.60	2	24.0	4.15	3	23.8	"
12		150	4:32.3	10.47	"	24.0	11.22	"	23.7	"
13		200	4:14.6	19.43	"	23.9	18.37	"	23.7	32.0
14		200	3:12.6	32.73	"	23.8	30.70	"	23.7	"
15		200	2:59.9	39.32	"	23.8	37.07	"	23.7	33.0
16		300	3:46.1	3.95	4	23.8	4.92	2	24.2	33.2
17		300	2:14.6	9.88	"	23.8	12.18	"	24.2	"
18		300	1:45.7	15.27	"	24.0	18.55	"	24.2	"
19		400	1:57.4	21.17	"	24.1	27.25	"	24.2	"
20		400	1:35.7	30.28	"	24.3	40.33	"	24.2	"
21		400	1:27.0	35.90	"	24.0	45.60	"	24.2	33.3

Original differences

#3 fluid	0.00
#1 fluid	2.20"
#2 fluid	0.00
#4 fluid	0.00

EXPERIMENTAL DATA

Table X

SUSPENSION B 8.8% SOLIDS

Test No.	Flow Rate			Pressure Drop							Suspension Temp. °C.
	Volume ml.	Weight lbs.	Time mins. & seconds	3/4" Tube			1 1/4" Tube				
				Manometer Difference inches	Fluid No.	Fluid Temp. °C.	Manometer Difference inches	Fluid No.	Fluid Temp. °C.		
1	1000		1:02.7	7.30	3	26.5	18.05	1	26.6	30	
2		50	14:51.8	12.49	"	26.6	31.69	"	26.6	"	
3	1000		1:05.0	13.00	"	26.6	30.60	"	26.5	"	
4		50	4:21.2	16.70	"	26.6	34.83	"	26.5	"	
5		50	3:29.6	25.4	"	26.6	38.65	"	26.5	"	
6		50	5:41.2	1.70	2	26.4	8.10	3	26.5	31	
7		100	3:40.1	8.00	"	26.5	15.52	"	26.7	"	
8		200	5:23.7	13.65	"	26.6	19.15	"	26.6	"	
9		200	4:23.2	19.00	"	26.6	23.52	"	26.7	"	
10		200	3:19.5	28.83	"	26.5	23.2	"	26.5	"	
11		200	2:59.1	36.16	"	26.3	37.50	"	26.3	"	
12		200	2:34.4	45.76	"	26.3	44.23	"	26.2	"	
13		200	2:35.6	3.62	4	26.0	4.43	2	26.3	"	
14		300	1:49.0	13.93	"	25.9	13.93	"	26.3	"	
15		400	1:48.6	23.84	"	25.9	29.02	"	26.3	"	
16		400	1:33.8	30.73	"	25.9	40.00	"	26.3	32	

Original differences

Fluid	inches
#1	3.40
#2	0.00
#3	0.20
#4	0.00

EXPERIMENTAL DATA

Table XI

SUSPENSION C 14.3% SOLIDS

Test No.	Flow Rate			Pressure Drop						Suspension Temp. °C.
	Volume ml.	Weight lbs.	Time mins. & seconds	3/4" Tube		1 1/4" Tube				
				Manometer Difference inches	Fluid No. Temp. °C.	Manometer Difference inches	Fluid No. Temp. °C.	Fluid Temp. °C.		
1	11		61.2	1.98	3	23.9	19.85	1	23.6	28.3
2	100		68.6	14.88	"	23.9	40.28	"	23.6	28.3
3	11		55.9	0.25	2	24.0	2.40	3	24.3	28.3
4	100		66.6	1.05	"	24.0	5.23	"	24.3	28.3
5	250		27.7	2.05	"	24.2	10.13	"	24.3	28.3
6	250		78.4	1.50	"	24.2	8.35	"	24.3	28.3
7	1000		34.9	3.32	"	24.3	12.80	"	24.5	28.3
8		50	7:46.2	3.88	"	24.4	16.28	"	24.6	27.8
9		100	5:19.9	5.77	"	24.5	19.90	"	24.7	28.8
10		100	3:18.7	9.68	"	24.5	24.42	"	24.7	28.8
11		100	2:11.7	19.10	"	24.3	32.68	"	24.5	29.4
12		150	2:50.5	25.42	"	24.5	31.05	"	24.7	29.6
13		200	3:04.8	35.28	"	24.4	34.59	"	24.5	29.8
14		200	2:38.1	46.75	"	24.6	44.47	"	24.9	30.2
15		200	2:56.0	3.36	4		3.55	2	24.6	30.3
16		225	1:49.1	8.65	"		10.66	"	24.5	30.7
17		300	1:46.0	15.16	"		18.87	"	24.5	30.9
18		300	1:24.0	22.48	"		28.82	"	24.5	31.3
19		400	1:34.7	30.45	"		38.15	"	24.6	31.8
20		449.5	1:25.9	43.10	"		4.38	4	24.5	32.2

Original differences

Fluid	inches
#1	3.00
#2	0.00
#3	0.30
#4	0.00

EXPERIMENTAL DATA

Table XII

SUSPENSION D 21.2% SOLIDS

Test No.	Flow Rate			Pressure Drop						Suspension Temperature
	Volume	Weight	Time	3/4" Tube			1 1/4" Tube			
				Manometer Difference	Fluid No.	Fluid Temp.	Manometer Difference	Fluid No.	Fluid Temp.	
	ml.	lbs.	mins. & seconds	inches		°C.	inches		°C.	°C.
1	100		31.5	4.60	2	23.8	3.00	3	23.9	28.0
2	1000		39.5	5.95	"	23.8	4.85	"	23.9	28.0
3	1000		78.4	6.50	"	23.5	15.78	"	23.7	28.0
4		100	4:55.0	13.02	"	23.4	23.38	"	23.7	28.0
5	250		50.0	7.15	"	23.4	38.00	"	23.6	28.0
6		200	4:02.8	1.75	4		6.75	2		28.0
7		200	2:17.8	4.85	"		8.20	"		28.0
8		200	1:32.2	9.83	"		11.63	"		28.3
9		300	1:46.4	15.40	"		18.58	"		28.7
10		350	1:38.0	23.12	"		28.35	"		29.1
11		400	1:36.6	30.66	"		38.10	"		29.5
12		400	1:27.7	35.62	"		44.33	"		29.6
13		449.5	1:31.9	40.18	"		52.13	"		30.0

Original differences

Fluid	inches
#1	----
#2	0.00
#3	1.25
#4	0.00

EXPERIMENTAL DATA

Table XIII

SUSPENSION E 25.0% SOLIDS

Test No.	Flow Rate			Pressure Drop						Suspension Temperature
	Volume	Weight	Time	3/4" Tube			1 1/4" Tube			
				Manometer Difference	Fluid No.	Fluid Temp.	Manometer Difference	Fluid No.	Fluid Temp.	
	ml.	lbs.	mins.& seconds	inches		°C.	inches		°C.	°C.
1	1000		1:26.5	11.35	2		5.95	2		28.0
2	10		3:02.2	0.20	3	25.2	11.85	3	25.5	28.0
3	250		1:22.6	9.98	2		54.10	3	25.0	28.0
4	9.5		1:19.6	0.60	"		20.60	3	25.2	28.0
5	100		23.5	9.70	"		47.53	3	24.9	28.0
6	100		2:01.2	6.85	"		38.20	3	24.9	29.1
7	250		51.0	10.00	"		6.85	2		29.1
8	1000		21.6	15.50	"		8.40	"		29.1
9		200	1:30.7	10.10	4		13.82	"		29.2
10		200	2:31.6	4.17	"		12.22	"		29.3
11		200	4:10.3	2.10	"		11.07	"		29.4
12	1000		1:52.0	1.10	"		7.18	"		29.3
13		200	1:13.5	14.87	"		18.25	"		30.0
14		300	1:19.4	25.87	"		28.73	"		30.3
15		350	1:18.2	34.67	"		41.04	"		30.5
16		400	1:16.8	44.73	"		54.27	"		31.0

No original differences.

EXPERIMENTAL DATA

Table XIV

SUSPENSION F 31.9% SOLIDS

Test No.	Flow Rate			Pressure Drop				Suspension Temperature
	Volume	Weight	Time mins.& seconds	3/4" Tube		1 1/4" Tube		
				Manometer	Fluid	Manometer	Fluid	
				Difference	No.	Difference	No.	
	ml.	lbs.		inches		inches		°C.
1	10		2:11.9	0.13	4	3.45	2	29.0
2	250		40.4	1.03	"	8.70	"	29.0
3	1000		37.6	2.90	"	14.85	"	29.0
4	100		29.8	2.5	"	11.30	"	29.0
5	250		45.2	2.13	"	10.20	"	29.0
6	1000		43.1	3.15	"	13.80	"	29.0
7	1000		9.9	3.70	"	18.75	"	29.1
8		100	3:47.1	5.00	"	28.00	"	29.1
9		200	1:31.8	9.75	"	34.18	"	29.4
10		250	1:28.5	15.76	"	39.69	"	29.5
11		300	1:22.5	22.12	"	37.01	"	29.7
12		300	1:10.2	32.57	"	46.62	"	30.0
13		530	1:42.0	45.52	"	4.93	4	30.2
14		400	1:11.8	52.02	"	5.25	"	30.5

No original differences.

EXPERIMENTAL DATA

Table XV

SUSPENSION G 36.8% SOLIDS

Pressure Drop								
Test No.	Flow Rate			3/4" Tube		1 1/4" Tube		Suspension Temperature
	Volume	Weight	Time	Manometer Difference	Fluid No.	Manometer Difference	Fluid No.	
	<u>ml.</u>	<u>lbs.</u>	<u>seconds</u>	<u>inches</u>		<u>inches</u>		
1	1000		65.1	5.58	4	38.0	2	29.1
2	39.5		2:52.5	1.20	"	12.95	"	29.1
3	250		50.3	4.45	"	27.30	"	29.1
4	250		40.1	5.22	"	26.60	"	29.5
5	1000		18.0	7.08	"	44.85	"	30.0
6	1000		50.3	6.15	"	36.58	"	30.2
7	1000		14.9	7.60	"	44.60	"	31.0
8		50	2:18.5	8.47	"	48.60	"	31.7
9		100	2:38.8	9.20	"	4.66	4	32.2
10		200	1:51.5	11.22	"	5.44	"	32.7
11		300	1:47.1	14.47	"	5.90	"	32.5
12		300	1:27.5	21.50	"	6.05	"	32.7
13		300	1:13.9	29.48	"	6.40	"	32.9
14		400	1:28.5	36.34	"	6.58	"	33.5
15		400	1:22.2	41.20	"	6.49	"	33.7
16		400	1:10.6	53.52	"	7.03	"	34.3

No original differences

EXPERIMENTAL DATA

Table XVI

SUSPENSION H 39.2% SOLIDS

Test No.	Flow Rate			Pressure Drop				Suspension Temperature
	Volume	Weight	Time	3/4" Tube		1 1/4" Tube		
				Manometer	Fluid	Manometer	Fluid	
				Difference	No.	Difference	No.	
	ml.	lbs.	mins.& seconds	inches		inches		°C.
1	250		46.2	6.96	4	41.5	2	31.7
2	1000		46.5	8.70	"	46.22	"	31.7
3	150		1:10.2	3.70	"	2.00	4	31.7
4	1000		11.5	10.45	"	5.31	"	31.7
5		40	5:35.4	10.33	"	5.61	"	31.7
6		100	2:24.4	12.35	"	6.84	"	32.9
7		200	1:42.2	15.26	"	7.91	"	33.1
8		200	1:06.7	17.27	"	8.27	"	33.2
9		300	1:34.4	18.76	"	8.48	"	33.7
10		400	1:55.3	21.33	"	8.74	"	34.2
11		400	1:36.3	29.98	"	8.83	"	34.5
12		400	1:11.0	53.14	"	9.50	"	34.7

EXPERIMENTAL DATA

Table XVII

SUSPENSION J 40.4% SOLIDS

Test No.	<u>Flow Rate</u>			<u>Pressure Drop</u>				Suspension Temperature °C.
	<u>Volume</u>	<u>Weight</u>	<u>Time</u> mins.& seconds	<u>3/4" Tube</u>		<u>1 1/4" Tube</u>		
				<u>Manometer</u>	<u>Fluid</u>	<u>Manometer</u>	<u>Fluid</u>	
				<u>Difference</u>	<u>No.</u>	<u>Difference</u>	<u>No.</u>	
<u>ml.</u>	<u>lbs.</u>	<u>seconds</u>	<u>inches</u>		<u>inches</u>			
1	300		1:15.1	8.90	4	5.60	4	29.5
2	250		23.0	12.10	"	5.48	"	29.5
3	1000		17.3	13.35	"	7.22	"	29.5
4		50	4:12.1	14.82	"	7.98	"	29.5
5		100	2:53.5	16.39	"	8.78	"	29.9
6		100	2:00.8	17.15	"	9.21	"	30.5
7		200	2:03.7	19.20	"	9.80	"	30.6
8		300	1:27.7	23.18	"	10.97	"	30.6
9		300	1:12.8	29.47	"	11.07	"	31.0
10		300	1:00.4	42.84	"	11.55	"	31.0
11		423	1:15.4	52.67	"	11.88	"	31.4

VI Presentation of Results.

Computed Data from Preliminary Calculations.

The following tables present the velocities (ft./sec.) and pressure drops (ft. of flowing fluid.) for each of the flow tests. They are listed here for convenience as they enter into all of the flow rate-pressure drop calculations encountered later.

The velocities are readily obtainable from the flow data by either dividing the volume, of fluid collected, by the time of collection and the pipe cross-sectional area, or by dividing the weight of fluid collected, by the time of collection, fluid density, and pipe cross-sectional area. The pressure drop may be calculated from the observed manometer difference by multiplying the manometer difference by the effective specific gravity of the manometer fluid and then dividing this product by the density of the flowing fluid. Conversion constants will be required where the measurements are not in the same unit system.

COMPUTED DATA

Table XVIII

Water Run #1

Test No.	PIPE LINE			
	Velocity ft/sec		Pressure Drop ft. of water	
	Pipe Size 3/4"	1 1/4"	3/4"	1 1/4"
1	0.485	0.184	0.0412	--
2	0.720	0.273	0.0884	0.0080
3	0.857	0.324	0.121	0.0160
4	1.040	0.384	0.174	0.0204
5	1.135	0.430	0.204	0.0247
6	1.25	0.475	0.243	0.0271
7	1.34	0.508	0.278	0.0318
8	1.45	0.550	0.317	0.0357
9	1.32	0.499	0.275	0.0333
10	1.90	0.721	0.524	0.0499
11	2.49	0.943	0.840	0.0833
12	3.14	1.19	1.25	0.125
13	3.70	1.40	1.67	0.167
14	4.15	1.58	2.10	0.208
15	4.58	1.74	2.53	0.250
16	5.09	1.93	3.00	0.308
17	6.94	2.63	5.02	0.216
18	10.2	3.88	10.35	1.01
19	13.1	4.83	15.4	1.50
20	15.9	6.00	21.1	2.19
21	17.9	6.75	26.5	2.77

COMPUTED DATA

Table XIX

Water Run #2

Test No.	Velocity ft/sec		Pressure Drop ft. of water	
	Pipe Size	3/4" 1 1/4"	3/4" 1 1/4"	
1		0.371 0.140	0.0153	0.00353
2		0.436 0.165	0.0303	--
3		0.514 0.1955	0.0419	0.00595
4		0.572 0.2170	0.0535	0.00620
5		0.660 0.250	0.0714	0.00803
6		0.715 0.271	0.0846	0.00981
7		0.777 0.2945	0.0978	0.0114
8		0.938 0.355	0.150	0.0120
9		1.020 0.386	0.188	0.0121
10		1.188 0.450	0.231	0.0163
11		1.33 0.503	0.283	0.0187
12		1.44 0.547	0.329	0.0225
13		1.55 0.587	0.376	0.0271
14		1.63 0.617	0.409	0.0291
15		1.71 0.647	0.445	0.0318
16		1.83 0.691	0.589	0.0379
17		2.485 0.944	0.854	0.092
18		3.15 1.19	1.27	0.124
19		3.40 1.286	1.51	0.148
20		4.07 1.54	1.99	0.215
21		4.65 1.76	2.52	0.251
22		5.00 1.895	2.92	0.287
23		5.68 2.155	3.55	0.367
24		6.40 2.420	4.44	0.424
25		10.70 4.05	10.98	1.09
26		16.4 6.22	22.97	2.15
27		18.5 7.00	28.15	2.66
28		20.8 7.87	34.7	3.46

COMPUTED DATA

Table XX

Water Run #3

Test No.	Pipe Size	Velocity	Pressure Drop
	Inches	ft/sec	ft. of water
1	1 $\frac{1}{4}$	0.02275	0.000267
2	1 $\frac{1}{4}$	0.0266	0.000378
3	1 $\frac{1}{4}$	0.0367	0.000525
4	3/4	0.0548	0.000972
5	3/4	0.212	0.00885
6	3/4	0.364	0.0178
7	3/4	0.381	0.0258
8	3/4	0.482	0.0354
9	3/4	0.533	0.0429

Water Run #4

Test No.	Pipe Size	Velocity ft/sec		Pressure Drop ft. of water	
		3/4"	1 1/4"	3/4"	1 1/4"
1		0.0928	0.0352	0.00445	--
2		0.116	0.0477	0.00578	--
3		0.168	0.0637	0.00792	--
4		0.310	0.118	0.0148	--
5		0.425	0.161	0.0332	--
6		0.470	0.178	0.0437	--
7		0.635	0.241	0.0769	0.000387
8		0.828	0.314	0.1250	0.00331
9		1.11	0.422	0.2080	0.00931
10		1.31	0.498	0.292	0.0160
11		1.55	0.588	0.382	0.0225
12		1.71	0.650	0.463	0.0278
13		1.75	0.664	0.438	0.0504
14		3.165	1.20	1.30	0.132
15		4.07	1.55	2.075	0.213
16		4.91	1.86	2.76	0.287
17		5.81	2.20	3.75	0.382
18		6.34	2.40	4.38	0.442
19		7.09	2.69	5.26	0.540
20		13.10	5.02	15.9	1.56
21		18.2	6.89	27.4	2.74
22		19.5	7.39	31.4	3.01

COMPUTED DATA

Table XXI

Run A June 10th 1948

PIPE LINE

Test No.	Pipe Size	Velocity ft/sec		Pressure Drop ft. of fluid	
		3/4"	1 1/4"	3/4"	1 1/4"
1		0.0346	0.0132	0.000787	0.000328
2		0.109	0.0414	0.00497	0.000976
3		0.417	0.159	0.0349	0.00142
4		0.566	0.216	0.0636	0.00206
5		0.639	0.242	0.0945	0.00396
6		0.870	0.331	0.135	0.00605
7		1.014	0.386	0.180	0.00913
8		1.07	0.406	0.192	0.0129
9		1.21	0.460	0.230	0.0245
10		1.35	0.514	0.287	0.0385
11		1.61	0.612	0.384	0.0363
12		2.62	0.999	0.873	0.0982
13		3.74	1.43	1.623	0.161
14		4.95	1.88	2.73	0.269
15		5.30	2.02	3.28	0.344
16		6.32	2.41	4.14	0.411
17		10.6	4.04	10.4	1.018
18		13.5	5.14	16.0	1.55
19		16.1	6.16	22.2	2.275
20		19.8	7.55	31.8	3.365
21		21.6	8.24	37.6	3.81

Solids Concentration 2.5%

Density of Suspension 63.0 lbs/ft³

COMPUTED DATA

Table XXII

Run B June 14th 1948

PIPE LINE

Test No.	Pipe Size	Velocity ft/sec		Pressure Drop ft. of fluid	
		3/4"	1 1/4"	3/4"	1 1/4"
1		0.167	0.0634	0.0588	0.0129
2		0.267	0.102	0.0989	0.0249
3		0.161	0.0610	0.1030	0.0239
4		0.915	0.348	0.1330	0.0277
5		1.14	0.433	0.203	0.0310
6		0.700	0.266	0.134	0.0653
7		2.16	0.822	0.632	0.125
8		2.95	1.12	1.08	0.154
9		3.62	1.38	1.50	0.189
10		4.77	1.82	2.28	0.268
11		5.33	2.02	2.68	0.303
12		6.19	2.36	3.62	0.358
13		8.76	3.33	3.60	0.350
14		13.20	5.02	13.86	1.37
15		17.5	6.66	23.70	2.30
16		19.1	7.26	30.60	3.16

Solids Concentration 8.8%

Density of Suspension 65.0 lbs/ft³

COMPUTED DATA

Table XXIII

Run C

June 17th 1948

PIPE LINE

Test No.	Pipe Size	Velocity ft/sec		Pressure Drop ft. of fluid	
		3/4"	1 1/4"	3/4"	1 1/4"
1		0.00188	0.000715	0.0183	0.00852
2		0.0152	0.00578	0.122	0.0268
3		0.00206	0.000782	0.0191	0.0214
4		0.0157	0.00596	0.0803	0.0439
5		0.0943	0.0358	0.157	0.0830
6		0.0334	0.0172	0.115	0.0688
7		0.299	0.114	0.254	0.104
8		0.457	0.177	0.296	0.132
9		1.37	0.52	0.441	0.121
10		2.20	0.833	0.74	0.192
11		3.31	1.26	1.46	0.262
12		3.84	1.46	1.94	0.248
13		4.72	1.79	2.70	0.277
14		5.55	2.10	3.57	0.353
15		4.98	1.89	3.23	0.271
16		9.00	3.41	8.31	0.814
17		12.37	4.68	14.6	1.44
18		15.6	5.91	21.6	2.20
19		18.5	7.00	29.3	2.92
20		22.8	8.65	41.4	4.22

Solids Concentration 14.3%

Density of Suspension 67.1 lbs/ft³

COMPUTED DATA

Table XXIV

Run D

June 21st 1948

PIPE LINE

Test No.	Pipe Size	Velocity ft/sec		Pressure Drop ft. of fluid	
		3/4"	1 1/4"	3/4"	1 1/4"
1		0.0332	0.0126	0.338	0.0134
2		0.264	0.1005	0.434	0.0278
3		0.133	0.057	0.474	0.111
4		1.41	0.538	1.13	0.169
5		0.0522	0.0198	0.522	0.281
6		3.45	1.31	1.61	0.493
7		6.08	2.32	4.46	0.598
8		9.05	3.44	9.03	0.850
9		11.8	4.47	14.20	1.36
10		14.9	5.66	21.30	2.07
11		17.3	6.56	28.20	2.78
12		19.0	7.23	32.7	3.24
13		20.4	7.75	36.9	3.80

Solids Concentration 21.2%

Density of Suspension 71.2 lbs/ft³

COMPUTED DATA

Table XXV

Run E June 22nd 1948

PIPE LINE

Test No.	Pipe Size	Velocity ft/sec		Pressure Drop ft. of fluid	
		3/4"	1 1/4"	3/4"	1 1/4"
1		0.121	0.0459	0.805	0.422
2		0.000791	0.000301	0.00146	0.0867
3		0.03165	0.0119	0.708	0.398
4		0.00125	0.000474	0.0426	0.151
5		0.0444	0.0169	0.688	0.350
6		0.00862	0.00328	0.487	0.281
7		0.0512	0.0195	0.710	0.487
8		0.462	0.184	1.10	0.596
9		8.04	3.40	9.02	0.981
10		5.36	2.03	3.73	0.866
11		3.24	1.23	1.88	0.785
12		0.0934	0.0354	0.984	0.510
13		11.0	4.18	13.3	1.295
14		15.3	5.82	23.1	2.04
15		18.2	6.92	31.0	2.92
16		21.15	8.03	40.0	3.85

Solids Concentration 25.0%

Density of Suspension 73.2 lbs/ft³

COMPUTED DATA

Table XXVI

Run F

June 24th 1948

Test No.	Pipe Size	Velocity ft/sec		Pressure drop ft. of fluid	
		3/4"	1 1/4"	3/4"	1 1/4"
1		0.00783	0.00301	0.11	0.231
2		0.0646	0.0246	0.877	0.583
3		0.278	0.1055	2.44	0.995
4		0.0350	0.0133	2.11	0.765
5		0.104	0.0394	1.80	0.684
6		0.242	0.0921	2.60	0.925
7		1.055	0.401	3.12	1.26
8		1.68	0.639	4.22	1.88
9		8.33	3.17	8.20	2.30
10		10.8	4.11	13.3	2.66
11		13.1	4.98	18.6	2.48
12		16.3	6.21	27.4	3.13
13		19.9	7.55	38.4	4.15
14		21.3	8.10	43.8	4.43

Solids Concentration 31.85%

Density of Suspension 77.5 lbs/ft³

COMPUTED DATA

Table XXVII

Run G June 28th 1948

PIPE LINE

Test No.	Pipe Size	Velocity ft/sec		Pressure drop ft. of fluid	
		3/4"	1 1/4"	3/4"	1 1/4"
1		0.161	0.0160	4.55	2.47
2		0.00153	0.000584	0.978	0.840
3		0.0520	0.0197	3.63	1.77
4		0.0652	0.0247	4.26	1.73
5		0.580	0.220	5.77	2.91
6		0.208	0.790	5.02	2.37
7		0.702	0.266	6.19	2.895
8		1.35	0.509	6.90	3.39
9		2.34	0.889	7.50	3.80
10		6.65	2.52	9.15	4.43
11		10.40	3.95	11.80	4.81
12		12.75	4.84	17.55	4.93
13		15.1	5.73	24.00	5.22
14		16.7	6.37	29.60	5.34
15		18.1	6.86	33.50	5.28
16		21.1	8.00	43.60	5.73

Solids Concentration 36.8%

Density of Suspension 79.8 lbs/ft³

COMPUTED DATA

Table XXVIII

Run H

June 30th 1948

Test No.	Pipe Size	Velocity ft/sec		Pressure drop ft. of fluid	
		3/4"	1 1/4"	3/4"	1 1/4"
1		0.0565	0.0215	5.60	2.68
2		0.2245	0.0855	7.00	2.95
3		0.0224	0.0085	2.975	1.61
4		0.910	0.345	8.41	4.27
5		0.0434	0.0165	8.32	4.52
6		2.52	0.956	9.94	5.50
7		7.13	2.70	12.3	6.36
8		10.9	4.14	13.9	6.65
9		11.6	4.40	15.1	6.82
10		12.65	4.80	17.2	7.025
11		15.1	5.74	24.5	7.10
12		20.55	7.80	42.7	7.64

Solids Concentration 39.2%

Density of Suspension 81.2 lbs/ft³

COMPUTED DATA

Table XXIX

Run J

July 2nd 1948

PIPELINE

Test No.	Pipe Size	Velocity ft/sec		Pressure drop ft. of fluid	
		3/4"	1 1/4"	3/4"	1 1/4"
1		0.0417	0.0158	7.75	4.43
2		0.114	0.0432	9.56	4.34
3		0.604	0.2295	10.55	5.70
4		0.712	0.270	11.8	6.30
5		2.07	0.786	12.95	6.94
6		2.98	1.13	13.55	7.28
7		5.83	2.21	15.20	7.76
8		12.30	4.67	18.3	8.66
9		14.80	5.62	23.3	8.75
10		17.9	6.79	33.85	9.24
11		20.2	7.67	41.6	9.38

Solids Concentration 40.4%

Density of Suspension 82.4 lbs/ft³

FINAL CALCULATIONS AND CORRELATION OF RESULTS

Suspension properties:

Equation (91) gives the relationship between the shearing stress (lbs/ft²) and the viscosimeter load. (gms).

$$S = \frac{A r w}{12 \times 454 R (2 \pi l (A_1^2 + A_2^2) + \frac{1}{2} \pi A_1^3)} \quad (91)$$

The following values of the constants in equation (91) were obtained from the supplementary data:

$$A = 0.25 \text{ inches}$$

$$r = 0.537 \text{ "}$$

$$R = 2.844 \text{ "}$$

$$l = 1.367 \text{ "}$$

$$A_1 = 0.625 \text{ "}$$

$$A_2 = 0.595 \text{ "}$$

Substitution in equation (91) yields

$$S = 0.00221 w$$

For the particular case of the zero rate of shear

$$m^1 = 0.00221 u \quad (110)$$

The mathematical analysis of a Stormer viscosimeter indicated that the viscosity or coefficient of rigidity of the material being tested was related to the slope of the viscosimeter data (λ) by means of a constant K such that

$$\nu = K \lambda \quad (98)$$

and

$$\eta_s = K \lambda \quad (109)$$

The calibration data for the particular viscosimeter used (Tables 1, Figs. 17 & 18) indicated that K was not quite constant but varied slightly with λ . For this reason the relationship between ν or η_s and λ is presented graphically in figures (19) and (20). Figure (20) is an expansion of the lower range of figure (19). It is recommended that figure (20) be used for slope values up to 5.5 or 5.6 and figure (19) be used for interpreting slope values greater than 5.6 gms. sec./ Rev.

A few points at the lower viscosities were checked and the coordinates have been marked on figure (17), as crosses and squares.

Using equation (110) and the viscosimeter calibration charts (Figs 19, 20) the suspension viscosimeter data (Table IV, Figs. 25, 26) were interpreted as yield values and coefficients of rigidity. The values so obtained are presented below in tabular and graphical form.

Figure (27) shows the relationship between the yield value (m^1) and the percent solids. The shape of the graph indicates an exponential relationship of the general form

$$m^1 = A (e^{ax} - 1) \quad (111)$$

where a, A are constants

x is the percent solids.

Figure (28) correlates the data as $\ln(m^1 + 0.001)$ vs. x to establish the equation:

$$m^1 = 0.001 (e^{0.158x} - 1) \quad (112)$$

Either figure (28) or equation (112) may be used to smooth the data. Figure (29) presents smoothed yield values correlated with percent solids. These values which are also tabulated below, were used in subsequent calculation.

Figure (30) presents the relationship between the coefficients of rigidity and the percent solids.

Again an exponential form is suggested. The coefficient of rigidity is temperature sensitive particularly at values of the same magnitude as the carrier fluid viscosity. This effect is assumed to be due to the liquid present and independent of the solid. By subtracting the viscosity of the carrier fluid from the coefficient of rigidity the difference, the effect due to the solid, should be unaffected by small changes in temperature. Values of this difference ($\gamma_s - \mu = \Delta$) are tabulated below for reference. In correlating the coefficients of rigidity with percent solids figure (31) was prepared. Instead of attempting to relate the coefficients of rigidity directly to percent solids, $\ln(\gamma_s - \mu + 0.042)$ was plotted against (x) the percent solids. Figure (31) gives rise to the following equation

$$\gamma_s = \mu + 0.042 (e^{0.159x} - 1) \quad (113)$$

This form of equation allows the temperature effect to be taken into consideration via the viscosity of the carrier fluid.

Figure (32) illustrates the relationship between the smoother coefficients of rigidity and the percent solids. The values used are tabulated below (Table XXXI) together with values of $(\gamma_s - \mu)$. These smoothed data were used in subsequent calculations.

VI

CALCULATED RESULTS

Table XXX

SUSPENSION PROPERTIES

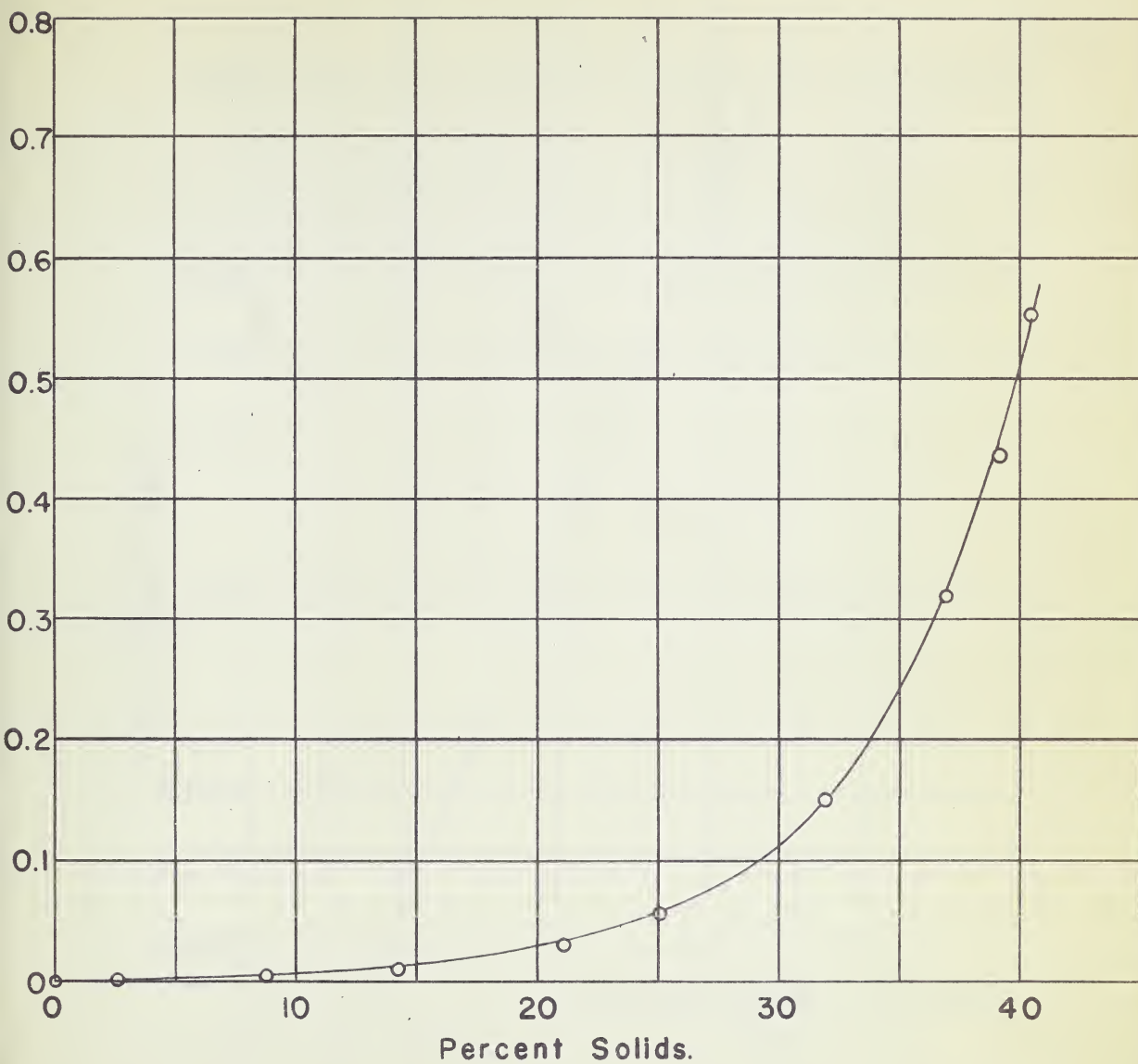
Run	% Solids	Density	Yield Load	Viscosimeter data slope	Yield Value	Coefficient of Rigidity	Smoothed	
							Yield Value	Coefficient of Rigidity
		lbs/ft ³	gms.	gms.secs. rev.	lbs ft ²	lbs ft.sec.	lbs ft ²	lbs ft.sec.
A	2.5	63.0	0	3.88	--	0.000526	0.0005	
B	8.8	65.0	1.0	4.02	0.00221	0.00064	0.0030	
C	14.3	67.1	4.0	4.27	0.00884	0.00082	0.0085	
D	21.2	71.2	14	4.64	0.03095	0.00118	0.0270	
E	25.0	73.2	25	4.83	0.0553	0.00132	0.0500	
F	31.9	77.5	68	6.87	0.150	0.0047	0.1480	
G	36.8	79.8	144	8.14	0.318	0.00655	0.315	
H	39.2	81.2	197	10.0	0.436	0.0103	0.470	
J	40.4	82.4	250	13.0	0.553	0.0159	0.560	

See Table XXXI
below.

Table XXXI

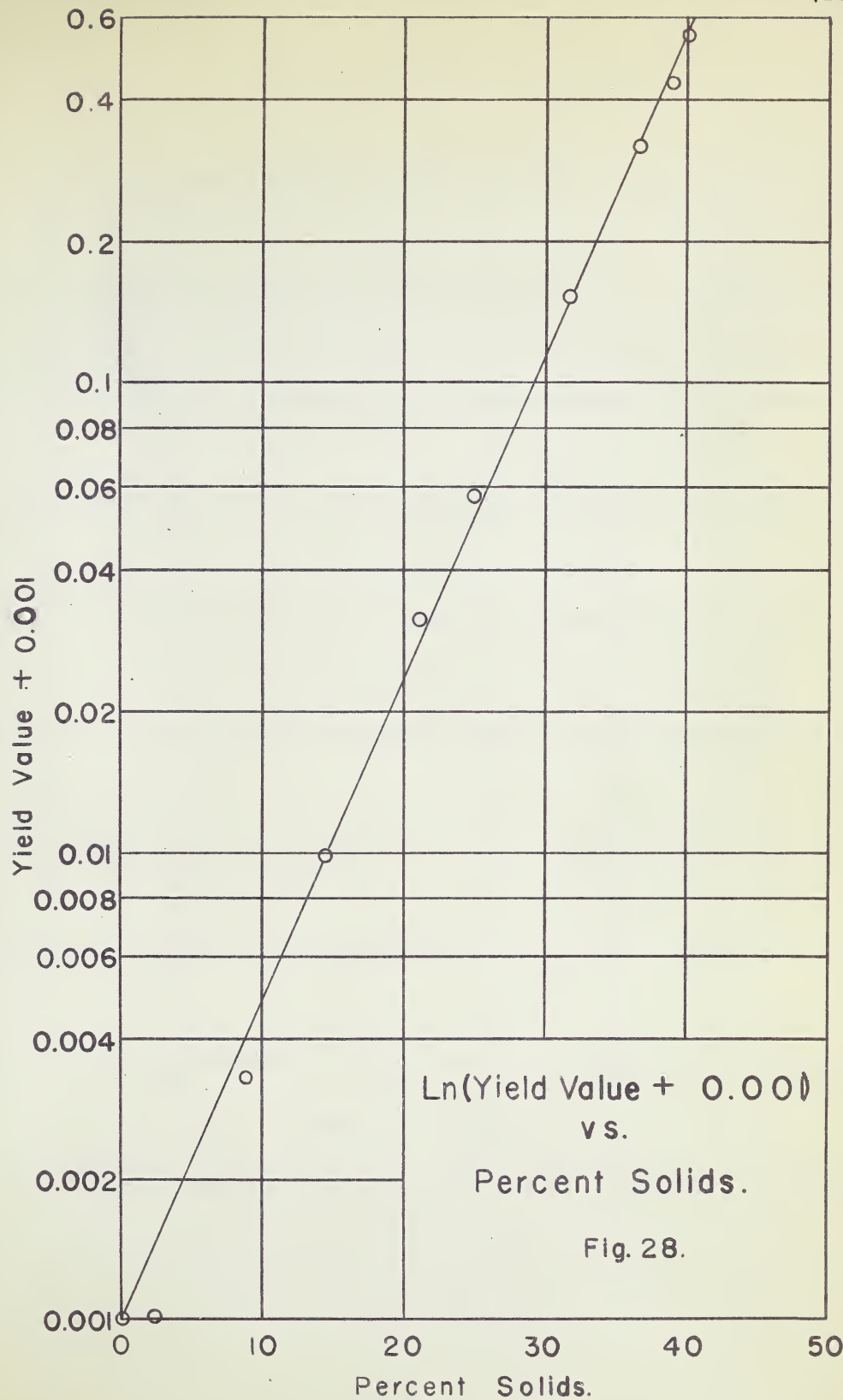
VARIATION OF η WITH TEMPERATURE

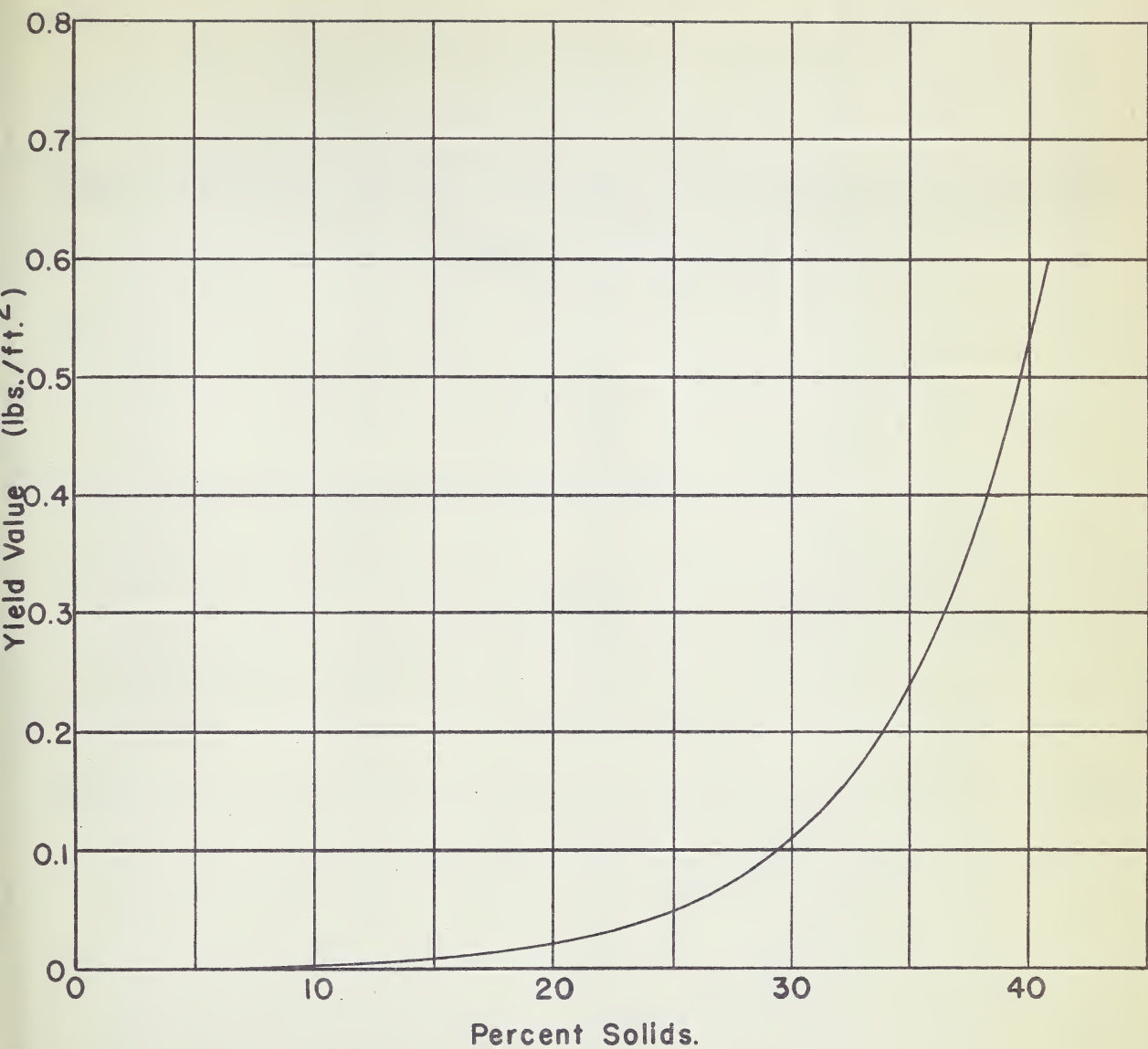
Run	η	25° C.	27° C.	29° C.	31° C.	33° C.	35° C.
A	0.0 ₄ 30	0.00063	0.000604	0.000579	0.000556	0.000535	0.000515
B	0.0 ₄ 82	0.000682	0.000654	0.000631	0.000608	0.000587	0.000567
C	0.0 ₃ 20	0.00080	0.000774	0.00744	0.00726	0.00705	0.000685
D	0.0 ₃ 56	0.001,16	0.00113	0.00111	0.00109	0.00107	0.00105
E	0.001,06	0.00166	0.00163	0.00161	0.00159	0.00157	0.00155
F	0.003,23	0.00383	0.00380	0.00378	0.00376	0.00374	0.00372
G	0.006,98	0.00758	0.00755	0.00753	0.00751	0.00749	0.00747
H	0.0107	0.0113	0.0113	0.0113	0.0112	0.0112	0.0112
J	0.0150	0.0156	0.0156	0.0156	0.0155	0.0155	0.0155



Yield Value vs. Percent Solids.

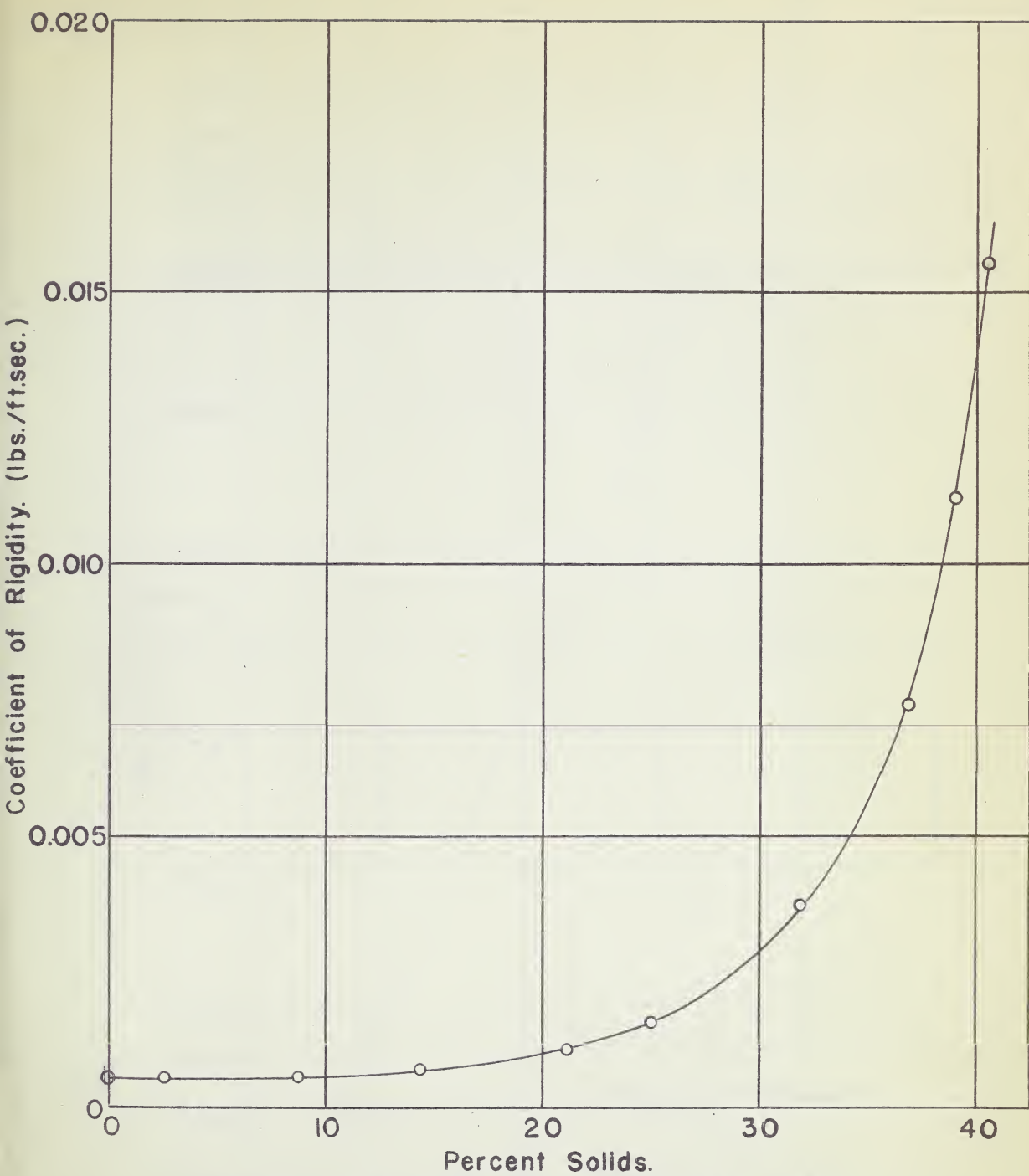
Fig. 27.





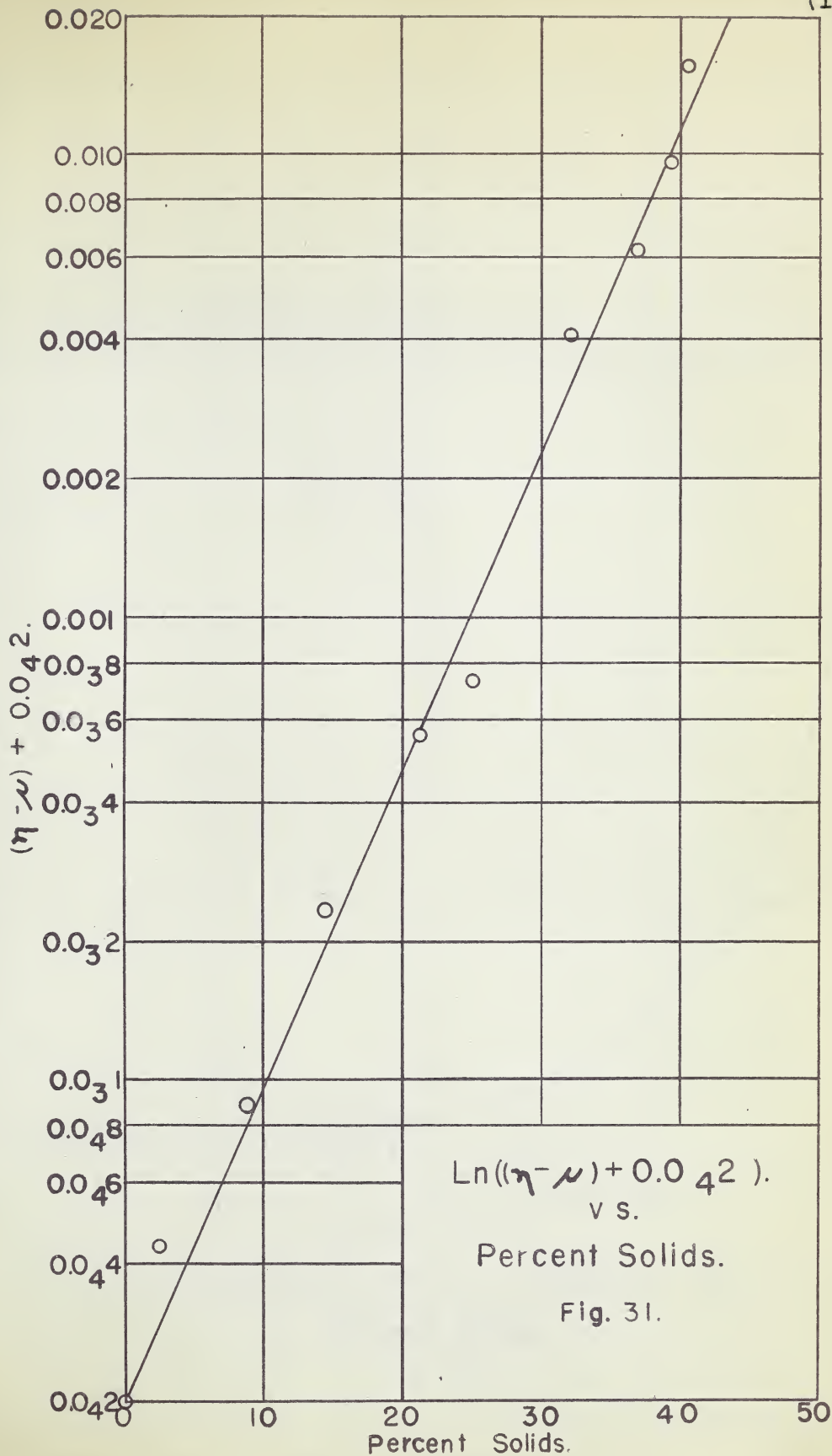
Smoothed Yield Value vs. Percent Solids.

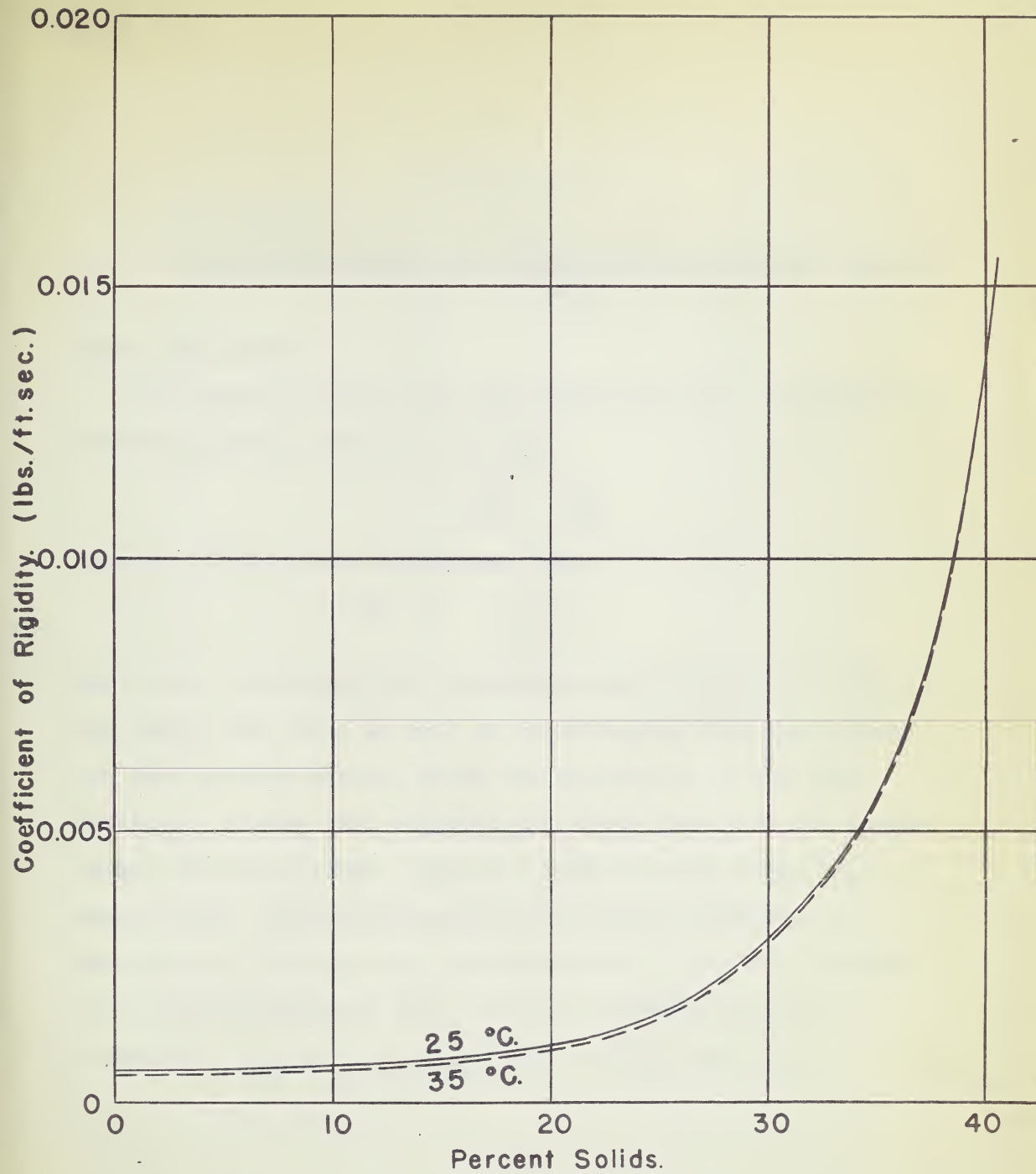
Fig. 29.



Coefficient of Rigidity vs. Percent Solids.

Fig. 30.





Smoothed Coefficient of Rigidity vs.
Percent Solids.

Fig. 32.

FINAL CALCULATIONS AND CORRELATION OF RESULTS (cont'd)

Water flow runs:

The friction factors for the water runs were calculated by means of equation (21) in the form

$$f = - \frac{\Delta P}{\rho V^2} \cdot \frac{\beta D}{2L}$$

Reynolds numbers were calculated from

$$N_{Re} = \frac{DV\rho}{\mu}$$

The values so obtained are tabulated below (Tables 32 - 35).

The water test runs, as well as establishing flow conditions for zero percent solids, check the smoothness of the test sections. Figure (33) compares the water data with the theoretical friction factor - Reynolds number relationship for smooth pipe. In the streamline flow region Poiseuille's theoretical line was used for comparison and in the turbulent flow region Nik^{ur}adse's line, which is obtained from the equation $\frac{1}{4f} = 2 \log N_{Re} \sqrt{4f} - 0.8$, was used.

RESULTS

Table XXXII

Water Test Run #1

Test No.	<u>Reynolds Number</u>		<u>Friction Factor</u>	
	Pipe Size	3/4" 1 1/4"	3/4" 1 1/4"	
1		3,340 2,050	0.00922 0.00915	
2		4,940 3,040	0.00895 0.0130	
3		5,900 3,600	0.00870 0.0118	
4		7,170 4,270	0.00874 0.0114	
5		7,820 4,780	0.00832 0.0103	
6		8,620 5,290	0.00821 0.0105	
7		9,240 5,650	0.00811 0.0100	
8		10,000 6,120	0.00795 0.0115	
9		9,100 5,550	0.00826 0.00820	
10		13,100 8,020	0.00764 0.00804	
11		17,200 10,500	0.00716 0.00754	
12		21,700 13,200	0.00668 0.00729	
13		25,500 15,600	0.00642 0.00712	
14		28,600 17,600	0.00642 0.00706	
15		31,600 19,500	0.00632 0.00706	
16		35,000 21,300	0.00611 0.00706	
17		47,800 29,300	0.00547 --	
18		70,400 43,200	0.00524 0.00572	
19		90,300 53,700	0.00472 0.00550	
20		109,500 66,700	0.00438 0.00520	
21		123,000 75,000	0.00435 0.00519	

CALCULATED RESULTS

Table XXXIII

Water Test Run #2

Test No.	Pipe Size	<u>Reynolds Number</u>		<u>Friction Factor</u>	
		3/4"	1 1/4"	3/4"	1 1/4"
1		2,150	1,310	0.00477	0.0154
2		2,520	1,550	0.00843	--
3		2,970	1,840	0.00837	0.0129
4		3,310	2,040	0.00863	0.0113
5		3,820	2,350	0.00863	0.0110
6		4,140	2,550	0.00873	0.0114
7		4,500	2,770	0.00849	0.0113
8		5,420	3,340	0.00900	0.00813
9		5,900	3,630	0.00952	0.00695
10		6,880	4,230	0.00863	0.00687
11		7,700	4,730	0.00843	0.00633
12		8,340	5,140	0.00837	0.00643
13		8,970	5,510	0.00826	0.00663
14		9,440	5,800	0.00810	0.00654
15		9,900	6,080	0.00800	0.00651
16		10,600	6,500	0.00926	0.00777
17		14,400	8,880	0.00726	0.00881
18		18,200	11,700	0.00668	0.00747
19		19,700	12,050	0.00690	0.00767
20		23,500	14,500	0.00632	0.00776
21		26,900	16,550	0.00613	0.00693
22		28,900	17,800	0.00614	0.00702
23		32,900	20,250	0.00668	0.0119
24		37,000	22,800	0.00568	0.00618
25		61,900	38,100	0.00540	0.00569
26		95,000	58,500	0.00448	0.00475
27		107,000	65,800	0.00435	0.00464
28		120,500	74,000	0.00422	0.00477

CALCULATED RESULTS

Table XXXIV

Water Test Run #3

June 8th 1948

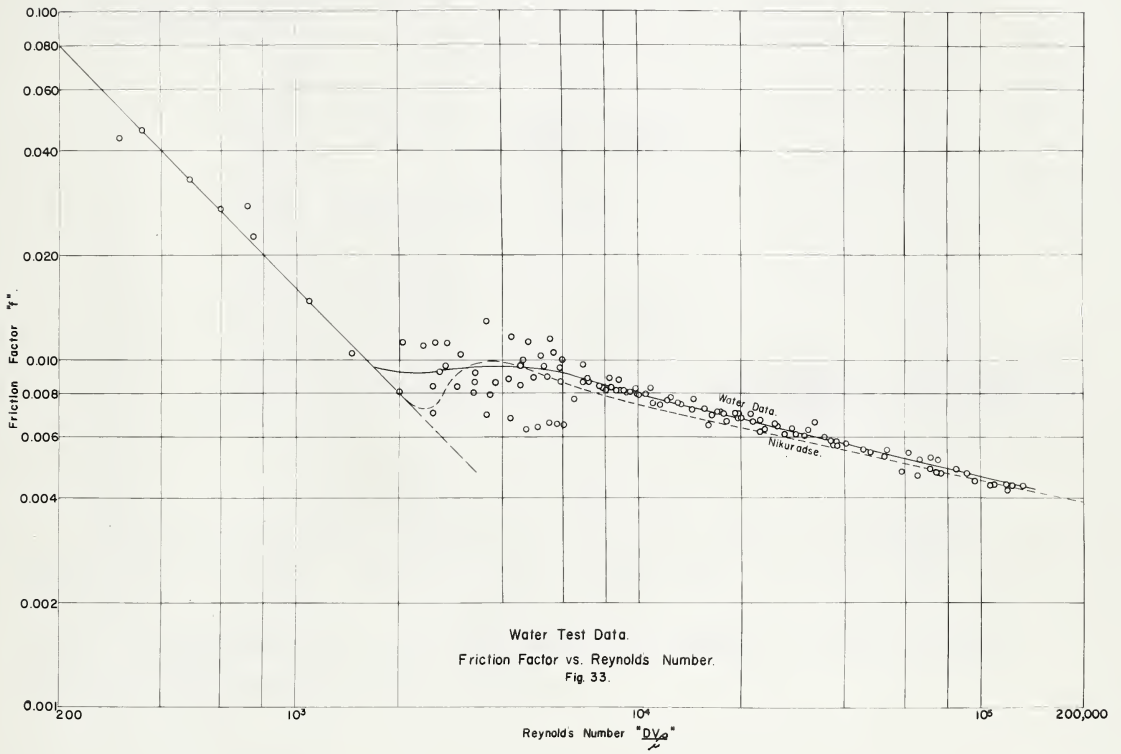
<u>Test No.</u>	<u>Pipe Size inches</u>	<u>Reynolds Number</u>	<u>Friction Factor</u>
1	1 1/4	300	0.0432
2	1 1/4	351	0.0456
3	1 1/4	484	0.0329
4	3/4	724	0.0277
5	3/4	1458	0.0104
6	3/4	2500	0.00706
7	3/4	2615	0.00938
8	3/4	3310	0.00806
9	3/4	3660	0.00795

Table XXXV

Water Test Run #4

July 9th 1948

<u>Test No.</u>	<u>Reynolds Number</u>		<u>Friction Factor</u>	
	<u>Pipe Size</u>	<u>3/4" 1 1/4"</u>	<u>3/4" 1 1/4"</u>	
1	594	366	0.0272	No pressure reading
2	743	496	0.0226	
3	1,080	662	0.0148	
4	1,980	1,230	0.00812	
5	2,720	1,680	0.00970	
6	3,010	1,850	0.0104	
7	4,060	2,510	0.0101	
8	5,300	3,260	0.00965	
9	7,100	4,380	0.00891	
10	8,280	5,180	0.00896	
11	9,810	6,120	0.00838	
12	10,800	6,750	0.00833	
13	11,100	6,900	0.00754	0.00976
14	20,050	12,500	0.00685	0.00785
15	25,100	16,100	0.00659	0.00652
16	30,300	19,400	0.00604	0.00710
17	36,800	22,900	0.00585	0.00675
18	40,500	25,000	0.00575	0.00655
19	45,400	28,000	0.00553	0.00638
20	84,800	52,200	0.00487	0.00529
21	119,000	71,600	0.00437	0.00483
22	123,000	76,800	0.00436	0.00472



FINAL CALCULATIONS AND CORRELATION OF RESULTS (cont'd)

Suspension flow runs:

The literature review indicated that, for suspensions, values of the following dimensionless ratios might be of use in establishing relationships to predict pressure drops from flow rates.

$$a. \quad "f" = - \frac{\Delta P}{V^2 \rho_s} \cdot \frac{\beta D}{2L}$$

$$b. \quad N_{Re(i)} = \frac{DV\rho_s}{\mu_i}$$

$$c. \quad N_{Re(ii)} = \frac{DV\rho_s}{\eta_s}$$

$$d. \quad N_{Re(iii)} = \frac{DV\rho_s}{\eta_s} \left[\frac{1-4}{3} \left(\frac{2Lm'}{R\Delta P} \right) + \frac{1}{3} \left(\frac{2Lm'}{R\Delta P} \right)^4 \right]$$

These ratios were calculated and are tabulated below (Tables 36 to 44). It was found convenient to apply all the "corrections" as modified Reynolds numbers and to leave the friction factor unaltered.

CALCULATED RESULTS

Table XXXVI

Run A

Test No.	Pipe Size	<u>Friction Factor</u>		<u>Reynolds Number</u>		<u>Reynolds Number</u>		<u>Reynolds Number</u>	
		3/4"	1 1/4"	$\frac{DV\sqrt{s}}{\mu}$ 3/4"	1 1/4"	$\frac{DV\sqrt{s}}{\eta_s}$ 3/4"	1 1/4"	$\frac{DV\sqrt{s}}{\eta_s} \left[1 - \frac{4}{3} \left(\frac{\mu}{\eta_s \rho} \right) + \frac{1}{3} \left(\frac{\mu}{\eta_s \rho} \right)^4 \right]$ 3/4"	1 1/4"
1		0.0345	0.161	318	197	265	164	-	-
2		0.0220	0.0488	1,003	617	836	512	-	-
3		0.0119	0.0480	3,830	2,470	3,200	1,970	743	
4		0.0105	0.0377	5,220	3,220	4,840	2,680	3,860	
5		0.0122	0.00577	5,880	3,610	4,900	3,000	4,230	
6		0.00937	0.00475	8,000	4,920	6,660	4,100	6,120	16.2
7		0.00923	0.00525	9,320	5,750	7,780	4,780	7,220	908
8		0.00891	0.00672	9,850	6,050	8,210	5,030	7,660	2,012
9		0.00832	0.00985	11,100	6,850	9,500	5,840	8,960	3,920
10		0.00832	0.0125	12,400	7,650	10,600	6,520		5,160
11		0.00780	0.00828	14,800	9,110	12,600	7,760		6,090
12		0.00669	0.00840	24,100	14,900	20,600	12,700		11,700
13		0.00611	0.00671	34,400	21,300	30,000	24,400		
14		0.00590	0.00627	45,500	28,000	39,700	24,400		
15		0.00616	0.00711	48,700	30,100	43,500	26,900		
16		0.00548	0.00603	58,200	35,900	51,700	32,100		
17		0.00487	0.00533	97,500	60,200	87,000	53,700		
18		0.00461	0.00502	124,000	76,500	111,000	68,300		
19		0.00456	0.00512	148,000	91,800	132,000	81,800		
20		0.00428	0.00505	182,000	112,500	162,000	100,000		
21		0.00424	0.00480	199,000	123,000	177,000	109,500		

CALCULATED RESULTS

Table XXXVII

Run B

Test Pipe No.	Friction Factor		Reynolds Number		Reynolds Number		Reynolds Number	
	Size - 3/4"	1 1/4"	$\frac{DV_s}{\mu_L}$	$\frac{DV_s}{\mu_L}$	$\frac{DV_s}{\mu_s}$	$\frac{DV_s}{\mu_s}$	$\frac{DV_s}{\mu_s} \left[1 - \frac{4}{3} \left(\frac{2L}{RAP} \right) + \frac{1}{3} \left(\frac{2L}{RAP} \right)^4 \right]$	$\frac{DV_s}{\mu_s}$
1	0.111	0.275	1,020	623	1,145	704	3.4	
2	0.0732	0.205	1,620	1,100	1,830	1,130	503	
3	0.210	0.553	975	600	1,100	677	328	
4	0.00795	0.0189	5,540	3,420	6,260	3,860	2,790	
5	0.00822	0.0141	6,900	4,260	7,810	4,810	4,920	111
6	0.0144	0.0791	4,230	2,620	5,360	3,300	2,410	1,050
7	0.00690	0.0159	13,100	8,080	16,500	10,200	14,500	6,420
8	0.00654	0.0105	17,850	11,000	22,600	13,900		9,730
9	0.00600	0.00853	21,900	13,600	27,700	17,100		12,900
10	0.00527	0.00692	28,800	17,900	36,400	22,600		
11	0.00497	0.00636	32,200	19,900	40,800	25,000		
12	0.00497	0.00551	37,400	23,200	47,700	29,500		
13	0.00257	0.00270	53,000	32,800	67,500	41,600		
14	0.00420	0.00465	80,000	49,400	102,000	62,600		
15	0.00407	0.00442	106,000	65,500	135,000	83,200		
16	0.00442	0.00513	116,000	71,400	149,000	91,800		

CALCULATED RESULTS

Table XXXVIII

Run C

Test No.	<u>Friction Factor</u>		<u>Reynolds Number</u>		<u>Reynolds Number</u>		<u>Reynolds Number</u>	
			$\frac{DV_{23}}{\nu_c}$		$\frac{DV_{23}}{\eta_g}$		$\frac{DV_{23}}{\eta_g} \left[1 - \frac{q}{3} \left(\frac{2Lm'}{R\Delta P} \right) + \frac{1}{3} \left(\frac{2Lm'}{R\Delta P} \right)^2 \right]$	
Pipe Size	3/4"	1 1/4"	3/4"	1 1/4"	3/4"	1 1/4"	3/4"	1 1/4"
1	273	1410	17.9	11.0	10.8	6.68	-	-
2	27.7	66.5	145	89.0	87.5	54.0	-	-
3	238	268	19.6	12.0	11.9	7.31	-	-
4	17.1	106	149	91.9	90.3	55.7	-	-
5	0.932	5.55	896	551	551	340	3.31	30.6
6	5.43	36.6	318	196	198	121	-	-
7	0.150	0.685	2,840	1,760	1,780	1,100	414	1.10
8	0.0717	0.362	4,440	2,720	2,720	1,710	925	168
9	0.0123	0.0384	13,300	8,220	8,150	5,020	4,370	276
10	0.00806	0.0237	21,400	13,200	13,100	8,040	9,440	7,490
11	0.0070	0.0141	32,500	20,000	20,000	12,400	17,200	6,180
12	0.00696	0.0100	37,900	23,200	23,200	14,300		6,760
13	0.00637	0.00741	46,600	28,800	28,500	17,500		9,220
14	0.00626	0.00685	55,000	33,800	33,600	20,600		
15	0.00685	0.00650	49,700	30,600	30,600	18,800		
16	0.00543	0.00599	89,700	55,200	55,200	33,900		
17	0.00502	0.00564	125,000	78,200	75,800	46,600		
18	0.00488	0.00539	157,000	97,500	92,600	58,600		
19	0.00452	0.00510	191,500	118,000	115,000	70,700		
20	0.00420	0.00482	236,000	145,000	142,000	87,400		

CALCULATED RESULTS

Table XXXIX

Run D

Test No.	<u>Friction Factor</u>		<u>Reynolds Number</u>		<u>Reynolds Number</u>		<u>Reynolds Number</u>	
			$\frac{DV \rho}{\mu}$		$\frac{DV \rho}{\mu}$		$\frac{DV \rho}{\mu} \left[1 - \frac{4}{3} \left(\frac{2Lm'}{RDP} \right) + \frac{1}{3} \left(\frac{2Lm'}{RDP} \right)^4 \right]$	
Pipe Size	3/4"	1 1/4"	3/4"	1 1/4"	3/4"	1 1/4"	3/4"	1 1/4"
1	16.2	7.22	330	203	137	82.4	-	-
2	0.380	0.236	2,620	1,620	1,090	672	447	
3	2.5	2.92	1,320	917	550	381	2.2	
4	0.0299	0.0496	14,000	5,440	5,840	3,600	2,730	
5	10.2	61.3	519	319	218	132	5.45	
6	0.0071	0.0246	34,300	21,100	14,300	8,750	8,870	2,350
7	0.00638	0.00950	60,500	37,300	25,200	15,500	21,700	5,970
8	0.00585	0.00616	90,900	55,300	37,400	23,200		13,000
9	0.00537	0.00581	110,000	71,900	49,000	30,100		
10	0.00506	0.00551	151,000	91,100	61,900	38,100		
11	0.00497	0.00553	178,000	106,000	71,900	44,200		
12	0.00477	0.00532	196,000	116,000	80,500	49,600		
13	0.00468	0.00543	212,000	125,000	86,500	53,200		

CALCULATED RESULTS

Table XL

Run E

Test No.	<u>Friction Factor</u>		<u>Reynolds Number</u>		<u>Reynolds Number</u>		<u>Reynolds Number</u>	
	$\frac{DV \rho_s}{\mu_s}$		$\frac{DV \rho_s}{\eta_s}$		$\frac{DV \rho_s}{\eta_s}$		$\frac{DV \rho_s}{\eta_s} \left[1 - \frac{4}{3} \left(\frac{2Lm'}{R\alpha P} \right) + \frac{1}{3} \left(\frac{2Lm'}{R\alpha P} \right)^2 \right]$	
Pipe Size	3/4"	1 1/4"	3/4"	1 1/4"	3/4"	1 1/4"	3/4"	1 1/4"
1	2.90	17.1	1,030	633	358	220	1.79	24.2
2	123	81,800	6.74	4.15	2.34	1.44	-	-
3	37.3	239	272	167	93.6	56.9	7.2	-
4	144	57,400	10.8	6.64	37.0	22.7	-	-
5	18.4	105	386	238	132	81.4	13.6	-
6	345	2,140	75.0	46.2	25.6	15.8	-	-
7	14.3	109.5	445	275	152	93.9	9.88	0.469
8	0.272	1.51	4,020	2,590	1,370	886	136	-
9	0.00705	0.00722	69,900	47,900	23,900	16,400	2,100	5,340
10	0.00685	0.0152	47,100	29,000	15,900	9,770	11,100	2,450
11	0.00943	0.0445	28,500	17,600	9,640	5,930	4,370	1,120
12	5.95	34.9	822	505	279	171	11.7	-
13	0.00578	0.00647	98,000	60,200	32,900	20,300	-	9,750
14	0.00520	0.00616	136,000	83,700	45,800	28,200	-	-
15	0.00483	0.00522	164,000	101,000	54,400	33,700	-	-
16	0.00471	0.00511	192,000	117,000	63,600	39,000	-	-

CALCULATED RESULTS

Table XLI

Run F

Test No.	<u>Friction Factor</u>		<u>Reynolds Number</u>		<u>Reynolds Number</u>		<u>Reynolds Number</u>	
			$\frac{DV \rho}{\mu}$		$\frac{DV \rho}{\mu}$		$\frac{DV \rho}{\mu} \left[1 - \frac{4}{3} \left(\frac{2L}{ReP} \right) + \frac{1}{3} \left(\frac{2L}{ReP} \right)^4 \right]$	
Pipe Size	3/4"	1 1/4"	3/4"	1 1/4"	3/4"	1 1/4"	3/4"	1 1/4"
1	94.3	2,180	72.2	45.1	10.5	6.53	-	
2	11.1	82.5	596	369	86.6	53.8	-	
3	1.67	7.68	2,570	1,580	372	229	2.90	
4	90.6	370	323	200	46.8	28.9	1.20	
5	8.8	37.8	960	591	139	85.5	-	
6	2.34	9.42	2,230	1,380	324	200	4.86	
7	0.142	0.669	9,750	6,000	1,410	870	152	37.4
8	0.0785	0.394	18,000	9,590	2,250	1,390	658	131
9	0.00622	0.0196	77,800	48,100	11,200	6,880	7,190	805
10	0.00601	0.0134	101,000	62,200	14,500	8,950	11,100	2,760
11	0.00569	0.00874	123,000	75,500	17,500	10,900		2,880
12	0.00543	0.00695	154,000	98,200	22,100	13,600		5,460
13	0.00511	0.00624	180,000	114,600	26,800	16,500		8,550
14	0.00514	0.00588	201,000	123,000	28,700	17,700		

CALCULATED RESULTS

Table XLIII

Run G

Test No.	<u>Friction Factor</u>		<u>Reynolds Number</u>		<u>Reynolds Number</u>		<u>Reynolds Number</u>	
			$\frac{DV\beta}{\mu}$		$\frac{DV\beta}{\eta_s}$		$\frac{DV\beta_s}{\eta_s} \left[1 - \frac{4}{3} \left(\frac{2.1\eta}{\eta_s \rho} \right) + \frac{1}{3} \left(\frac{2.1\eta}{\eta_s \rho} \right)^4 \right]$	
Pipe Size	3/4"	1 1/4"	3/4"	1 1/4"	3/4"	1 1/4"	3/4"	1 1/4"
1	9.28	56.8	1,530	941	112	68.9	1.23	6.39
2	2,205	211,000	14.6	0.900	1.06	0.66	-	-
3	70.9	390	494	304	36.1	22.3	-	-
4	529	243	626	387	45.3	27.9	1.50	-
5	0.906	5.14	5,670	3,430	404	249	21	8.46
6	6.12	32.5	2,000	1,244	145	89.2	0.435	12.7
7	0.664	3.50	6,890	4,240	490	300	40.7	1.5
8	0.200	1.12	13,550	8,270	944	575	139	14.4
9	0.722	0.412	23,750	14,600	1,630	1,000	324	84
10	0.0109	0.0592	67,900	41,800	4,640	2,870	1,510	496
11	0.00575	0.0263	106,000	65,500	7,270	4,460	3,370	557
12	0.00569	0.0180	132,000	81,200	8,920	5,440	5,660	1,300
13	0.00554	0.0136	156,000	96,200	10,650	6,470	7,780	1,790
14	0.00559	0.0113	175,000	107,800	11,700	7,200	-	2,095
15	0.00538	0.00959	189,000	116,000	12,700	7,750	-	2,120
16	0.00517	0.00766	223,000	138,000	14,800	9,040	-	3,030

CALCULATED RESULTS

Table XLIII

Run H

Test No.	<u>Friction Factor</u>		<u>Reynolds Number</u>		<u>Reynolds Number</u>		<u>Reynolds Number</u>	
	Pipe Size		$\frac{DV}{\mu} \frac{\rho}{\gamma}$		$\frac{DV}{\mu} \frac{\rho}{\gamma}$		$\frac{DV}{\mu} \frac{\rho}{\gamma} \left[1 - \frac{4}{3} \left(\frac{2.6}{Re} \right)^4 + \frac{1}{3} \left(\frac{2.6}{Re} \right)^4 \right]$	
	3/4"	1 1/4"	3/4"	1 1/4"	3/4"	1 1/4"	3/4"	1 1/4"
1	9.27	496	552	345	26.3	16.2	3.6	
2	7.32	34.6	2,195	1,370	105	64.5	-	
3	312	1,050	219	136	10.4	6.42	-	
4	0.537	3.06	9,160	5,720	424	261	19.5	
5	23.3	1,420	437	274	20.2	12.5	0.909	0.0625
6	0.0795	0.515	26,200	16,350	1,170	722	52.7	60.5
7	0.0127	0.0743	74,200	46,200	3,320	2,040	927	768
8	0.00616	0.0333	113,000	70,700	5,080	3,130	1,790	997
9	0.00590	0.0304	122,000	75,700	5,410	3,320	2,160	700
10	0.00564	0.0261	134,500	83,700	5,900	3,620	2,760	829
11	0.00564	0.0185	162,000	101,000	7,040	4,330	4,570	1,030
12	0.00532	0.0108	220,000	137,600	9,570	5,890	7,470	1,660

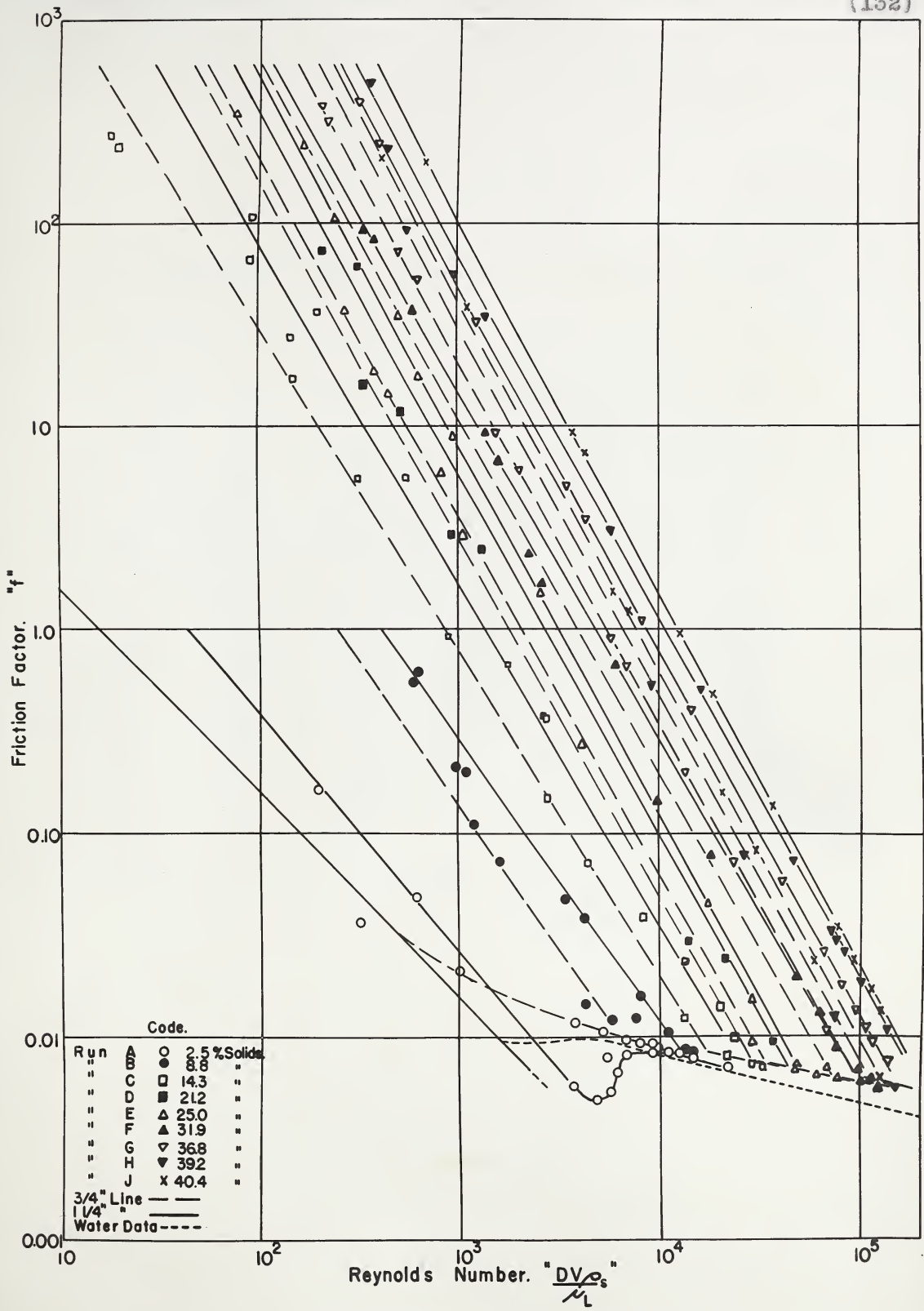
Table XLIV

Run J

Test No.	<u>Friction Factor</u>		<u>Reynolds Number</u>		<u>Reynolds Number</u>		<u>Reynolds Number</u>	
	Pipe Size		$\frac{DV}{\mu} \frac{\rho}{\gamma}$		$\frac{DV}{\mu} \frac{\rho}{\gamma}$		$\frac{DV}{\mu} \frac{\rho}{\gamma} \left[1 - \frac{4}{3} \left(\frac{2.6}{Re} \right)^4 + \frac{1}{3} \left(\frac{2.6}{Re} \right)^4 \right]$	
	3/4"	1 1/4"	3/4"	1 1/4"	3/4"	1 1/4"	3/4"	1 1/4"
1	234	1,470	409	252	14.3	8.86		1.01
2	38.7	199	1,120	688	39.5	24.2	0.868	2.2
3	1.52	9.25	5,990	3,690	209	129	14.0	0.257
4	1.23	7.40	7,060	4,350	248	153	33.2	8.41
5	0.159	0.959	20,600	12,800	720	444	137	0.444
6	0.0805	0.486	30,200	18,600	1,000	638	228	107
7	0.0236	0.136	59,100	36,300	2,030	1,250	593	215
8	0.00632	0.0340	125,000	76,700	4,280	2,640	1,710	642
9	0.00561	0.0237	152,000	93,400	5,150	3,180	2,645	324
10	0.00557	0.0171	183,000	113,000	6,220	3,840	4,150	1,070
11	0.00514	0.0132	209,000	129,000	7,020	4,340	5,120	1,270

Suspension flow runs: (cont'd)

To investigate any relationship between the friction factor "f" and $N_{Re(i)} = \frac{DV\sqrt{s}}{\mu}$ figures (34) and (35) were constructed. Figure (34) makes use of the data for $f > 0.011$. Figure (35) presents the data in the range $f < 0.011$ on a larger scale to show the effect of the percent solids to better advantage. The code which identifies the points in figures (34) to (50) is given on figure (34) and also on a flap inside the back cover of the thesis. This flap may be opened out and used in conjunction with the figures.



Friction Factor vs. Reynolds Number.

Fig. 34.

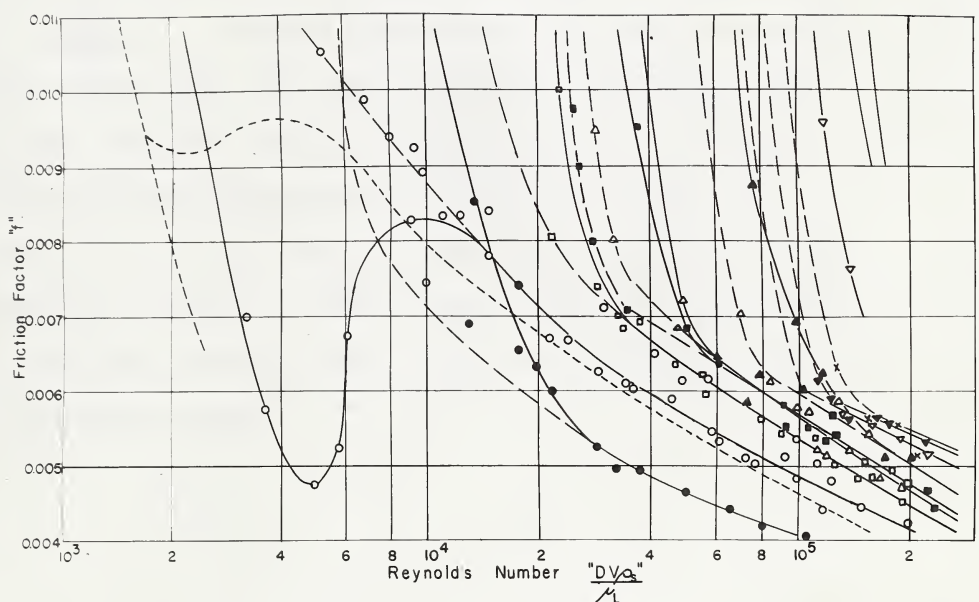


Fig. 35. Friction Factor vs. Reynolds Number.

(See Fig. 34 for code.)

Suspension flow runs: (cont'd)

Figures (36) and (37) below presents the suspension flow data as friction factor vs $N_{Re(ii)}$
 $= \frac{DV\eta_s}{\eta_s}$. Figure (36) covers the range $f < 0.011$ and figure (37) the range $f > 0.011$. On figure (37) a line labeled "Limit of Reliability of η " marks the boundary above and to the right of which the use of η_s is not justified by the viscosimeter data. However, it will be shown later that this limitation is not very serious and η_s may be used beyond its justifiable range.

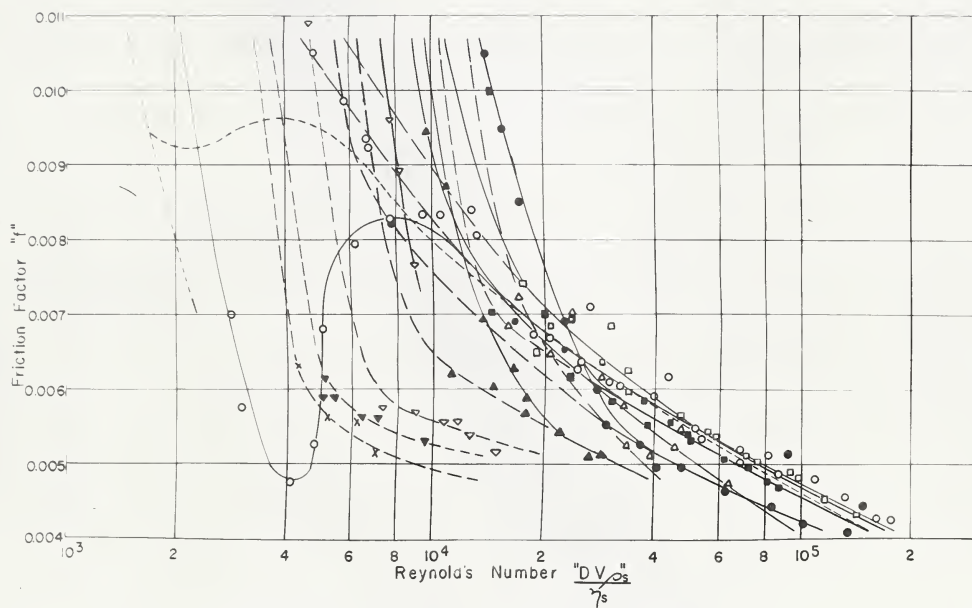


Fig 36. Friction Factor vs. Reynolds Number.

(See Fig 34 for code.)

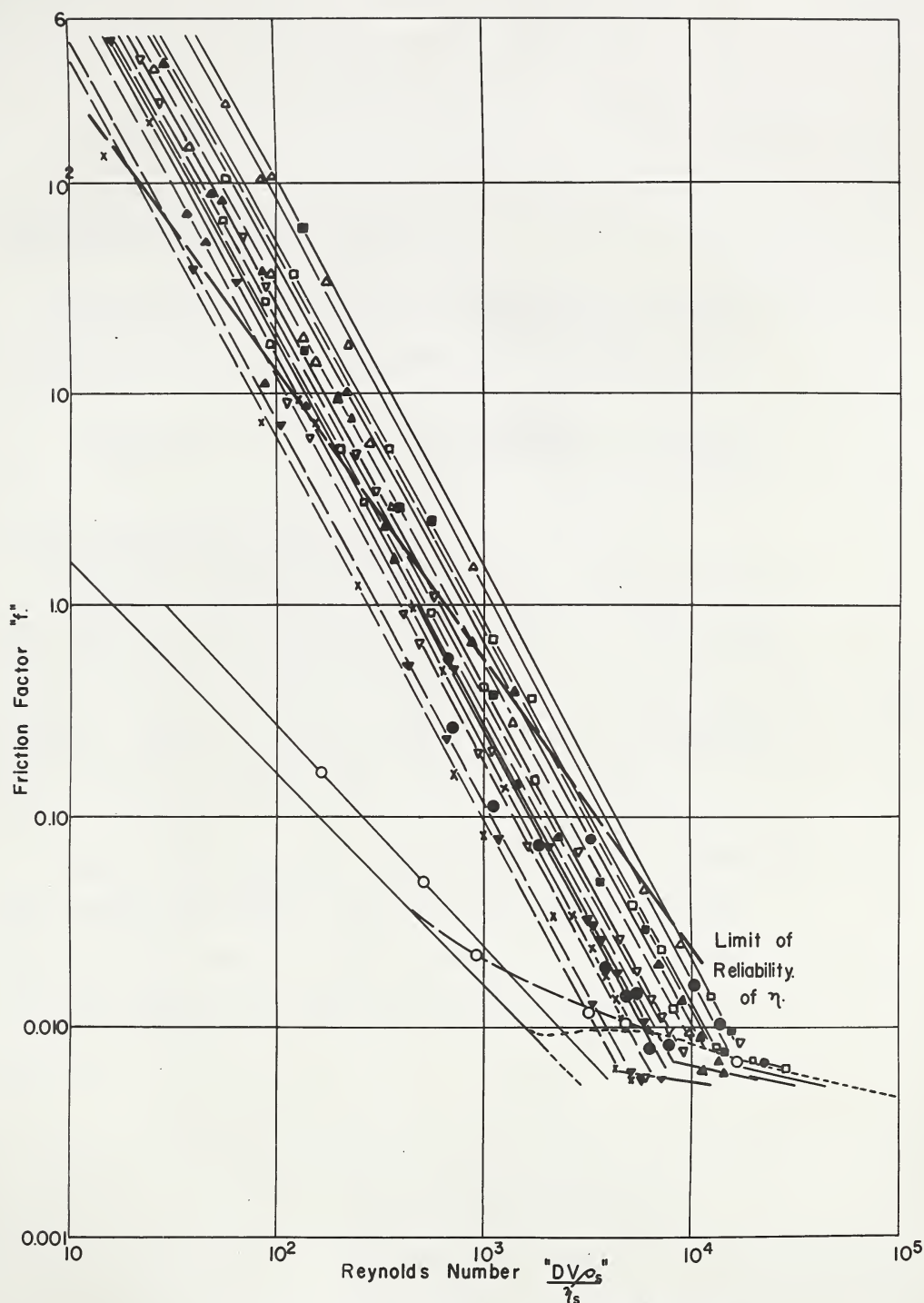


Fig. 37. Friction Factor vs. Reynolds Number.

(See Fig. 34 for code.)

Suspension flow runs: (cont'd)

Figure 38 illustrates the relationship between the friction factor and the modified Reynolds number

$$N_{Re(III)} = \frac{DV\beta}{\gamma_s} \left[1 - \frac{4}{3} \frac{(2Lm')}{(RAP)} + \frac{1}{3} \frac{(2Lm')^4}{(RAP)} \right]$$

in the streamline flow region.

Since the limit of reliability of γ_s , if taken on the same basis as in figure (37), should fall on the same line as the data only the extreme limit of γ_s is marked. Again the data indicate that it is probably safe to use γ_s outside its justifiable range.

Figure (39) combines figure (38) for the streamline flow region and figure (36) for the turbulent flow region. The range covered by each of the modified Reynolds numbers is indicated at the bottom of the figure.

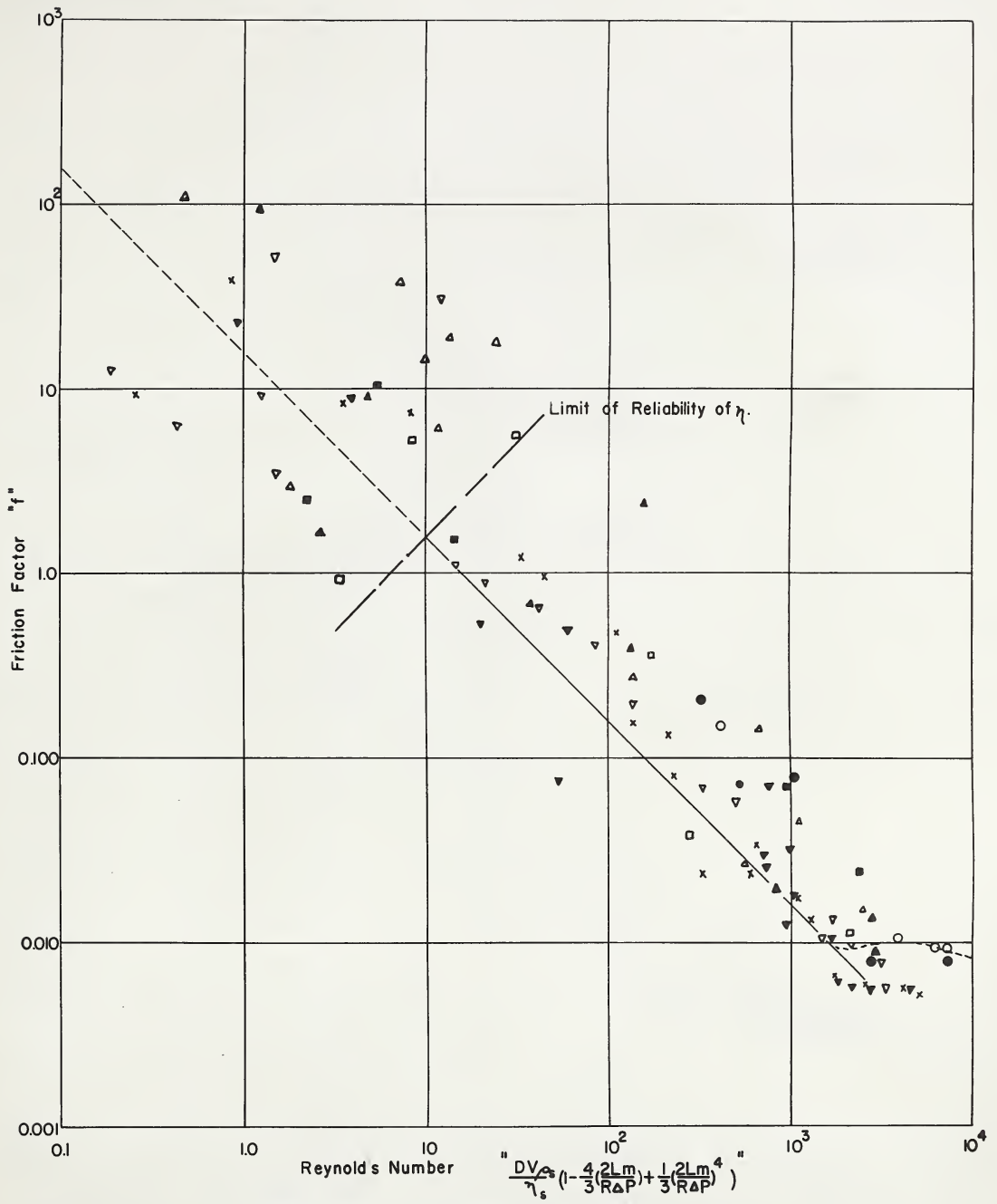


Fig.38. Friction Factor vs. Reynolds Number.

(See Fig.34 for code.)

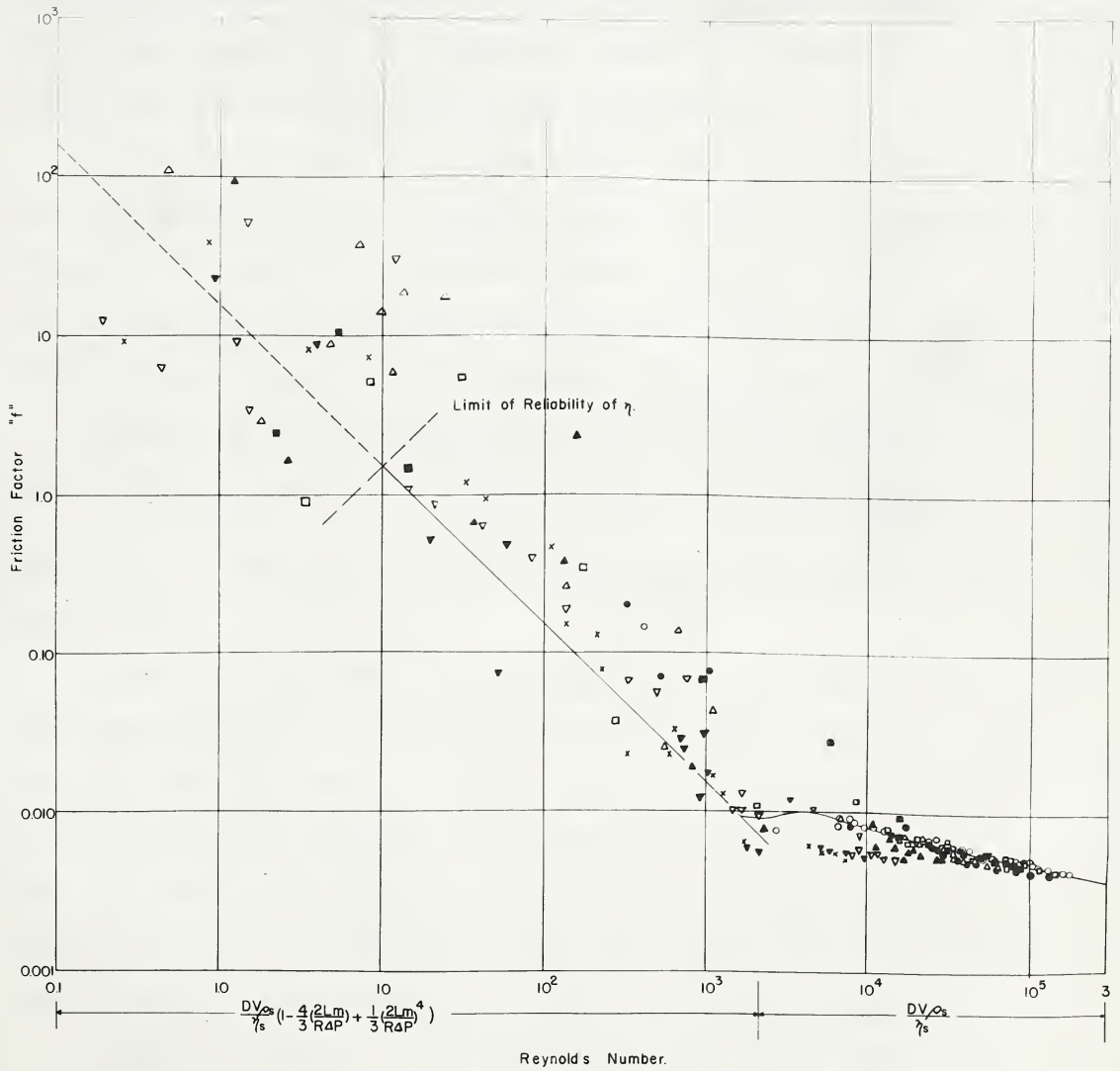


Fig 39 Friction Factor. vs. Reynolds Number.

(See Fig.34 for code.)

Suspension Flow Runs (cont'd)

Dimensional analysis indicated that a further ratio $\left(\frac{D_m \beta}{\sqrt{\eta_s}}\right)$, called the yield ratio, might be useful in establishing pressure drop - flow rate relationships. To locate the relative position of lines of equal values of the yield ratio with respect to the friction factor and Reynolds number the following procedure was followed.

Values of "f" were read from figure (37) at different percent solids and pipe diameters but at a series of constant values of the modified Reynolds number $\left(\frac{DV\beta}{\eta_s}\right)$. Knowing the particular pipe diameter and suspension properties for each of these values of "f" the ratio $\left(\frac{D_m^2 \beta \beta}{\eta_s^2}\right)$ was calculated.

Dividing the ratio $\left(\frac{D_m^2 \beta \beta}{\eta_s^2}\right)$ by the modified Reynolds number $\left(\frac{DV\beta}{\eta_s}\right)$ results in values of the yield ratio $\left(\frac{D_m \beta}{\sqrt{\eta_s}}\right)$.

The values of "f" and the yield ratio $\left(\frac{D_m \beta}{\sqrt{\eta_s}}\right)$ are listed below (Table 45).

Figures (40) to (50) which follow table (45) illustrate the variation of the friction factor with yield ratio at constant Reynolds number. These figures also serve as a source of smoothed data on the relationship between the friction factor, the yield ratio, and the modified Reynolds number, since it is possible to read off values of the friction factor at any yield ratio for a series of Reynolds numbers.

A table of smoothed data obtained in the above manner is presented below (Table 46).

CALCULATED RESULTS

TABLE XLV

Friction Factor "f" and Yield Ratio $\frac{Dm^2}{V\eta}$

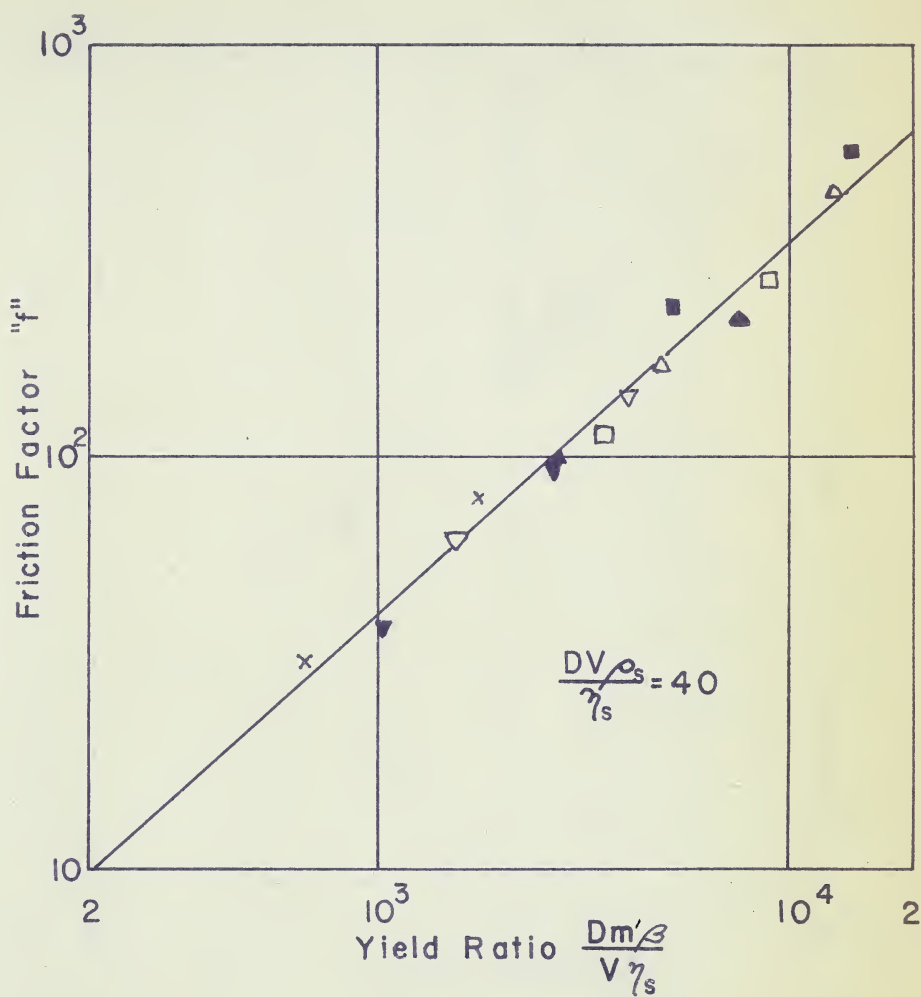
Pipe size.	Friction Factor		Yield Ratio		Friction Factor		Yield Ratio	
	<u>3/4"</u>	<u>1 1/4"</u>	<u>3/4"</u>	<u>1 1/4"</u>	<u>3/4"</u>	<u>1 1/4"</u>	<u>3/4"</u>	<u>1 1/4"</u>
Reynolds No. 40					Reynolds No. 100			
% Solids								
2.5			393	1040			158	415
8.8			2070	5450			829	2185
14.3	116	270	3530	9000	22.5	52.5	1410	3600
21.2	238	560	5250	13900	46.0	102.0	2100	5540
25.0	168	440	4900	12900	32.0	84.0	1960	5170
31.9	100	220	2780	7300	19.5	41.5	1110	2920
36.8	64	140	1550	4070	12.0	26.5	620	1630
39.2	39	93	1020	2680	7.5	17.8	407	1070
40.4	32	80	660	1.740	6.1	15.0	267	6950
Reynolds No. 400					Reynolds No. 1,000			
2.5			39.3	104	0.021	0.024	15.8	41.5
8.8			207	545	0.255		82.9	
14.3	1.84	4.4	353	900	0.350	0.82	141	360
21.2	3.9	8.1	525	1390	0.75	1.5	210	554
25.0	2.7	6.8	490	1290	0.52	1.18	196	517
31.9	1.62	3.45	278	730	0.31	0.65	111	292
36.8	0.98	2.18	155	407	0.18	0.41	62	163
39.2	0.62	1.41	102	268	0.116	0.265	40.7	107
40.4	0.50	1.13	66	174	0.095	0.210	26.4	69.5
Reynolds No. 4,000					Reynolds No. 6,000			
2.5	0.0111	0.0048	3.93	10.4	0.0098	0.008	2.64	6.92
8.8	0.020		20.7		0.0094	0.0148	13.8	36.4
14.3	0.0295	0.068	35.3	90.0	0.014	0.032	23.5	60.0
21.2	0.062	0.114	52.5	139	0.030	0.054	35.0	92.4
25.0	0.044	0.090	49.0	129	0.021	0.043	32.7	86.1
31.9	0.0245	0.054	27.8	73	0.012	0.026	18.5	48.7
36.8	0.0144	0.0318	15.5	40.7	0.0069	0.016	10.3	27.2
39.2	0.0094	0.0220	10.2	26.8	0.00575	0.0108	6.8	17.9
40.4	0.0075	0.0160	6.60	17.4	0.00537	0.0094	4.4	11.6

CALCULATED RESULTS

TABLE XLV (Cont'd)

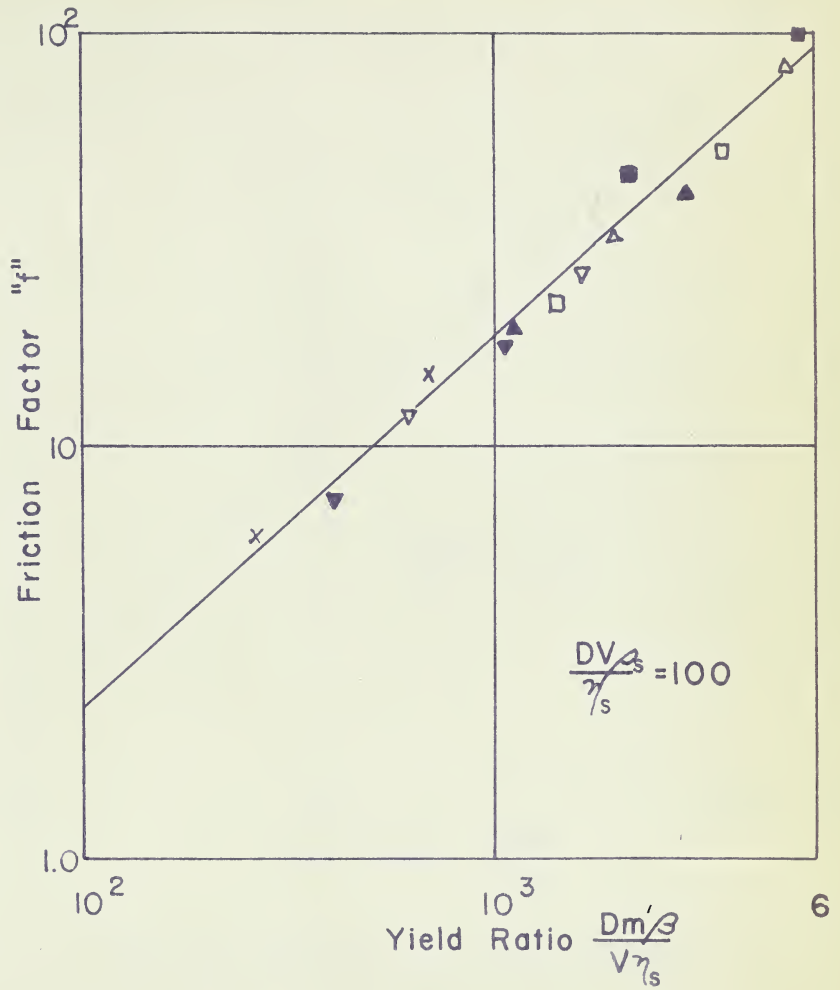
Friction Factor "f" and Yield Ratio $\frac{D_{m/2}}{V_7}$

Pipe Size.	Friction Factor		Yield Ratio		Friction Factor		Yield Ratio	
	<u>3/4"</u>	<u>1 1/4"</u>	<u>3/4"</u>	<u>1 1/4"</u>	<u>3/4"</u>	<u>1 1/4"</u>	<u>3/4"</u>	<u>1 1/4"</u>
Reynolds No. 8,000					Reynolds No. 10,000			
% Solids								
2.5	0.0089	0.0083	1.97	5.19	0.00828	0.00815	1.58	4.15
8.8	0.00815	0.0155	10.4	27.4	0.00658	0.021	8.29	21.8
14.3	0.00965	0.0195	17.6	45.0	0.00896	0.0130	14.1	36.0
21.2	0.0178	0.034	26.3	69.3	0.0119	0.021	21.0	55.4
25.0	0.0125	0.025	24.5	64.7	0.0091	0.0165	19.6	51.7
31.9	0.00745	0.0155	13.9	36.5	0.00646	0.0100	11.1	29.2
36.8	0.00575	0.00915	7.76	20.4	0.00558		6.2	16.3
39.2	0.00545		5.1	13.4	0.0053		4.07	10.7
40.4	0.00520		3.30	8.69			2.64	6.95
Reynolds No. 20,000					Reynolds No. 40,000			
2.5	0.00678	0.00678	.79	2.08	0.00580	0.00580	0.393	1.04
8.8	0.0062	0.0076	4.15	10.9	0.00517	0.00517	2.07	5.45
14.3	0.0071	0.0071	7.05	18.0	0.00588	0.00588	3.53	9.00
21.2	0.0065	0.0076	10.5	27.7	0.00560	0.00560	5.25	13.9
25.0	0.00655	0.00665	9.80	25.9	0.00592	0.00542	4.90	12.9
31.9	0.0055	0.0056	5.55	14.6				
36.8	0.00505		3.10	8.2				
39.2			2.03	5.4				
40.4			1.32	3.48				
Reynolds No. 100,000								
2.5	0.00474	0.00474	0.158	0.415				
8.8	0.00422	0.00422	0.829	2.18				
14.3	0.00469	0.00469	1.41	3.60				
21.2	0.00454	0.00454	2.10	5.54				
25.0								
31.9								
36.8								
39.2								
40.4								



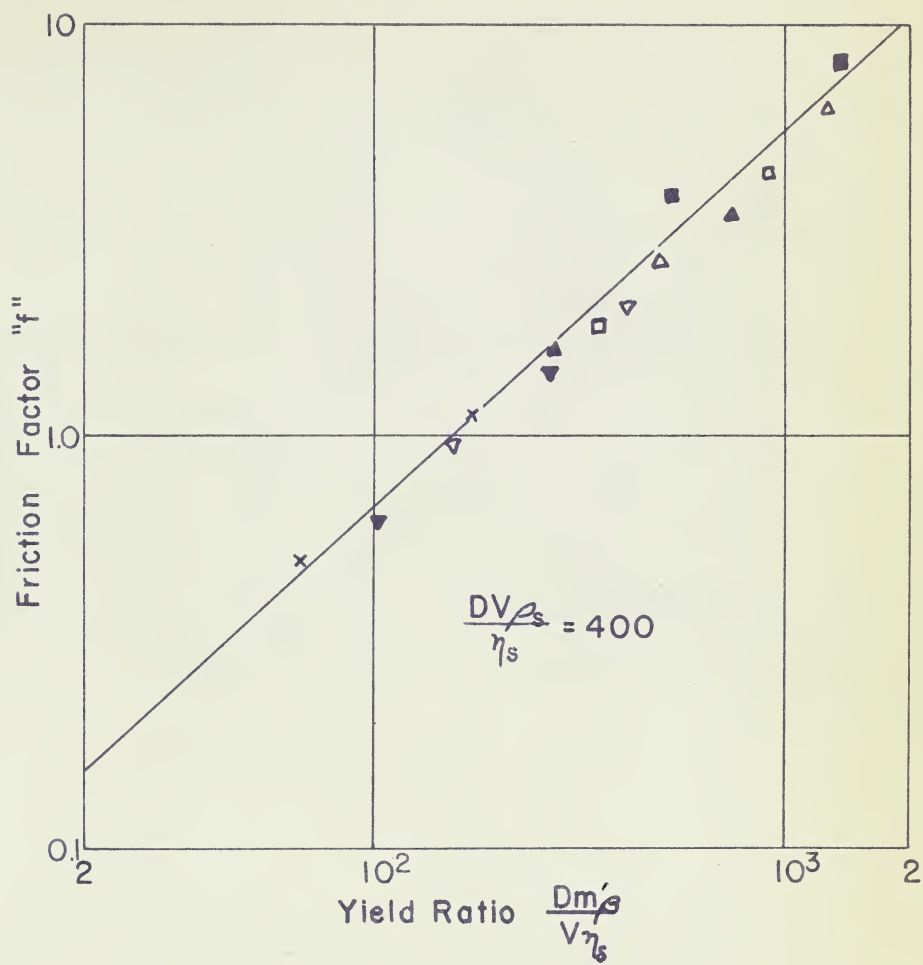
Friction Factor vs. Yield Ratio

Fig. 40



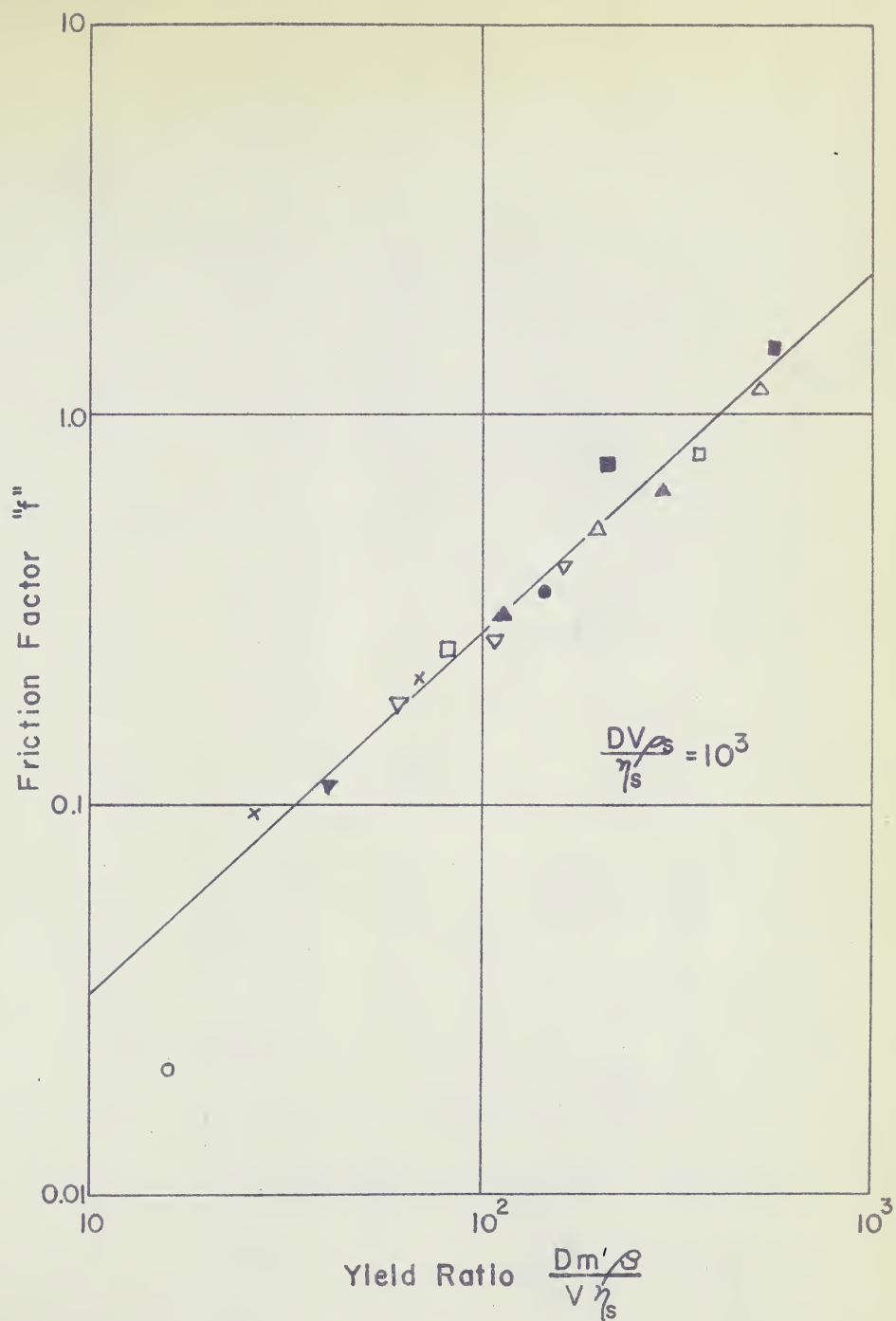
Friction Factor vs. Yield Ratio

Fig. 41



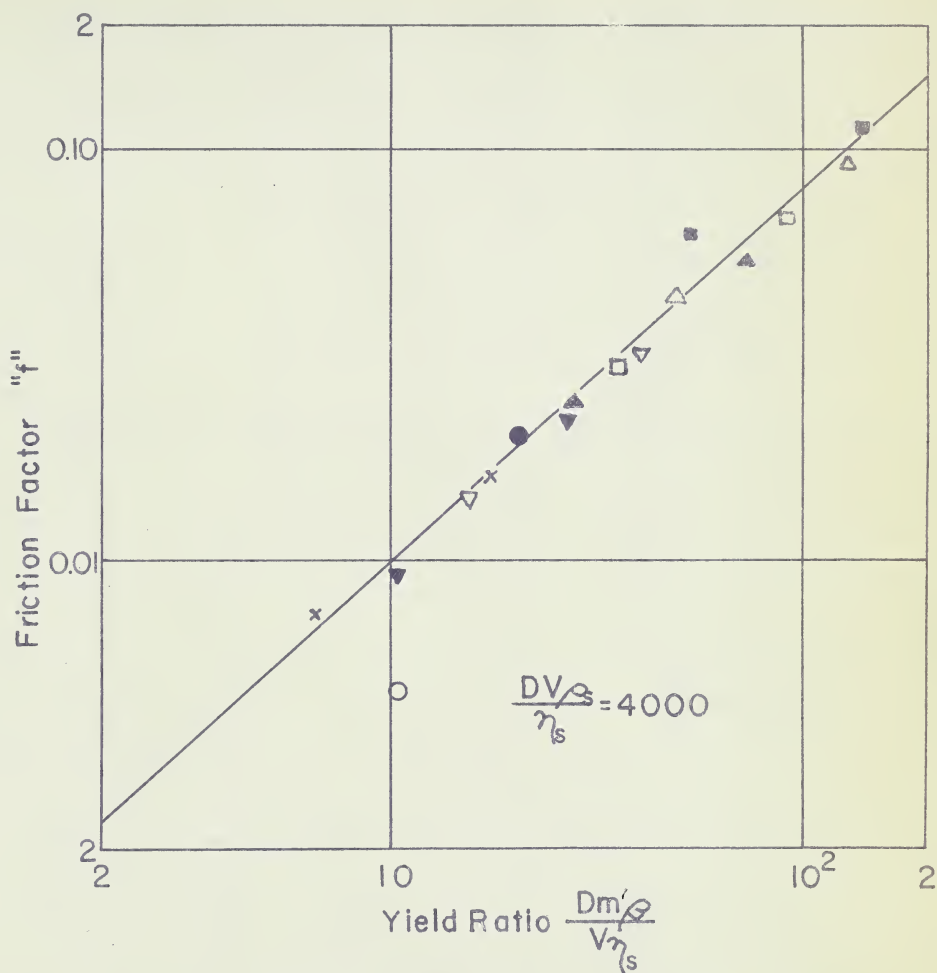
Friction Factor vs. Yield Ratio

Fig. 42.



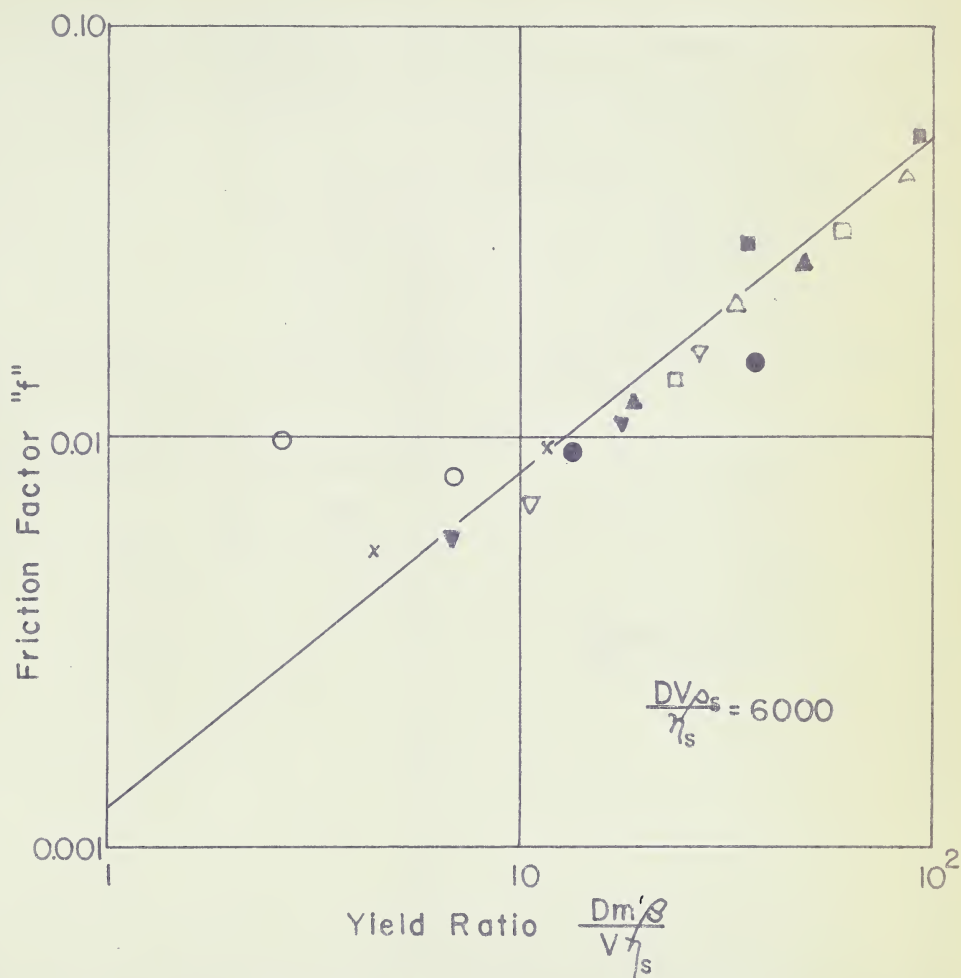
Friction Factor vs. Yield Ratio

Fig. 43.



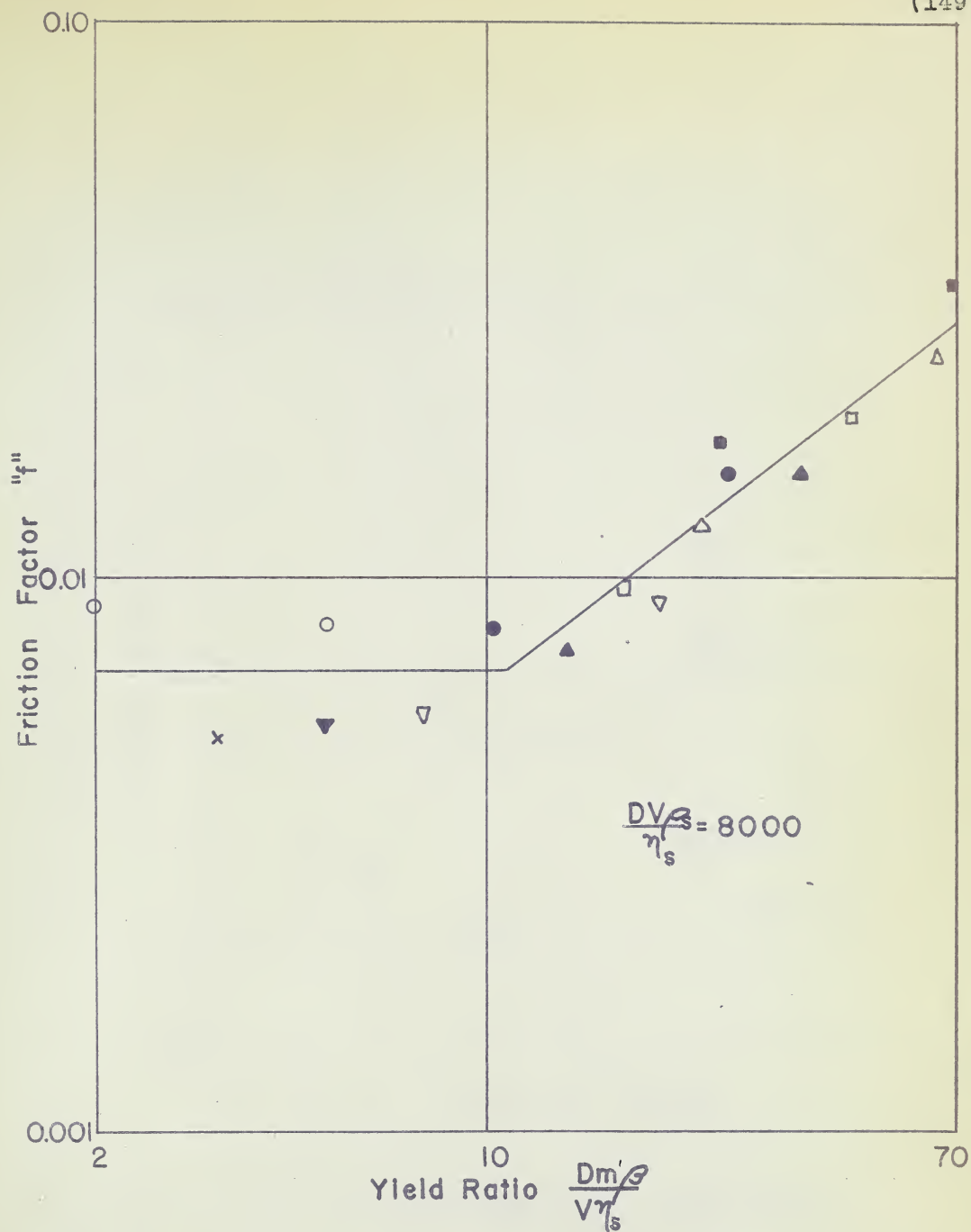
Friction Factor vs. Yield Ratio.

Fig. 44.



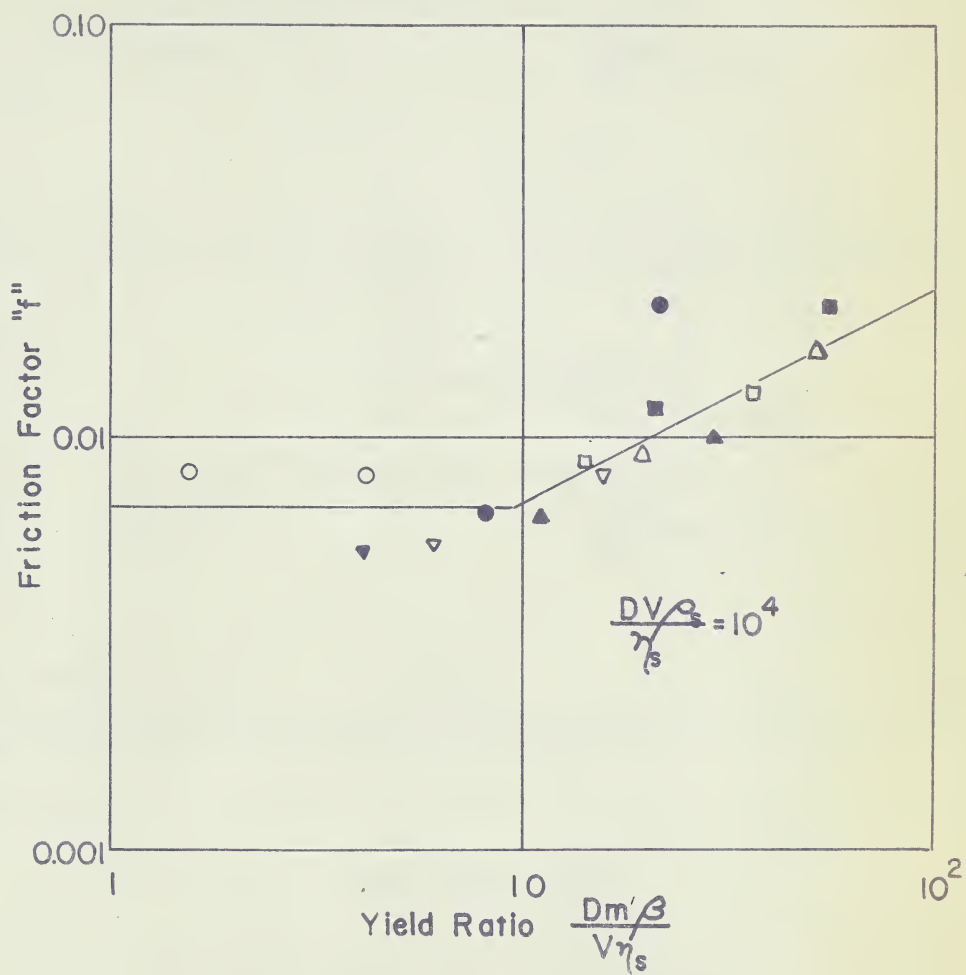
Friction Factor vs. Yield Ratio.

Fig. 45.



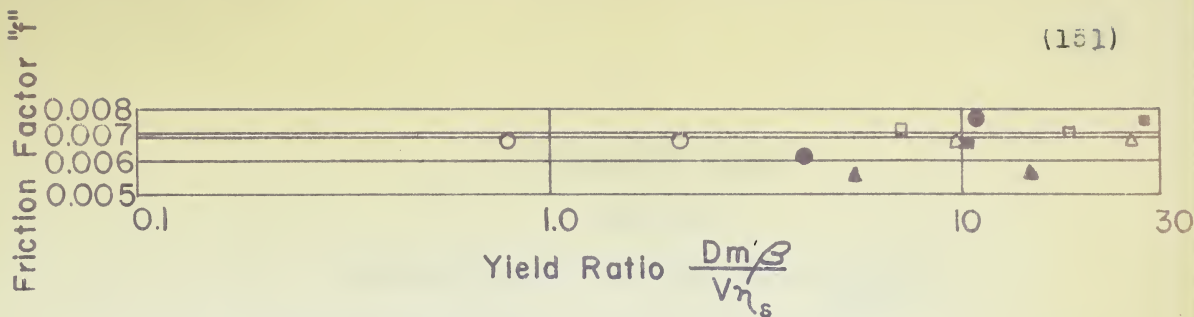
Friction Factor vs. Yield Ratio.

Fig. 46.



Friction Factor vs. Yield Ratio.

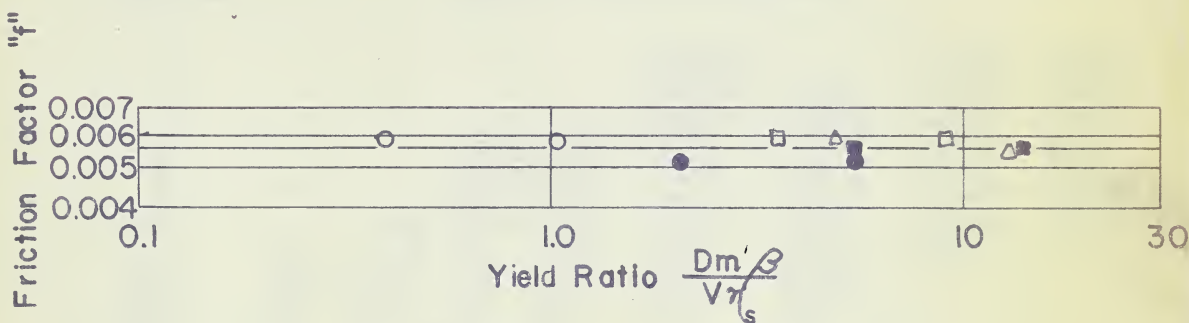
Fig. 47.



Friction Factor vs. Yield Ratio.

Fig. 48.

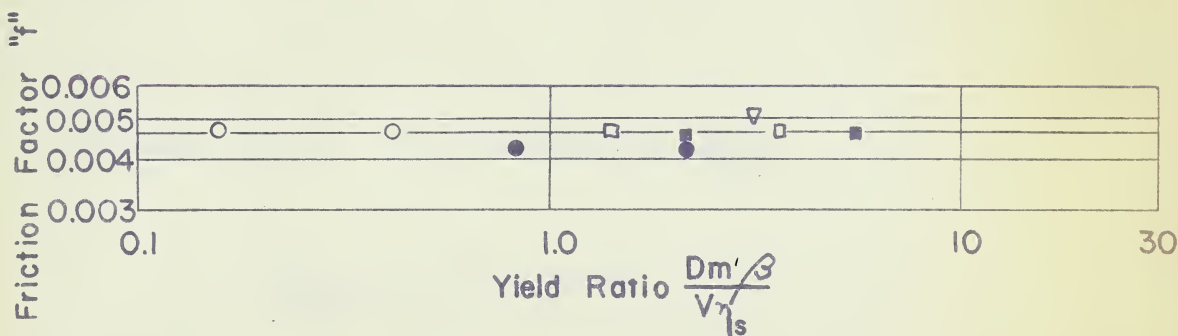
$$\frac{DV\beta}{\eta_s} = 2 \times 10^4$$



Friction Factor vs. Yield Ratio.

Fig. 49.

$$\frac{DV\beta}{\eta_s} = 4 \times 10^4$$



Friction Factor vs. Yield Ratio.

Fig. 50.

$$\frac{DV\beta}{\eta_s} = 10^5$$

CALCULATED RESULTS

TABLE XLVI

Smoothed Values of the Yield Ratio		$\frac{D m' \beta}{V \gamma_s}$							
$\frac{D V \beta}{\gamma_s}$	=	40	100	400	1,000	4,000	6,000	8,000	10,000
$\frac{D m' \beta}{V \gamma_s}$	Values of the friction factor								
1					0.00125			0.0068	0.0068
3					0.00335	0.0031	0.0068	0.0068	0.0068
6					0.0063	0.0054	0.0068	0.0068	0.0068
10			0.086	0.033	0.010	0.0082	0.0068	0.0068	0.0068
30			0.255	0.091	0.0270	0.02	0.0149	0.012	0.012
60			0.43	0.17	0.0505	0.033	0.0255	0.0174	0.0174
100		2.35	0.63	0.275	0.080	0.053	0.0375	0.025	0.025
300	14	6.25	1.8	0.75	0.216	0.13	0.086		
600	26.5	11.6	3.4	1.44	0.41	0.225			
1000	42	18.5	5.5	2.3	0.64	0.34			
3000	112	52	15	6.3					
6000	220	92							
10,000	335	142							
30,000	900	380							
60,000	1680								
100,000	2650								

At $\frac{D V \beta}{\gamma_s} > 2 \times 10^4$ "f" is independent of $\frac{D m' \beta}{V \gamma_s}$

$\frac{D V \beta}{\gamma_s}$	=	2×10^4	4×10^4	10^5
f		0.0068	0.0056	0.0046

Suspension Flow Runs (cont'd)

Table (47) lists values of the yield ratio for all the tests.

Figure (51) illustrates the relationship between the friction factor and the modified Reynolds number when the yield ratio is a parameter. The lines of constant yield ratio were positioned using the data of table (46). The positions of these lines were checked by locating the flow data as points with the numerical value of the yield ratio beside them.

No limitation has been placed on the coefficient of rigidity in figure(51). It appears that for any given percent solids the values of the coefficients of rigidity used apply equally well over the whole flow range.

CALCULATED RESULTS

TABLE XLVII

Values of the Yield Ratio for all Data

Run Pipe Size Test No.	A		B		C	
	<u>3/4</u>	<u>1 1/2</u>	<u>3/4</u>	<u>1 1/2</u>	<u>3/4</u>	<u>1 1/2</u>
	Yield Ratio		$\frac{D m^{1/3}}{V^{1/2}}$			
1	56.4	242	61.0	262	12350	52700
2	17.9	76.9	38.1	16.22	1515	650
3	4.68	20.0	63.3	27.20	11210	48200
4	1.85	14.8	10.12	47.70	1472	633
5	3.05	13.2	8.94	38.30	250	1072
6	2.24	9.64	16.23	70.50	704	3020
7	1.93	8.25	5.26	22.60	79.8	342
8	1.83	7.87	3.85	16.52	51.1	219.5
9	1.65	7.09	3.14	13.43	17.45	74.9
10	1.48	6.33	2.38	10.20	10.86	46.9
11	1.24	5.32	2.13	9.20	7.33	31.4
12	0.761	3.26	1.85	7.93	6.31	27.0
13	0.544	2.33	1.31	5.61	5.14	22.1
14	0.412	1.77	0.869	3.73	4.37	18.85
15	0.392	1.68	0.656	2.81	4.94	21.2
16	0.329	1.41	0.606	2.60	2.74	11.76
17	0.196	0.841			1.99	8.58
18	0.154	0.660			1.58	6.80
19	0.129	0.552			1.35	5.83
20	0.100	0.462			1.097	4.71
21	0.0965	0.412				

CALCULATED RESULTS

TABLE XLVII

Values of the Yield Ratio for all Data

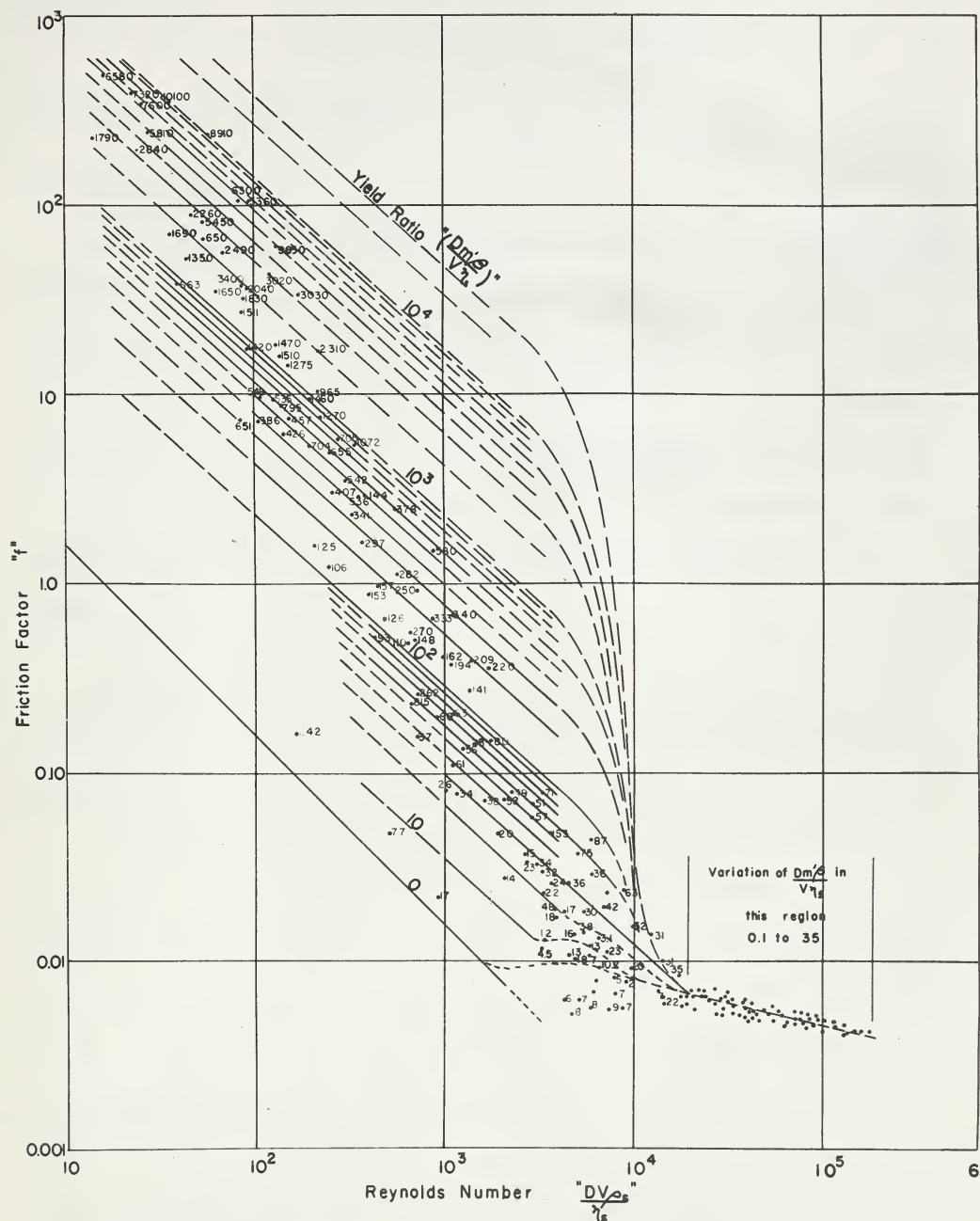
Run Pipe Size Test	D		E		F	
	3/4	1 $\frac{1}{4}$	3/4	1 $\frac{1}{4}$	3/4	1 $\frac{1}{4}$
	Yield Ratio		$\frac{D m/\beta}{\sqrt{\beta}}$			
1	1510	651	536	2310	10500	44500
2	194	81.5	82000	353000	1280	5450
3	378	144.0	2040	8910	297	1270
4	35.7	152.5	52500	226000	2260	10100
5	965	4150	1470	6300	705	3400
6	14.6	62.5	7600	32500	341	1460
7	8.28	35.3	1275	5360	78.1	333
8	5.55	23.8	141	580	49.2	209
9	4.29	18.5	8.14	34.3	9.78	42.2
10	3.41	14.6	12.2	52.4	7.68	32.7
11	2.93	12.6	20.2	86.7	6.32	27.0
12	2.72	11.65	705	3030	5.07	21.7
13	2.53	10.85	5.90	25.6	4.16	17.7
14			4.30	18.4	3.88	16.7
15			3.61	15.5		
16			3.10	13.4		

CALCULATED RESULTS

TABLE XLVII

Values of the Yield Ratio for all Data

Run	G		H		J	
Pipe Size	<u>3/4</u>	<u>1 1/2</u>	<u>3/4</u>	<u>1 1/2</u>	<u>3/4</u>	<u>1 1/2</u>
Test No.	Yield Ratio		$\frac{D}{V} \frac{m'}{\beta}$			
1	548	2490	1550	6580	1790	7750
2	56300	244000	386	1650	663	2840
3	1690	7320	3860	16600	125	535
4	1350	5810	95.2	409	106	457
5	153	655	2000	8550	36.8	157
6	426	1830	34.4	148	25.6	109.5
7	126	542	12.15	52.3	13.5	56.0
8	65.8	282	7.97	34.0	6.17	26.6
9	37.9	162	7.48	32.1	5.15	22.1
10	13.3	57.1	6.86	29.4	4.26	18.3
11	8.52	36.5	5.75	24.6	3.76	16.1
12	6.95	29.8	4.24	18.1		
13	5.87	25.1				
14	5.31	23.2				
15	4.92	21.0				
16	4.20	18.1				



Friction Factor vs. Reynolds Number
Parameter — Yield Ratio.

Fig. 51.

VII Discussion of Results.

Calibration of Equipment.

The Viscosimeter:

The equation relating the yield load on the viscosimeter (u) to yield value (m^1) was found to be $m^1 = 0.00221 u$ (110)

The relationship between viscosity or coefficient of rigidity and the slope of the viscosimeter data (λ) is not a linear function as was expected. It is represented graphically in figures (19) and (20). Figure (20) is an extension of the lower range of figure (19) to straighten and clarify the correlation.

Certain limitations are placed upon the results by the use of a Stormer viscosimeter to measure yield values and coefficients of rigidity. These are discussed below.

A minimum viscosimeter load of ten grams was found necessary to facilitate the use of the instrument. The minimum speed was taken as being about $\frac{1}{2}$ R.P.S. so as not to prolong the measurements to such an extent that settling or a time^{effect} would become apparent. The maximum speed at which the instrument may be operated is restricted by the necessity of maintaining streamline flow conditions within the suspension sample. These limits are marked on the viscosimeter data figures, as dotted lines, wherever the figures extend beyond the limits.

NOTE: In transforming viscosimeter R.P.S. to Reynolds numbers it is very difficult to evaluate the rate of shear directly. The following method is suggested as an alternative. The viscosimeter load at any percent solids is related to the R.P.S. through figures (17) and (18). The load may be converted to a shearing stress at the pipe wall by multiplying by 0.00221. Knowing the shearing stress and the percent solids the appropriate Reynolds number may be obtained from the tabulated data. Since the data in this thesis are presented as pressure drops and not shearing stresses it is suggested that equation (114), given in the appendix, be used to carry out the necessary transformation.

As a result of the above restrictions on the use of the viscosimeter the range of modified Reynolds numbers $\left(\frac{DV\beta}{\eta_s}\right)$ is limited by the extent to which η_s has been justified by the viscosimeter data. However, this restriction does not appear to be very serious since the data correlate as well beyond the limit of reliability of as they do within the limit. (Figs. 36, 37, 38, 39). A further result of the restrictions on the use of the viscosimeter is that the exact value of the yield value (m) is in doubt. The symbol m' is being used for the experimental yield values since the exact behaviour of the suspensions at zero rate of shear is unknown. It is pointed out later in the discussion that more precise measurements of the yield values are required. This indicates that some method of measurement is required which will not be hampered by settling or ageing.

The Manometer Fluids:

The effective specific gravities of manometer fluids 1, 3, 5, 6 vary with temperature. Figures 21, 22, 23 and 24 present the calibration data (Table 3) in graphical form. Over the range of temperatures employed the relationship between temperature and effective specific gravities is linear.

For the air over water (fluid #2) the effective specific gravity changes by 1/10 of 1% for a temperature change of 12°C. so no calibration is necessary. Similarly the water over mercury (fluid #4) changes its effective specific gravity by 1/10 of 1% for a temperature change of 5°C. and no calibration is necessary.

Pipeline Smoothness.

In the description of the flow circuit it was mentioned that special care had been exercised to obtain smooth test sections. As a check on this, data from four test runs, using water as the fluid, were plotted as friction factor vs. Reynolds Number. (Figure 33). One of these tests was made at the conclusion of the slurry runs to show that no roughening had taken place. The data compare favourable with Poiseuilles predictions for streamline flow and Nikuradses equation for turbulent flow in a theoretically smooth tube. There is a slight roughness present but the effect is small.

Rheology:

The data of the preliminary investigation (Table 2) indicate that the clay suspensions behave as true plastics.

This is indicated also by the viscosimeter data obtained during the measurement of the suspension properties. The viscosimeter data are not extensive enough to establish conclusively what occurs at low rates of shear.

It has been found possible to correlate the yield values and coefficients of rigidity of the clay suspensions with the percent solids. The equations representing these relationships are:

$$m^1 = 0.001 (e^{0.158x-1}) \quad (112)$$

$$\text{and } \eta_s = \mu + 0.042 (e^{0.159x-1}) \quad (113)$$

where m^1 = the yield value (lbs/ft²)

η_s = the coefficient of rigidity (lbs/ft.sec.)

x = the percent solids (%)

μ = the viscosity of the carrier fluid

(lbs/ft.sec.) at the temperature of the suspension. While these equations apply to the clay suspensions used in this investigation, it is not recommended that they be applied to other materials. A peculiarity of these equations is that the exponents of "e" are, within the limits of experimental error, the same. It is not known whether this is a specific property of the clay used or whether it is general for all suspensions.

The effect of temperature on the coefficient of rigidity is taken care of by including the viscosity of the carrier fluid as a separate term in the equation for the coefficient of rigidity. This assumes that the effect of the solid on the coefficient of rigidity is independent of temperature. The fact that the data may be correlated by equation (113) appears to justify the assumption.

Pressure drop - Rate of Flow Correlations.

Figure (34) presents the pressure drop-rate of flow data as a graph of the friction factor (f) vs. Reynolds number ($N_{Re(i)}$) calculated from $\frac{DV\rho_s}{\eta_s}$. In the streamline region the effect of solids concentration and diameter are both apparent. The higher percent solids and larger diameter increase the friction factor. Figure (35) presents the data for friction factors less than 0.011 on a slightly larger scale. It is noted that although the diameter effect disappears at the higher rates of flow there is still a family of curves the position of which depends on the percent solids.

Since the use of the viscosity of water in computing Reynolds number results in a family of curves the position of which is dependent on both percent solids and diameter, plots of (f) vs $(\frac{DV\rho_s}{\eta_s})$ were constructed (Figs. 36, 37). The lower limits of Reynolds number on these plots are defined by the extent to which the coefficients of rigidity are known to be accurate. A dashed line on the graph marks these limits.

In the streamline flow region the effect of the percent solids and diameter are still apparent. However, there is now an inversion in the effect due to the solids concentration. Up to about 22% solids the friction factor increases with percent solids. Above this concentration the friction factor decreases with percent solids. It does not return to the same value as that for 0% solids.

Figure (38) presents the data of the streamline region correlated as friction factor vs. $N_{Re(III)} = \frac{DV\rho}{\eta} \left[\frac{1-4(2Lm')}{3(R\Delta P)} + \frac{1(2Lm')^4}{3(R\Delta P)} \right]$. The lowest limit of $N_{Re(III)}$ which is justified by the viscosimeter data is marked by a dashed line. The data, while following the general trend $f = \frac{16}{N_{Re(III)}}$, are scattered to a great extent. This scattering appears to be due to the form of the term $\left[\frac{1-4(2Lm')}{3(R\Delta P)} + \frac{1(2Lm')^4}{3(R\Delta P)} \right]$ since it is not present until this term enters the correlation.

Due to the fact that the yield value (m^1) is obtained by extrapolation of a graph, and by neglecting the possibility of friction in the viscosimeter, errors of from 5 to 10% may be present. The effect of errors of this magnitude in the yield value is multiplied greatly when the yield value is used in the computation of $N_{Re(III)}$. This indicates that a more precise measurement of the yield value is required. Table (48) illustrates the range of errors in $\left[\frac{1-4(2Lm')}{3(R\Delta P)} + \frac{1(2Lm')^4}{3(R\Delta P)} \right]$ which may be the result of errors in the yield value alone without allowing for errors in the other factors present.

TABLE XLVIII

Effect of Errors in the Yield Value

	Point H6		Point B2	
	Value	Errors	Value	Errors
m'	0.47	± 5% ± 0.025	± 10% ± 0.047	0.003 ± 5% ± 0.00015 ± 0.0003
$\frac{4(2Lm')}{3(R\Delta P)}$	0.936	± 5% ± 0.0564	± 10% ± 0.0936	0.761 ± 5% ± 0.038 ± 0.076
$\frac{1}{3} (2Lm')^4$	0.081	± 20% ± 0.0195	± 40% ± 0.0324	0.036 ± 20% ± 0.0072 ± 0.0144
$\left[\frac{1-4(2Lm')}{3 R\Delta P} + \frac{1(2Lm')^4}{3(R\Delta P)} \right]$	0.045	± 170% ± 0.0759	± 280% ± 0.126	0.275 ± 16.4 % ± 0.045 ± 0.090

Figure (39) combines figures (38) and (36) over the ranges to which they apply. This figure may be used with extremely accurate values of the rheological properties to predict pressure drops for suspensions flowing in smooth pipes. This method is not recommended since it involves trial and error computations.

Figures 40 to 50 were constructed to give smoothed values of the yield ratio $\frac{(Dm'/\beta)}{V\eta_s}$. These figures also show the linear relationship between the friction factors and yield ratios at constant Reynolds numbers. A very significant factor is indicated in that for $\frac{DV\beta_s}{\eta_s} > 2 \times 10^4$ the friction factor is constant for all known values of the yield ratio. It has already been shown (Fig. 36) that at values of $\frac{DV\beta_s}{\eta_s} > 2 \times 10^4$ the friction factor for suspensions could be related to $\frac{DV\beta_s}{\eta_s}$ by means of the usual friction factor - Reynolds number diagram for water.

Dimensional analysis indicated that the three ratios expected to affect the friction factor are $\left(\frac{DV\beta_s}{\eta_s}\right)$, $\left(\frac{\Delta}{D}\right)$, $\left(\frac{Dm'/\beta}{V\eta_s}\right)$. The effect of $\left(\frac{\Delta}{D}\right)$ has been kept negligible by the use of smooth pipe. The effect of $\left(\frac{Dm'/\beta}{V\eta_s}\right)$ disappears for values of $\left(\frac{DV\beta_s}{\eta_s}\right)$ greater than or equal to 2×10^4 . Both $\left(\frac{DV\beta_s}{\eta_s}\right)$ and $\left(\frac{Dm'/\beta}{V\eta_s}\right)$ have an effect at $\left(\frac{DV\beta_s}{\eta_s}\right)$ less than 2×10^4 . A transition region appears to exist for the range $4 \times 10^3 < \left(\frac{DV\beta_s}{\eta_s}\right) < 2 \times 10^4$.

Figure 51 presents the relationship between the friction factor "f" and $\left(\frac{DV\beta_s}{\eta_s}\right)$ with values of $\left(\frac{Dm'/\beta}{V\eta_s}\right)$ as parameters. The observed data are plotted with their values of $\left(\frac{Dm'/\beta}{V\eta_s}\right)$ beside them to check the positions of the constant yield ratio lines.

The experimental data indicate that the use of the two dimensionless ratios $\left(\frac{DV\beta}{\eta_s}\right)$ and $\left(\frac{Dm'\beta}{V\eta_s}\right)$ gives a more reliable method of predicting flow rate-pressure drop relationships than does Bingham's equation. This method does away with the necessity of trial and error computations.

RECOMMENDED METHOD OF PRESSURE DROP ESTIMATION.

It is recommended that the following steps be carried out to estimate the pressure drop due to the flow of a suspension in a smooth pipeline.

1. Obtain the yield value and coefficient of rigidity of the suspension by means of a calibrated viscosimeter.
2. Calculate the Reynolds number $\left(\frac{DV\beta}{\eta_s}\right)$.
3. If the value of $\left(\frac{DV\beta}{\eta_s}\right)$ is greater than 2×10^4 , it may be used with the regular Reynolds number friction factor line for water to obtain the friction factor.
4. If the value of $\left(\frac{DV\beta}{\eta_s}\right)$ is less than 2×10^4 calculate the yield ratio $\left(\frac{Dm'\beta}{V\eta_s}\right)$.
5. Use figure (51) and the two dimensionless ratios $\left(\frac{DV\beta}{\eta_s}\right)$, $\left(\frac{Dm'\beta}{V\eta_s}\right)$ to obtain the friction factor.
6. The friction factor may then be employed in equation (17) to predict the pressure drop.

VIII CONCLUSIONS

1. A versatile experimental unit for the study of pipe line pressure drops of suspensions has been developed.

2. The flow of clay suspensions over the range of concentrations encountered in this investigation may be interpreted on the assumption that the suspensions are true plastics.

3. The yield values (m^1) for the clay suspensions encountered in this investigation are related to the percent solids of the suspension (x) by the equation

$$m^1 = 0.001 (e^{0.158x-1}) \quad (112)$$

4. The coefficients of rigidity η_s under the same conditions, are related to the percent solids (x) by the equation.

$$\eta_s = \mu + 0.042 (e^{0.159x-1}) \quad (113)$$

where μ is the viscosity of water at the temperature of the suspension.

5. It is possible to estimate pressure drops, for true plastic suspensions flowing in smooth pipes, from independent measurements of the yield values, coefficients of rigidity and density of the suspensions, and knowing the velocity of flow and diameter of the pipe.

5(a) Two dimensionless ratios $\left(\frac{Dm'\beta}{V\eta_s}\right)$ and $\left(\frac{DV\beta}{\eta_s}\right)$ may be used, in conjunction with a chart given in this report, to estimate the pressure drop of suspensions flowing at low rates.

5(b) The dimensionless ratio $\left(\frac{DV\beta}{\eta_s}\right)$ may be used with the

conventional Reynolds number chart to estimate the pressure drop of suspensions at high rates of flow (ie $\frac{DV_s}{\eta_s} > 2 \times 10^4$)

6. Bingham's equations for pressure drop estimation of true plastics at low rates of flow requires a very accurate measurement of the yield value. It is not recommended that these equations be used with independently measured rheological properties.

7. The use of the dimensionless ratio $\left(\frac{DV_s}{\eta_s}\right)$ to predict pressure drops for a suspension in turbulent flow is to be recommended as an approximation only.

IX Bibliography.

1. Babbitt, H. E. and Caldwell, D. H.: U. of Illinois Bulletin #12 November 14, 1939.
2. Babbitt, H. E. and Caldwell, D. H.: U. of Illinois Bulletin #13 November 19, 1940.
3. Bingham, E. C.: Fluidity and Plasticity. McGraw Hill (1922).
4. Buckingham, E.: On the Flow of Plastic Materials, Proc. Am. Soc. Test Matls. (1921) p.1154.
5. Handbook of Chemistry and Physics: Chemical Rubber Publishing Co., Cleveland, Ohio.
6. Hatschek, E.: Viscosity of Liquids. Bell, London, (1928).
7. Houwink, R.: Elasticity, Plasticity and Structure of Matter. Cambridge University Press (1937).
8. McMillen, W. L.: Chem. Eng. Progress 44 537 (1948). Simplified Pressure-Loss Calculations for Plastic Flow.
9. Parent, J. D.: Predicting Fluid Friction Data for Sludges. Chem. and Met. Eng. 51 #1, 101, (1944).
10. Reiner, M.: Lectures in Theoretical Rheology. Rubin Mass, Jerusalem (1943).
11. Scott-Blair, G. W., and Crowther, E.M.: Flow of Clay Pastes Through Narrow Tubes. J. Phy. Chem. 33 321 (1920).
12. Staudinger, H.: Ber. Deutsch Chem. Ges. 62 2893 (1929).
13. de Waele, A.: Manifestation of Interfacial Forces in Dispersed Systems. J. Am. Chem. Soc. 48 2760 (1926).
14. Walker, Lewis, McAdams and Gilliland: Principles of Chemical Engineering. McGraw Hill (1937).
15. Williamsen, R. V.: Estimation of Brushing and Flow Properties of Paint from Plasticity Data. Ind. Eng. Chem. 21 1111 (1929).

(Numbers 8, 10, 12 and 15 are quoted by Winding, C. C., Baumann, C. P., and Krenich, W. L.: Viscosities of GR-S latices. Chem. Eng. Progress (Trans. Section) 43 527 (1947)).

X APPENDIX

Theoretical Derivations

The following symbols will be used.

- h = head loss due to friction per unit length ($f + 16s/16 \text{ ft.}$)
 L = Length of pipe (ft.)
 Q = Rate of flow ($\text{ft}^3/\text{sec.}$)
 r = Radius from any point within a pipe to the centre of the pipe (ft.)
 R = Radius of pipe (ft.)
 r_0 = Radius within a pipe at which the shearing stress equals the yield value (ft.)
 S = Shearing stress in (lbs/ft^2)
 S_p = Shearing stress at the pipe wall (lbs/ft^2)
 S_r = Shearing stress in a circular pipe at a distance r from the centre (lbs/ft^2)
 m = Shearing stress at the yield point of a plastic material (lbs/ft^2)
 V = Mean velocity of flow in a pipe (ft/sec)
 v_0 = Velocity of a plug of radius r_0 (ft/sec)
 v_r = Velocity at a distance r from the centre of a pipe (ft/sec)
 v_R = velocity at the wall of the pipe (ft/sec)
 ν = coefficient of viscosity ($\text{lbs}/\text{ft}.\text{sec}$)
 η = coefficient of rigidity ($\text{lbs}/\text{ft}.\text{sec}$)
 β = a proportionality constant ($\frac{\text{lbs. mass. ft}}{\text{lbs. force sec}^2}$)
 $= 32.1740 \frac{\text{lbs. mass ft}}{\text{lbs. force sec}^2}$
 ρ = density of flowing substance (lbs/ft^3)
 ΔP = pressure drop related to S_p by $S_p = \frac{R\Delta P}{2L}$ (114)
 $\& S_r$ by $S_r = \frac{r\Delta P}{2L}$ (lbs/ft^2) (115)

The following is the method of Bingham, also used by Babbitt and Caldwell, and Parent, applied to a true plastic.

$$\text{By definition } \eta = (S-m) \frac{dx}{dv} \beta \quad (116)$$

for a circular pipe equation (116) becomes

$$dv = - \frac{\beta}{\eta} (S_r - m) dr \quad (117)$$

$$\text{or } dv = - \frac{\beta}{\eta} \left[\frac{r \Delta P}{2L} - m \right] dr \quad (118)$$

The velocity at any distance r from the centre of the pipe between the plug of radius r_0 and the pipe wall is obtained by integrating equation (118) from $r = R$ to $r = r$ to give

$$v_r = - \frac{\beta}{\eta} \int_R^r \left[\frac{\Delta P r}{2L} - m \right] dr = \frac{\beta}{\eta} \left[\frac{\Delta P r^2}{4L} - m r \right]_R^r \quad (119)$$

$$v_r = \frac{\beta}{\eta} \left[\frac{\Delta P}{4L} (R^2 - r^2) - m (R - r) \right] \quad (120)$$

The velocity of the solid plug is obtained by setting

$r = r_0$ in equation (120) to give

$$v_0 = \frac{\beta}{\eta} \left[\frac{\Delta P R^2}{4L} + \frac{L m^2}{\Delta P} - m R \right] \quad (121)$$

The volumetric rate of flow is given by the expression

$$Q = \pi r_0^2 v_0 + 2\pi \int_{r_0}^R r v_r dr \quad (122)$$

$$\text{but } \pi r_0^2 v_0 = \frac{\pi 4m^2 L^2}{\Delta P^2} \frac{\beta}{\eta} \left[\frac{(\Delta P) R^2}{4L} + \frac{L m^2}{\Delta P} - m R \right] \quad (123)$$

$$\text{and } 2\pi \int_{r_0}^R r v_r dr = \frac{2\pi\beta}{\eta} \int_{r_0}^R \left[\frac{\Delta P}{4L} (R^2 r - r^3) - m (R r - r^2) \right] dr \quad (124)$$

$$\begin{aligned} 2\pi \int_{r_0}^R r v_r dr &= \frac{2\pi\beta}{\eta} \left[\frac{R^4 \Delta P}{16L} - \frac{R^3 m}{6} - \frac{\Delta P}{4L} \left(\frac{R^2 r_0^2}{2} - \frac{r_0^4}{4} \right) \right. \\ &\quad \left. + m \left(\frac{R r_0^2}{2} - \frac{r_0^3}{2} \right) \right] \quad (125) \end{aligned}$$

substituting for r_o $r_o = \frac{2mL}{\Delta P}$ (126)

$$2\pi \int_0^R r v_r dr = \frac{2\pi\beta}{\gamma} \left[\frac{R^4 \Delta P}{16L} - \frac{R^3 m}{6} - \frac{R^2 L m^2}{2(\Delta P)} + \frac{2RL^2 m^2}{\Delta P^2} - \frac{5}{3} \frac{L^3 m^4}{(\Delta P)^3} \right] \quad (127)$$

Substituting in equation 122 give

$$Q = \frac{\pi\beta}{\gamma} \left[\frac{R^4 \Delta P}{8L} - \frac{R^3 m}{3} + \frac{2}{3} \frac{L^3 m^4}{(\Delta P)^3} \right] \quad (128)$$

$$= \frac{R^4 \pi\beta}{8L\gamma} \Delta P \left[1 - \frac{4}{3\Delta P} \left(\frac{2Lm}{R} \right) + \frac{1}{3\Delta P^4} \left(\frac{2Lm}{R} \right)^4 \right] \quad (129)$$

as an expression for velocity

$$V = \frac{R^2 \beta}{8L\gamma} \Delta P \left[1 - \frac{4}{3\Delta P} \left(\frac{2Lm}{R} \right) + \frac{1}{3\Delta P^4} \left(\frac{2Lm}{R} \right)^4 \right] \quad (130)$$

If the final expression is desired in terms of shear replacing ΔP by its equivalent from equation //4 results in

$$V = \frac{R\beta S_p}{4\gamma} \left[1 - \frac{4}{3} \frac{m}{S_p} + \frac{1}{3} \left(\frac{m}{S_p} \right)^4 \right] \quad (131)$$

or $V = \frac{R\beta}{4\gamma} \left[S_p - \frac{4}{3} m + \frac{1}{3} \frac{m^4}{S_p^3} \right] \quad (132)$

Babbitt and Caldwell went further and simplified equation (132) by assuming $\beta = 32$ so equation (132) becomes

$$V = \frac{4D}{\gamma} \left[S_p - \frac{4}{3} m + \frac{1}{3} \frac{m^4}{S_p^3} \right] \quad (133)$$

Their experimental data indicated that if $\frac{m}{S_p}$ is small (a high rate of shear) it is permissible to drop the last term of (133) resulting in

$$V = \frac{4D}{7} \left[S_p - \frac{4}{3} m \right] \quad (134)$$

from which it is possible to obtain

$$S_p = \frac{4}{3} m + \eta \frac{V}{4D} \quad (135)$$

Parent employs equation (131) as Bingham gave it

$$V = \frac{D S_p}{8} \left[1 - \frac{4}{3} \frac{m}{S_p} + \frac{1}{3} \left(\frac{m}{S_p} \right)^4 \right] \quad (131)$$

He points out that for a Newtonian fluid in streamline

$$\text{motion} \quad f = \frac{16}{DV} \rho \quad (19)$$

which when substituted for f in the equation (17) yields

$$-\Delta P = \frac{32 \mu V L}{(2R)^2} \quad (20)$$

$$\text{Letting } \frac{hg}{\beta} = \frac{-\Delta P}{\rho L} = \frac{32 \mu V}{4R^2 \rho} \quad (136)$$

Parent suggests μ' as an apparent viscosity so that for a plastic material equation (136) becomes

$$\frac{hg}{\beta} = \frac{32 V \mu'}{4 \rho R^2} \quad (137)$$

Substituting the expression

$$S_p = \frac{2R \Delta P}{4L} \quad (114)$$

into (131) and replacing ΔP by

$$\Delta P = hL \rho \frac{g}{\beta} \quad (138)$$

the resulting expression for the velocity V is

$$V = \frac{4hg\rho R^2}{32\eta} \left[1 - \frac{16}{3} \frac{\rho m}{g\rho h 2R} + \frac{256}{3} \left(\frac{\rho m}{g\rho h 2R} \right)^4 \right] \quad (139)$$

Comparing this with equation (137) shows that

$$\mu' = \frac{\eta}{\left[1 - \frac{16}{3} \frac{\rho m}{g\rho h 2R} + \frac{256}{3} \left(\frac{\rho m}{g\rho h 2R} \right)^4 \right]} \quad (140)$$

Substituting this in equation (137) gives

$$h = \frac{32 V \eta}{4g\rho R^2 \left[1 - \frac{16}{3} \left(\frac{\rho m}{g\rho h^2 R} \right) + \frac{256}{3} \left(\frac{\rho m}{g\rho h^2 R} \right)^4 \right]} \quad (141)$$

Parent's treatment of equation (141) has been described in the literature review.

The following derivation is given according to Buckingham's method. The starting equation is

$$-\frac{dv}{dr} = \frac{\beta}{\eta} \left(\frac{\Delta P r}{2L} - m \right) \quad (142)$$

For $\frac{\Delta P r}{2L} < m$ there is no shear so the material inside

$r_0 = \frac{2mL}{\Delta P}$ moves as a solid plug. Between r_0 and R the material yields, moving in streamline motion and v_r is the velocity at the wall. Integrating (142) between r and R gives

$$v_r - v_R = -\frac{\beta}{\eta} \int_R^r \left(\frac{\Delta P r}{2L} - m \right) dr = \frac{\beta}{\eta} \left[\frac{\Delta P}{4L} (R^2 - r^2) - m(R-r) \right] \quad (143)$$

$$\text{from which } v_r = \frac{\beta}{\eta} \left[\frac{\Delta P}{4L} (R^2 - r^2) - m(R-r) \right] + v_R \quad (144)$$

The speed of the plug is obtained by setting $r = r_0$

$$\text{so } v_0 - v_R = -\int_{R}^{r_0} \left(\frac{\Delta P r}{2L} - m \right) dr \quad (145)$$

$$\begin{aligned} &= -\frac{\beta}{\eta} \left\{ \left[\frac{\Delta P r^2}{4L} \right]_R^{r_0} - \left[m r \right]_R^{r_0} \right\} \\ &= -\frac{\beta}{\eta} \left\{ \frac{\Delta P r_0^2}{4L} - \frac{\Delta P R^2}{4L} - m r_0 + m R \right\} \\ &= \frac{\beta}{\eta} \left\{ \frac{\Delta P R^2}{4L} - m R - \frac{\Delta P r_0^2}{4L} + m r_0 \right\} \end{aligned}$$

$$\text{by definite } r_0 = \frac{2Lm}{\Delta P} \quad (126)$$

$$\text{squaring } r_0^2 = \frac{4L^2 m^2}{\Delta P^2} \quad (146)$$

$$\text{so } v_o - v_R = \frac{\beta}{\eta} \left[\frac{\Delta P R^2}{4L} - mR - \frac{\Delta P}{4L} \frac{4L^2 m^2}{\Delta P^2} + \frac{m^2 L m}{\Delta P} \right]$$

$$\text{or } v_o - v_R = \frac{\beta}{\eta} \left[\frac{\Delta P R^2}{4L} - mR + \frac{L m^2}{\Delta P} \right] \quad (147)$$

$$\text{or } v_o = \frac{\beta}{\eta} \left[\frac{\Delta P R^2}{4L} - mR + \frac{L m^2}{\Delta P} \right] + v_R \quad (148)$$

The volumetric rate of discharge is given by

$$Q = \pi r_o^2 v_o + 2\pi \int_{r_o}^R v_r r dr \quad (122)$$

substituting for r_o , v_o , v_r gives

$$Q = \pi \left(\frac{2Lm}{\Delta P} \right)^2 \left\{ \frac{\beta}{\eta} \left[\frac{\Delta P R^2}{4L} - mR + \frac{L m^2}{\Delta P} \right] + v_R \right\} + 2\pi \int_{r_o}^R \left\{ \frac{\beta}{\eta} \left[\frac{\Delta P}{4L} (R^2 - r^2) - m(R-r) \right] + v_R \right\} r dr \quad (149)$$

Dividing by πR^2 to get V average gives

$$V = \left\{ \frac{4\beta}{\eta} \frac{L^2 m^2}{\Delta P^2 R^2} \left[\frac{\Delta P R^2}{4L} + \frac{m^2 L}{\Delta P} - mR \right] + v_R \left(\frac{4L^2 m^2}{\Delta P^2 R^2} \right) + \frac{2\beta}{R^2 \eta} \left[\frac{\Delta P R^4}{16L} - \frac{m}{6} R^3 + v_R \frac{R^2}{2} \right] - \frac{R^2 L m^2}{2\Delta P} + \frac{2RL^2 m^3}{\Delta P^2} - \frac{5}{3} \frac{L^3 m^4}{\Delta P^3} - \frac{2v_R}{\Delta P^2} L^2 m^2 \right\} \quad (150)$$

Simplification yields

$$V = \frac{R^2 \beta}{8L \eta} \Delta P \left\{ 1 - \frac{4}{3\Delta P} \left(\frac{2Lm}{R} \right) + \frac{1}{3\Delta P^4} \left(\frac{2Lm}{R} \right)^4 \right\} + v_R \quad (151)$$

Buckingham assumed that the slip at the wall v_R occurred in a Newtonian layer of thickness ℓ and viscosity $\frac{1}{\phi}$. In this

$$\text{layer} \quad - \frac{dv}{dr} = \frac{\phi r \Delta P \beta}{2L} \quad (152)$$

approximately $-\frac{dv}{dr} = \frac{v_R}{\ell}$ and $r = R$ so

$$v_R = \frac{\ell \phi R \Delta P \beta}{2L} \quad (153)$$

Equation (153) may be substituted in (151) to give

$$v = \frac{R^2 \beta}{8L \eta} \Delta P \left\{ 1 - \frac{4}{3\Delta P} \left(\frac{2Lm}{R} \right) + \frac{1}{3\Delta P^4} \left(\frac{2Lm}{R} \right)^4 \right\} + \frac{\ell \phi R \Delta P \beta}{2L} \quad (154)$$

Scott-Blair and Crowther redefined their terms letting $\ell \phi / R$ be replaced by $\frac{\ell \phi}{R}$ and replacing ΔP by $\Delta P - \Delta p$ to give

$$v = \frac{R^2 \beta}{8L \eta} \Delta P \left\{ 1 - \frac{4}{3\Delta P} \left(\frac{2Lm}{R} \right) + \frac{1}{3\Delta P^4} \left(\frac{2Lm}{R} \right)^4 \right\} + \frac{R^2 \beta \ell \phi (\Delta P - \Delta p)}{2L} \quad (155)$$

Δp is the pressure required to initiate motion (i.e. cause slip at the wall).

McMillen (14) makes use of Binham's equation

$$-\frac{dv}{dr} = \beta \frac{(S-m)}{\eta} \quad (117)$$

Since $S = \frac{\Delta P r}{2L}$ is the shear at any radius and $\frac{\Delta P r_0}{2L}$ is the shear at the plug boundary any shearing stress at a radius greater than r_0 is $\frac{r}{r_0}$ times as great as the shearing stress or yield value m at the plug boundary

Equation (117) may be rewritten as

$$-\frac{dv}{dr} = \beta \frac{m}{\eta} \left(\frac{r}{r_0} - 1 \right) \quad (156)$$

Integrating (156) to obtain the velocity gives

$$v = \int_0^v dv = -\beta \frac{m}{\eta} \frac{r}{R} \int_{r_0}^r \left(\frac{r}{r_0} - 1 \right) dr \quad (157)$$

$$= -\beta \frac{m}{2\eta r_0} (R^2 - 2Rr_0 + 2r_0 r - r^2) \quad (158)$$

Substituting r_o for r yields the velocity of the plug

$$V_p = \frac{m\beta}{2\eta r_o} (R^2 - 2Rr_o + 2r_o^2 - r_o^2) \quad (159)$$

$$= \frac{m\beta}{2\eta r_o} (R^2 - 2Rr_o + r_o^2) \quad (160)$$

$$= \frac{m\beta}{2\eta r_o} (R - r_o)^2 \quad (161)$$

The volumetric rate of flow where shearing occurs between layers is given by

$$\begin{aligned} QR_{ro} &= - \int_R^{r_o} 2\pi r v dr \\ &= \frac{\beta m}{\eta r_o} \int_R^{r_o} (R^2 r - 2Rr_o r + 2r_o^2 r - r^3) dr \end{aligned} \quad (162)$$

$$QR_{ro} = \frac{\beta m \pi}{12\eta r_o} (3R^4 - 4R^3 r_o - 6R^2 r_o^2 + 12Rr_o^3 - 5r_o^4) \quad (163)$$

The volumetric rate of flow of plug is

$$\begin{aligned} Q_{plug} &= \pi r_o^2 V_o \\ &= \frac{\beta \pi r_o m}{2\eta} (R - r_o)^2 \end{aligned} \quad (164)$$

The total volumetric rate of flow $Q = Q_p + QR_{ro}$

$$Q = \frac{\beta \pi r_o m}{2\eta} (R - r_o)^2 + \frac{\pi m \beta}{12\eta r_o} (3R^4 - 4R^3 r_o - 6R^2 r_o^2 + 12Rr_o^3 - 5r_o^4) \quad (165)$$

$$Q = \left[\left(\frac{\pi m \beta}{2\eta} \right) r^3 \right] + \left[\frac{\beta \pi m R^4}{4\eta r_o} - \frac{\beta \pi m R^3}{3\eta} - \frac{5\pi m \beta r_o^3}{12\eta} \right] \quad (166)$$

$$= \frac{\beta \pi m}{12r_o \eta} \left[(6r_o^4) + (3R^4 - 4r_o R^3 - 5r_o^4) \right] \quad (167)$$

$$Q = \frac{\beta \pi m}{12r_o \eta} \left[3R^4 - 4r_o R^3 + r_o^4 \right] \quad (\text{cf \#129}) \quad (168)$$

$$V_{avr} = \frac{\beta m}{12R^2 r_o \eta} \left[3R^4 - 4R^3 r_o + r_o^4 \right] \quad (169)$$

While the term r_0 remains in these equations they cannot be used conveniently. To make them more useful, McMillen writes them in terms of dimensionless quantities: c , the ratio of plug radius to tube radius (or diameters), x , the ratio of any layers radius to the tube radius, and certain combinations of the two. The resulting equations are given below

$$VR_{ro} = \frac{\beta R_m}{\eta} \left(\frac{1-2c+2cx-x^2}{2c} \right) \quad (170)$$

$$= \frac{\beta R_m}{\eta} n \quad (58)$$

$$V_p = \frac{\beta R_m}{\eta} \left(\frac{1-c}{2c} \right)^2 \quad (171)$$

$$= \frac{\beta R_{mb}}{\eta} \quad (59)$$

$$V_{avr} = \frac{\beta R_m}{\eta} \left(\frac{c^4-4c+3}{12c} \right) \quad (172)$$

$$= \frac{\beta R_m}{\eta} \alpha \quad (61)$$

The ratio of average velocity to maximum velocity (assumed plug velocity)

$$\frac{V_{avr}}{V_p} = \frac{\alpha}{b} = \gamma \quad (64)$$

Volumetric rate of flow

$$Q = \frac{\beta \pi R_m^3}{\eta} \alpha \quad (60)$$

Shearing stress at tube wall

$$S_p = \frac{\Delta P R}{2L} = \frac{m}{c} \quad (173)$$

$$\text{McMillen bases his Reynolds numbers on } N_{re} = \frac{\delta V}{\eta} \quad (174)$$

$$\text{where } \delta = R-r \quad (175)$$

to take into account the radial variation of velocity and viscosity

$$\text{so } NRe = \frac{\delta V \rho}{\eta} = (R-r) \frac{(Rm_n) \rho \delta^2}{\eta^2 (y)} \quad (176)$$

$$= \frac{\delta^2 R_m^2}{\eta^2} \rho n y (1-x) \quad (70)$$

It will be noted that $NRe = 0$ at the pipe wall where $x = 1$, NRe increases with δ and V till ^{the} rate of increase of δV equals the rate of increase of η , then decreases as η increases towards the plug boundary. The maximum Reynolds number is found at x_m

$$x_m = \frac{3c + 4c(1-c)^2}{3} \quad (67)$$

The velocity at this point may be obtained by substituting

$$n_m = \frac{1 - 2c + 2cx_m - x_m^2}{c} \quad (65)$$

$$\text{into } V = \frac{\delta R_m}{\eta} n_m \quad (58)$$

The maximum Reynolds number is obtained by substituting x_m for x , n_m for n and $(1 - \frac{c}{x_m})$ for y in the equation for NRe

$$\text{to give } NRe_{\max} = \frac{\delta^2 R_m^2}{\eta^2} \rho n_m (1 - \frac{c}{x_m})(1-x_m) \quad (177)$$

$$= \frac{\delta^2 R_m^2}{\eta^2} \rho z \quad (178)$$

The dimensionless ratios which are defined above are summarized as follows:

$$\alpha = \frac{c^4 - 4c + 3}{12c} \quad (62)$$

$$b = \frac{(1 - c)^2}{2c} \quad (63)$$

$$r = \frac{\alpha}{b} \quad (64)$$

$$\omega = \frac{1}{4C\alpha} \quad (66)$$

$$xm = c + \frac{4c(1 - c)^2}{3} \quad (67)$$

$$Z = n_m (1 - \frac{c}{Z_m}) (1 - xm) \quad (68)$$

$$n = \left(\frac{1 - 2c + 2cx - x^2}{2c} \right) \quad (65)$$

$$y = (1 - \frac{c}{x}) \quad (69)$$

McMillen suggests a method for obtaining the properties of a suspension from pressure drop measurements at two different flow rates in the same pipe. This method is based on the fact that for any ratio $\frac{c_2}{c_1}$ there exists under the same set of conditions only one ratio $\frac{\alpha_1}{\alpha_2}$

$$\text{Since } \frac{c_2}{c_1} = \frac{2m/Rc_1}{2m/Rc_2} = \frac{(\Delta P/L)_1}{\Delta P/L_2} = \frac{F_1}{F_2} \quad (179)$$

$$\text{and } \frac{\alpha_1}{\alpha_2} = \frac{Rm \alpha_1 / \beta n}{Rm \alpha_2 / \beta n} = \frac{V_{ave 1}}{V_{ave 2}} \quad (180)$$

the two ratios are readily obtainable, when the flow data are known. The actual values of α_1 , α_2 , c_2 , c_1 , are then obtainable by trial and error calculation. (Graphs

presented in (14) speed up this work.) The yield value may be calculated from either c value by

$$m = \frac{\Delta P R C}{2 L} \quad (173)$$

The coefficient of rigidity is then available from

$$\eta = \frac{\beta V_{ave} R m}{\alpha} \quad (61)$$

Run	Code Symbol	% Solids
A	○	2.5
B	●	8.8
C	□	14.3
D	■	21.2
E	△	25.0
F	▲	31.9
G	▽	36.8
H	▼	39.2
J	X	40.4

$\frac{3}{4}$ " Line ———

$1\frac{1}{4}$ " Line ———

Water Data - - - - -

